University of Potsdam
Institute of Earth and Environmental Science

Trends in precipitation over Germany and the Rhine basin related to changes in weather patterns

Cumulative dissertation
for the degree of “doctor rerum naturalium” (Dr. rer. nat.)
in Hydrology

submitted to the
Faculty of Science
at the University of Potsdam, Germany

by
Aline Murawski

Trends in precipitation over Germany and the Rhine basin related to changes in weather patterns

Dissertation submitted to the Faculty of Science at the University of Potsdam, Germany, for the degree of "doctor rerum naturalium" (Dr. rer. nat.) in Hydrology

Potsdam, December 2017

Author: Aline Murawski
University of Potsdam, Institute of Earth and Environmental Science, Potsdam, Germany
German Research Centre for Geosciences, Potsdam, Germany
murawski@gfz-potsdam.de

1st Referee: Prof. Dr. Bruno Merz
(Supervisor) University of Potsdam, Institute of Earth and Environmental Science, Potsdam, Germany
German Research Centre for Geosciences, Potsdam, Germany

2nd Referee: Prof. Dr.-Ing. Uwe Haberlandt
Leibniz University of Hannover, Institute of Hydrology & Water Resources Management, Hannover, Germany

3rd Referee: Prof. Dr. Harald Kunstmann
Institute for Meteorology and Climate Research (IMK-IFU), Karlsruhe Institute of Technology (KIT), Germany
University of Augsburg, Chair for Regional Climate and Hydrology, Institute of Geography, Augsburg, Germany

Published online at the
Institutional Repository of the University of Potsdam:
URN urn:nbn:de:kobv:517-opus4-412725
http://nbn-resolving.de/urn:nbn:de:kobv:517-opus4-412725

Acknowledgements

On cake-rich and cake-poor periods

This thesis is the final product of a long journey at GFZ and around the world. Many people contributed to its success and I want to acknowledge them here.

First of all I want to thank my supervisors and mentor – Prof. Bruno Merz and Dr. Sergiy Vorogushyn – for their supervision, frequent and fruitful discussions, for adjusting the goals of my PhD to the actual work progress, and for keeping a realistic view on how much can be done in the time given. Special thanks to Sergiy for numerous good advices, for the possibility to always rely on you, no matter what.

I want to thank Prof. Blöschl from TU Vienna, who is not only my second supervisor and hosted me during an inspiring research stay at his institute, but also funded the last months of my PhD work. Thanks to Dr. Kai Schröter for funding some months of my original PhD period.

I want to acknowledge my co-authors of the papers collected here for constructive discussions and their support in the writing processes. Special thanks to Dr. Lars Gerlitz for helping with the third manuscript on very short notice and helpful suggestions on the final thesis.

Thank you to Stefan Lüdtke for fast and reliable help with programming issues. If we hadn't you in the section, me and many others would have spent so much more time on tricky little problems, especially when using the computing cluster.

A heartily thanks to all of my colleagues in section 5.4 for a good time at GFZ, for lovely hours at the campfire during summer retreats, for honest and open discussions, and especially (mind the headline!) for plenty of cakes that have sweetened the days at work!

Thank you to my friends for their uncompromised friendship, no matter how often and how long I had to leave them for the various events of the PhD programme.

Thank you to my parents for their love and support during my life up to this point.

And last but surely not least, thank you to Tobias for the time together, travelling the world, and overcoming times of separation for weeks and months even across borders.

Contents

Summary

Precipitation as the central meteorological feature for agriculture, water security, and human well-being amongst others, has gained special attention ever since. Lack of precipitation may have devastating effects such as crop failure and water scarcity. Abundance of precipitation, on the other hand, may as well result in hazardous events such as flooding and again crop failure. Thus, great effort has been spent on tracking changes in precipitation and relating them to underlying processes. Particularly in the face of global warming and given the link between temperature and atmospheric water holding capacity, research is needed to understand the effect of climate change on precipitation.

The present work aims at understanding past changes in precipitation and other meteorological variables. Trends were detected for various time periods and related to associated changes in large-scale atmospheric circulation. The results derived in this thesis may be used as the foundation for attributing changes in floods to climate change. Assumptions needed for the downscaling of large-scale circulation model output to local climate stations are tested and verified here.

In a first step, changes in precipitation over Germany were detected, focussing not only on precipitation totals, but also on properties of the statistical distribution, transition probabilities as a measure for wet/dry spells, and extreme precipitation events. Shifting the spatial focus to the Rhine catchment as one of the major water lifelines of Europe and the largest river basin in Germany, detected trends in precipitation and other meteorological variables were analysed in relation to states of an "optimal" weather pattern classification. The weather pattern classification was developed seeking the best skill in explaining the variance of local climate variables. The last question addressed whether observed changes in local climate variables are attributable to changes in the frequency of weather patterns or rather to changes within the patterns itself. A common assumption for a downscaling approach using weather patterns and a stochastic weather generator is that climate change is expressed only as a changed occurrence of patterns with the pattern properties remaining constant. This assumption was validated and the ability of the latest generation of general circulation models to reproduce the weather patterns was evaluated.

Precipitation changes in Germany in the period 1951–2006 can be summarised briefly as negative in summer and positive in all other seasons. Different precipitation characteristics confirm the trends in total precipitation: while winter mean and extreme precipitation have increased, wet spells tend to be longer as well (expressed as increased probability for a

wet day followed by another wet day). For summer the opposite was observed: reduced total precipitation, supported by decreasing mean and extreme precipitation and reflected in an increasing length of dry spells. Apart from this general summary for the whole of Germany, the spatial distribution within the country is much more differentiated. Increases in winter precipitation are most pronounced in the north-west and south-east of Germany, while precipitation increases are highest in the west for spring and in the south for autumn. Decreasing summer precipitation was observed in most regions of Germany, with particular focus on the south and west. The seasonal picture, however, was again differently represented in the contributing months, e.g. increasing autumn precipitation in the south of Germany is formed by strong trends in the south-west in October and in the south-east in November. These results emphasise the high spatial and temporal organisation of precipitation changes.

The next step towards attributing precipitation trends to changes in large-scale atmospheric patterns was the derivation of a weather pattern classification that sufficiently stratifies the local climate variables under investigation. Focussing on temperature, radiation, and humidity in addition to precipitation, a classification based on mean sea level pressure, near-surface temperature, and specific humidity was found to have the best skill in explaining the variance of the local variables. A rather high number of 40 patterns was selected, allowing typical pressure patterns being assigned to specific seasons by the associated temperature patterns. While the skill in explaining precipitation variance is rather low, better skill was achieved for radiation and, of course, temperature. Most of the recent GCMs from the CMIP5 ensemble were found to reproduce these weather patterns sufficiently well in terms of frequency, seasonality, and persistence.

Finally, the weather patterns were analysed for trends in pattern frequency, seasonality, persistence, and trends in pattern-specific precipitation and temperature. To overcome uncertainties in trend detection resulting from the selected time period, all possible periods in 1901–2010 with a minimum length of 31 years were considered. Thus, the assumption of a constant link between patterns and local weather was tested rigorously. This assumption was found to hold true only partly. While changes in temperature are mainly attributable to changes in pattern frequency, for precipitation a substantial amount of change was detected within individual patterns. Magnitude and even sign of trends depend highly on the selected time period. The frequency of certain patterns is related to the long-term variability of large-scale circulation modes.

Changes in precipitation were found to be heterogeneous not only in space, but also in time – statements on trends are only valid for the specific time period under investigation. While some part of the trends can be attributed to changes in the large-scale circulation, distinct changes were found within single weather patterns as well. The results emphasise the need to analyse multiple periods for thorough trend detection wherever possible and add some note of caution to the application of downscaling approaches based on weather patterns, as they might misinterpret the effect of climate change due to neglecting within-type trends.

Zusammenfassung

Niederschlag als eine der wichtigsten meteorologischen Größen für Landwirtschaft, Wasserversorgung und menschliches Wohlbefinden hat schon immer erhöhte Aufmerksamkeit erfahren. Niederschlagsmangel kann verheerende Auswirkungen haben, wie z.B. Missernten und Wasserknappheit. Übermäßige Niederschläge andererseits bergen jedoch ebenfalls Gefahren in Form von Hochwasser oder Sturzfluten und wiederum Missernten. Daher wurde viel Arbeit in die Detektion von Niederschlagsänderungen und deren zugrundeliegende Prozesse gesteckt. Insbesondere angesichts von Klimawandel und unter Berücksichtigung des Zusammenhangs zwischen Temperatur und atmosphärischer Wasserhaltekapazität, ist großer Bedarf an Forschung zum Verständnis der Auswirkungen von Klimawandel auf Niederschlagsänderungen gegeben.

Die vorliegende Arbeit hat das Ziel, vergangene Veränderungen in Niederschlag und anderen meteorologischen Variablen zu verstehen. Für verschiedene Zeiträume wurden Tendenzen gefunden und mit entsprechenden Veränderungen in der großskaligen atmosphärischen Zirkulation in Zusammenhang gebracht. Die Ergebnisse dieser Arbeit können als Grundlage für die Attributierung von Hochwasserveränderungen zu Klimawandel genutzt werden. Die Annahmen für die Maßstabsverkleinerung („Downscaling“) der Daten von großskaligen Zirkulationsmodellen auf die lokale Skala wurden hier getestet und verifziert.

In einem ersten Schritt wurden Niederschlagsveränderungen in Deutschland analysiert. Dabei lag der Fokus nicht nur auf Niederschlagssummen, sondern auch auf Eigenschaften der statistischen Verteilung, Übergangswahrscheinlichkeiten als Maß für Trocken- und Niederschlagsperioden und Extremniederschlagsereignissen. Den räumlichen Fokus auf das Rheineinzugsgebiet, das größte Flusseinzugsgebiet Deutschlands und einer der Hauptwasserwege Europas, verlagernd, wurden nachgewiesene Veränderungen in Niederschlag und anderen meteorologischen Größen in Bezug zu einer „optimierten“ Wetterlagenklassifikation analysiert. Die Wetterlagenklassifikation wurde unter der Maßgabe entwickelt, die Varianz des lokalen Klimas bestmöglich zu erklären. Die letzte hier behandelte Frage dreht sich darum, ob die beobachteten Veränderungen im lokalen Klima eher Häufigkeitsänderungen der Wetterlagen zuzuordnen sind oder einer Veränderung der Wetterlagen selbst. Eine gebräuchliche Annahme für einen Downscaling-Ansatzmit Hilfe von Wetterlagen und einem stochastischen Wettergenerator ist, dass Klimawandel sich allein durch eine Veränderung der Häufigkeit von Wetterlagen ausdrückt, die Eigenschaften der Wetterlagen dabei jedoch konstant bleiben. Diese

Annahme wurde überprüft und die Fähigkeit der neuesten Generation von Zirkulationsmodellen, diese Wetterlagen zu reproduzieren, getestet.

Niederschlagsveränderungen in Deutschland im Zeitraum 1951–2006 lassen sich zusammenfassen als negativ im Sommer und positiv in allen anderen Jahreszeiten. Verschiedene Niederschlagscharakteristika bestätigen die Tendenz in den Niederschlagssummen: während mittlere und extreme Niederschlagstageswerte im Winter zugenommen haben, sind auch zusammenhängende Niederschlagsperioden länger geworden (ausgedrückt als eine gestiegene Wahrscheinlichkeit für einen Tag mit Niederschlag gefolgt von einem weiteren nassen Tag). Im Sommer wurde das Gegenteil beobachtet: gesunkene Niederschlagssummen, untermauert von verringerten Mittel- und Extremwerten und längeren Trockenperioden. Abseits dieser allgemeinen Zusammenfassung für das gesamte Gebiet Deutschlands, ist die räumliche Verteilung von Niederschlagsveränderungen deutlich heterogener. Vermehrter Niederschlag im Winter wurde hauptsächlich im Nordwesten und Südosten Deutschlands beobachtet, während im Frühling die stärksten Veränderungen im Westen und im Herbst im Süden aufgetreten sind. Das saisonale Bild wiederum löst sich für die zugehörigen Monate auf, z.B. setzt sich der Anstieg im Herbstniederschlag aus deutlich vermehrtem Niederschlag im Südwesten im Oktober und im Südosten im November zusammen. Diese Ergebnisse betonen die starken räumlichen Zusammenhänge der Niederschlagsänderungen.

Der nächste Schritt hinsichtlich einer Zuordnung von Niederschlagsveränderungen zu Änderungen in großskaligen Zirkulationsmustern, war die Ableitung einer Wetterlagenklassifikation, die die betrachteten lokalen Klimavariablen hinreichend stratifizieren kann. Fokussierend auf Temperatur, Globalstrahlung und Luftfeuchte zusätzlich zu Niederschlag, wurde eine Klassifikation basierend auf Luftdruck, Temperatur und spezifischer Luftfeuchtigkeit als am besten geeignet erachtet, die Varianz der lokalen Variablen zu erklären. Eine vergleichsweise hohe Anzahl von 40 Wetterlagen wurde ausgewählt, die es erlaubt, typische Druckmuster durch die zusätzlich verwendete Temperaturinformation einzelnen Jahreszeiten zuzuordnen. Während die Fähigkeit, Varianz im Niederschlag zu erklären, relativ gering ist, ist diese deutlich besser für Globalstrahlung und natürlich Temperatur. Die meisten der aktuellen Zirkulationsmodelle des CMIP5-Ensembles sind in der Lage, die Wetterlagen hinsichtlich Häufigkeit, Saisonalität und Persistenz hinreichend gut zu reproduzieren.

Schließlich wurden die Wetterlagen bezüglich Veränderungen in ihrer Häufigkeit, Saisonalität und Persistenz, sowie der Wetterlagen-spezifischen Niederschläge und Temperatur, untersucht. Um Unsicherheiten durch die Wahl eines bestimmten Analysezeitraums auszuschließen, wurden alle möglichen Zeiträume mit mindestens 31 Jahren im Zeitraum 1901–2010 untersucht. Dadurch konnte die Annahme eines konstanten Zusammenhangs zwischen Wetterlagen und lokalem Wetter gründlich überprüft werden. Es wurde herausgefunden, dass diese Annahme nur zum Teil haltbar ist. Während Veränderungen in der Temperatur hauptsächlich auf Veränderungen in der Wetterlagenhäufigkeit zurückzuführen sind, wurde für Niederschlag ein erheblicher Teil von Veränderungen innerhalb einzelner Wetterlagen gefunden. Das Ausmaß und sogar das Vorzeichen der Veränderungen hängt hochgradig vom untersuchten Zeitraum ab. Die Häufigkeit einiger Wetterlagen steht in direkter Beziehung zur langfristigen Variabilität großskaliger Zirkulationsmuster.

Niederschlagsveränderungen variieren nicht nur räumlich, sondern auch zeitlich – Aussagen über Tendenzen sind nur in Bezug zum jeweils untersuchten Zeitraum gültig. Während ein Teil der Veränderungen auf Änderungen der großskaligen Zirkulation zurückzuführen ist, gibt es auch deutliche Veränderungen innerhalb einzelner Wetterlagen. Die Ergebnisse betonen die Notwendigkeit für einen sorgfältigen Nachweis von Veränderungen möglichst verschiedene Zeiträume zu untersuchen und mahnen zur Vorsicht bei der Anwendung von Downscaling-Ansätzen mit Hilfe von Wetterlagen, da diese die Auswirkungen von Klimaveränderungen durch das Vernachlässigen von Wetterlagen-internen Veränderungen falsch einschätzen könnten.

1. Introduction

1.1 Background

For some people, the weather forecast is more exciting than any crime thriller: will it rain tomorrow? But even for those, who await tomorrow's weather more relaxed, precipitation is directly or indirectly an (or even the most) important feature of local weather, affecting fields as diverse as agriculture, water security, and human well-being, to name only a few. Both extremes of precipitation – droughts and floods – can have devastating effects and cause high damages. Some recent events in Germany still being in memory comprise the flash flood affecting Braunsbach in 2016 (Bronstert et al., 2017), floods in many Central European rivers in 2013 (Schröter et al., 2015), the Elbe flood in 2002 (Ulbrich et al., 2003), and (memory being refreshed due to its 20th anniversary this year) the Oder flood in 1997 (Keil et al., 1999). All these (exemplarily selected) events were caused by extremely high intensities of precipitation. The mentioned fluvial floods share even one more common feature – the generating precipitation events were associated with a "Vb cyclone". Droughts, on the other hand, as observed e.g. in 2003 in Central Europe, do not cause immediate damage and fatalities, but are often associated with increasing mortality (Robine et al., 2008) and lead to interruption of river navigation and crop failures, resulting in raised prices for consumers.

Given this hazardous potential of precipitation anomalies, changes in precipitation are of great interest in the face of climate change and also given the close relationship between temperature and atmospheric moisture content (Trenberth et al., 2003). Understanding past changes is a requirement for deducing future changes (Min et al., 2011). Moreover, having demonstrated the close link between precipitation and floods above, changes in precipitation are likely to cause changes in floods as well. Understanding the effect of climate variations on river flow will help to attribute changes in floods to climate change and take appropriate measures to mitigate increased risks.

This thesis focuses on two different, yet overlapping regions in central Europe – namely Germany and the Rhine catchment. The latter being the largest river basin in Germany, comprising almost one third of its area. The climate is moderate and generally humid with annual precipitation ranging from slightly above 400 mm year^{-1} in the north-east of Germany to more than 2500 mm year^{-1} in the Alps with clear differences between windward and lee sides of mountain ranges (see also Figure 1.1, page 13). Annual mean temperature ranges from $-4.7\,^{\circ}$C at the peak of Zugspitze (the highest mountain of Germany) to more than $10\,^{\circ}$C in the Upper Rhine Plain and around $8\,^{\circ}$C at the German coasts. Population density in the study region is rather heterogeneously distributed – metropolitan areas with more than 2000 inhabitants km^{-2} being surrounded by rural areas with less than 300 inhabitants km^{-2} (`de.statista.com`, accessed September 2017). Especially the Rhine catchment comprises one of the largest urban areas of Germany (the Ruhr Area), thus placing large numbers of people into generally flood-prone areas.

This significant exposure to floods is accompanied by increasing flood trends during the second half of the 20th century (Petrow and Merz, 2009). Observed trends are partly attributable to river training (Vorogushyn and Merz, 2013), and partly to increases in flood-producing precipitation (Pinter et al., 2006). Changes in the frequency and persistence of atmospheric circulation types can trigger these changes in precipitation (Petrow et al., 2009). Further increases in winter precipitation are expected under climate change, thus, in combination with earlier snowmelt, aggravating flood risk in the Rhine (te Linde et al., 2010). But already in the past, changes in precipitation have been observed. Hundecha and Bárdossy (2005) found increasing magnitude and frequency of heavy precipitation for all seasons but summer in the German part of the Rhine basin, which is also confirmed by Zolina et al. (2008) and Brienen et al. (2013). However, they also indicate region- and season-specific dependence of their results and found a low stability in time of these trends (analysed by 30-year moving windows). The present work expands the existing knowledge in two aspects: precipitation trends have been analysed for the whole of Germany using an unprecedentedly long and dense station record, and time-stability of trends has been investigated based not only on 30-year periods, but taking all periods into account with a length of 31 years up to the full record length of 110 years.

This brief summary points towards the importance of precipitation (changes) for flood generation in the Rhine basin and indicates the role of atmospheric circulation in driving these changes. Thus, this thesis will focus on (a) precipitation changes and (b) how precipitation and changes thereof can be related to atmospheric circulation. The results will enhance understanding of past changes in precipitation and shall lay the basis for future research on attributing changes in floods to climate change. In the following sections, the two main topics of this thesis are introduced by providing some background information.

1.1.1 Precipitation changes

A considerable amount of work has been dedicated to changes in precipitation during the past decades, with a number of authors reporting on increasing extremes for different regions and time periods (for an overview, see Table 2.1, page 22). The question arises, to which extent climate change will be (and was) affecting precipitation characteristics. One expectation is the intensification of extreme events due to atmospheric warming, following the Clausius–Clapeyron relationship (Bürger et al., 2014). Given the observed warming during the last century (see Figure 4.7, page 77, for observed temperature changes in the Rhine catchment), changes in heavy precipitation are to be expected likewise. Annual precipitation was increasing by around 1 mm year^{-1} during the last century in many parts of Germany and the Rhine catchment (see Figure 1.1, central panel). However, when changing the analysed period to only the second half of the century (Figure 1.1, right panel), the trends are different in quite some places and their spatial distribution is more heterogeneous. For the headwater region of the Rhine in the Swiss Alps, precipitation decreased considerably during the second half of the century, although the century-long trend is positive. This should rise awareness for the strong dependence of trend analyses on the actual period under investigation, which is further acknowledged in chapter 4 and illustrated in Figure 1.2. Another aspect evident from Figure 1.1 is the fact that regions with low annual precipitation (i.e. the north-east of Germany) are experiencing only low increases or even decreases in annual precipitation (depending on the analysed period), thus potentially aggravating water stress situations.

1.1.2 Large-scale atmospheric patterns

As already indicated above, observations of "weather" can be related to distinct, reoccurring atmospheric states. These states are better predictable than the actual weather characteristics and can easily be obtained from large-scale information such as general circulation models (GCMs), thus making the analysis of atmospheric states an appealing tool for inferring the effect

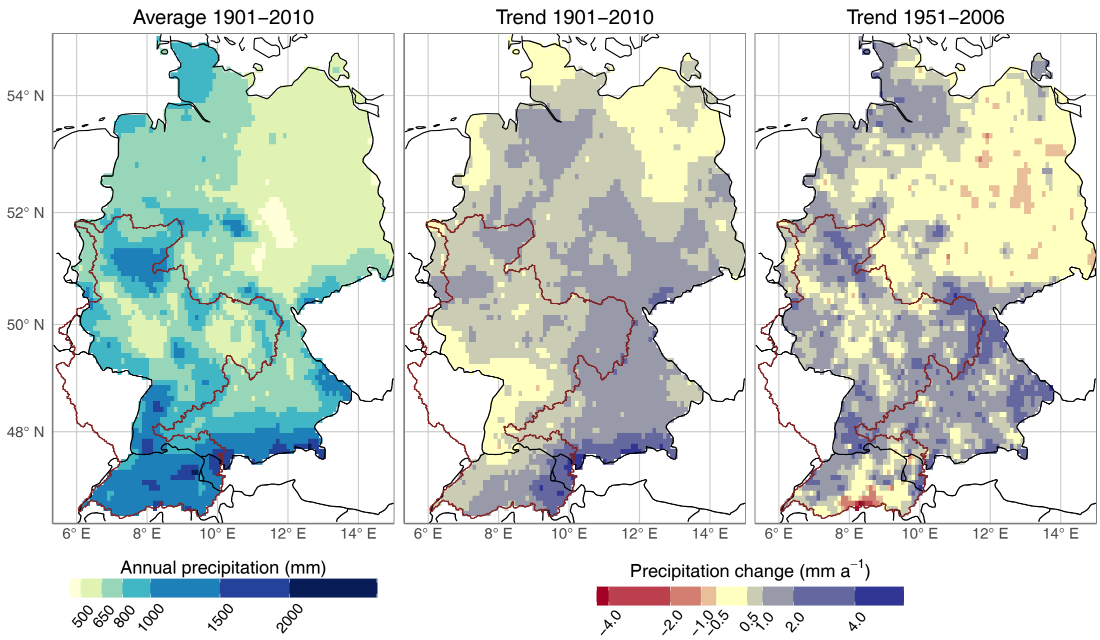

Figure 1.1: Annual precipitation for Germany and the Rhine catchment (left). Linear trend of annual precipitation for two selected time periods (center and right). Black outline indicates state borders, dark red outline shows the Rhine catchment up to the German-Dutch border. Same data set as used in chapter 3 and 4.

of climate change and for understanding atmospheric processes (Huth et al., 2008). By conditioning a stochastic weather generator on these atmospheric states, a valuable downscaling tool can be obtained for bridging the spatial gap between the global scale of GCMs and e.g. the local scale of hydrological catchment models. Analysing a finite number of atmospheric states rather than the virtually non-finite realisations of local weather itself reduces the complexity of the target. Changes in precipitation and other variables, such as temperature, can either be related to a changing occurrence of associated states or to a change of the states themselves.

Atmospheric states can be grouped into circulation or weather types (the difference between both being explained later) by classification to reduce complexity, analyse past changes of circulation, or to obtain a statistical downscaling tool to investigate past and future changes in climate. Huth et al. (2008) define classification as “a task of grouping entities (cases) so that they share common features (are similar) within each group, while being dissimilar between groups”. Groups can be spatial, i.e. defined regions that share the same climate features. A well-known example being the climate classification after Köppen, (Köppen and Geiger, 1930). The grouping can also refer to the temporal dimension, i.e. by grouping time periods (days, months, years, ...) that share common atmospheric or synoptic features. The latter is referred to further on.

Some well-known classifications comprise those after e.g. Hess-Brezowsky (Germany), Lamb (England), and Schüepp (Switzerland). All of them are subjective classifications, i.e. the assignment of cases (days) to a certain (pre-defined) type is done subjectively. Another group of classifications are objective classifications, which derive their types from the actual data, grouping them by e.g. clustering or correlation-based methods. A third group consists of objectivised versions of the formerly mentioned subjective classifications, i.e. using the same pre-defined types, but assigning individual cases depending on objective distance measures or threshold criteria. Objective (or objectivised) methods hold the advantage that they are efficiently applicable to large amounts of data, making them attractive for analysing long time series or ensembles of GCM runs. The downside of objective methods is, that their naming conventions for types are not intuitive (usually only a mere number), whereas names of subjective methods comprise some characteristics of the type (Huth et al., 2008).

Two fundamentally different strategies for classification are cluster analysis and principal component analysis. While the first assigns one defined type to each case, the latter results in modes of variability and each case can be expressed as a linear combination of several modes. The classification used in this thesis clearly belongs to the clustering methods and is compared to well-established large-scale circulation modes in chapter 4.

The aforementioned Vb cyclone, however, belongs to yet another type of classification – the "cyclone track typology" by van Bebber (1892). This classification categorises low-pressure areas by their trajectory which they take over several days. Nowadays hardly used, is the Vb cyclone the only widely known type of this classification as it is frequently associated with intense precipitation over Central Europe, transporting moisture from the Mediterranean northward and potentially leading to severe flooding. In contrast to other methods, the cyclone track typology classifies the development over several days (track). Usually, the focus is on single cases/days (however, there are options to classify sequences of days).

In chapter 3 of this thesis, a classification is established using the objective clustering method "SANDRA" (Simulated ANnealing and Diversified RAndomization). A brief description of the method is given in Philipp et al. (2007). This method offers the possibility to select and thus optimise the classification variables (subjective and objectivised methods usually pre-define the variables to use, e.g. mean sea level pressure, 500 hPa geopotential height), and has proven to have good or even superior performance compared to other methods (see subsection 3.3.1, page 44 for related references).

Depending on the variables used for classification, Huth et al. (2008) differentiates between circulation classifications, based e.g. on sea level pressure or geopotential height, and weather classifications, based on surface weather variables such as temperature and humidity amongst others. The resulting groups are hence called "circulation patterns" or "weather patterns". Although the classification used here somewhat mixes variables from both definitions, the term "weather pattern (classification)" is used throughout the thesis to distinguish from pure circulation classifications and emphasise the envisaged application in a climate change attribution study.

A pure circulation classification, based solely on variables defined at certain lower- and midtropospheric levels (Huth et al., 2008), allows for a clear separation between dynamic (circulation-based) and thermo-dynamic (pattern-internal) variability. Many studies (Cahynová and Huth, 2010, 2016; Huth, 2001; Küttel et al., 2011; Philipp et al., 2007) analysed, to which extent observed changes in temperature, precipitation, and other surface variables can be attributed to either type of variability. In terms of global warming one question to answer could be, if observed warming is due to an increased occurrence of "warm" patterns or due to a warming of the types itself. This kind of physical interpretation is often done on classifications using few types only (Belleflamme et al., 2014). However, these classifications often suffer from poor explained variances, i.e. large variability within each type (Huth et al., 2016).

In this thesis, the classification is developed particularly with regard to further application as a downscaling tool for an approach based on weather patterns and a stochastic weather generator. To condition a stochastic weather generator on weather patterns, the patterns are required to have a time-constant link to surface variables (i.e. no within-type trends) and to capture a preferably high fraction of variance of the variables under consideration (precipitation, temperature, ...). This is best achieved when expanding a classification by synoptic variables such as surface temperature and specific humidity, as done here and also suggested by Hewitson and Crane (2006). The inclusion of temperature in the classification has the further advantage of introducing a clear seasonal assignment to the patterns, thus allowing for a continuous classification throughout the whole year. A disadvantage is the loss of clear physical interpretability – global warming might either manifest as a trend within certain patterns, or as an increased occurrence of warm patterns at the expense of cold patterns. The optimisation of the classification for the specific application purpose requires for these more pragmatic compromises. Although the development of an "optimal" classification for a downscaling tool and the validation of the underlying assumptions (high explained variance, time-constant link to surface variables) is in the focus here, this thesis also assesses the physical basis of the weather patterns by integrating them into the context of established large-scale circulation modes.

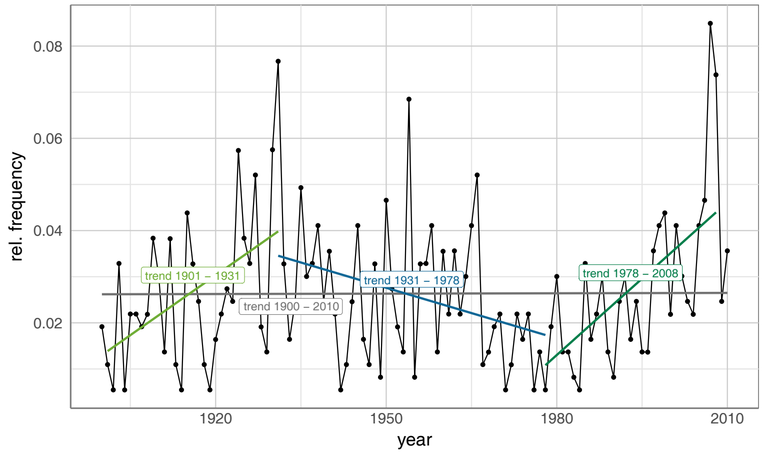

Figure 1.2: Example time series (annual frequency of weather pattern 18) to illustrate how trend direction and magnitude may differ, depending on the analysed period. Note the trend over the whole period being virtually zero.

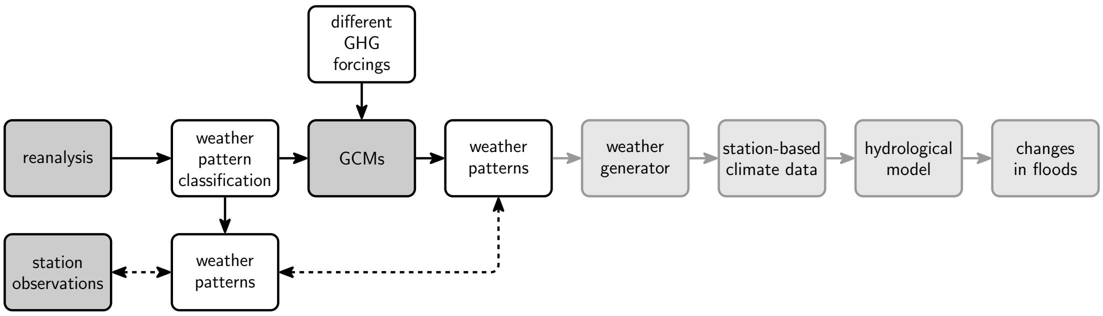

Figure 1.3: Outline of workflow towards attributing observed changes in floods to climate change. Steps that have to build on the results of this thesis are highlighted in light grey shading.

1.2 Objectives and research questions

Starting with a comprehensive investigation of precipitation changes in Germany, this thesis further analyses trends in different meteorological variables in relation to changes in the states of an optimised weather pattern classification. Aiming at the attribution of changes in floods to climate change using a downscaling approach based on weather patterns and a stochastic weather generator, the underlying assumptions for such a downscaling approach are validated here. To disentangle the effect of an anthropogenically influenced climate on floods (compared to a climate without human interference), a hydrological model can be employed using different climate data input. GCMs as from the current CMIP5 ensemble provide runs from both forcings (all greenhouse gases as observed vs. natural greenhouse gases only). However, the global scale of these models' output is not suitable for a regional hydrological model and thus some downscaling method has to be applied to bridge this spatial gap. Different approaches exists, see e.g. Maraun et al., 2010 for a review. One promising approach comprises a stochastic weather generator conditioned on weather patterns. This allows for generating long time series of meteorological variables as needed for the hydrological model. The workflow is outlined in Figure 1.3. However, some requirements are indispensable for this approach. Firstly, a weather pattern classification with high skill in explaining the variability of local weather variables is needed. Secondly, the link between weather patterns and local climate needs to be stationary, meaning that climate change will only manifest as a change in the occurrence of individual patterns.

These assumptions are tested here based on an optimised weather pattern classification developed for the Rhine basin. Thus, the applicability of the downscaling approach is validated and the precipitation changes detected for Germany can be further discussed in relation to changes in weather patterns. In addition to validating the downscaling approach, the thesis elaborates on several research questions which are shortly outlined in the following.

What changes in precipitation can be detected in the past century?
A thorough analysis of trends is sought with particular focus on a large range of precipitation characteristics, as well as on the spatial and temporal variability of trends. Despite the already existing body of literature on different aspects of trends in precipitation, this thesis aims at giving a general and comprehensive overview, extending previous studies in terms of number of analysed parameters, time period covered, spatial coverage, and quality of the data used.

Are precipitation changes rather decadal fluctuations or long-term trends (persistent in time)?
Trends in precipitation may change direction and magnitude in time (as exemplary shown for pattern frequency in Figure 1.2) which has already partly been acknowledged in the literature, as stated above. To get a more comprehensive picture of changes, multiple periods are considered for trend detection.

Can variability of daily precipitation be explained by weather patterns?
Values of daily precipitation are spread across a great range. Is it possible to stratify this range using weather patterns? A possibly narrow distribution of precipitation values is needed for developing an "optimal" weather pattern classification that can serve as a downscaling tool in climate change attribution.

Can precipitation trends be related to changes in large-scale atmospheric patterns?
Changes in precipitation (and other meteorological variables) may be driven by a changing frequency of occurrence of weather patterns, or by changing internal properties of these patterns. To which of these (between-type and within-type changes) can observed changes be related to? How do the weather patterns relate to large-scale atmospheric circulation?

1.3 Thesis outline and author contribution

The thesis combines two published papers and one submitted manuscript, whose findings answer the research questions stated above. All of them are the achievement of varying teams of authors, as listed in the respective chapters. This section provides an overview on the following chapters and distinguishes my contribution to each manuscript.

Published article: "High spatial and temporal organization of changes in precipitation over Germany for 1951–2006"
Focusses on the detection of trends in different precipitation characteristics across Germany.

Own contribution: data analyses; figures; text: data, methods, results; contributed to all other sections; revisions to the full text made by all authors.

Published article: "Can local climate variability be explained by weather patterns? A multi-station evaluation for the Rhine basin"
An "optimal" weather pattern classification is developed, aiming at maximising the amount of variation explained by weather patterns. Additionally and in regard to a future application in downscaling, GCM runs for the past century from the CMIP5 ensemble are evaluated for their skill in reproducing weather patterns characteristics.

Own contribution: data analyses; figures; text: data, methods, results; contributed to all other sections; revisions to the full text made by all authors.

Submitted manuscript: "Do changing weather types explain observed climatic trends in the Rhine basin? An analysis of within and between-type changes"
Trends in precipitation (amongst other variables) are analysed for different time periods, assessing the persistence of trends and completing the results on precipitation changes in the past

century. Weather patterns are analysed for between- and within-type changes and observed trends are related to atmospheric circulation modes.

Own contribution: data analyses; figures (except Figure 4.3 and respective computations); text (major part of): data, methods, results, discussion/conclusion; contributed to all other sections; revisions to the full text made by all authors.

2. High spatial and temporal organization of changes in precipitation over Germany for 1951–2006

Abstract

Temporal changes in daily precipitation observed at more than 2300 stations in Germany during the second half of the 20th century are analysed. Compared to other studies, this analysis is based on a very high spatial density of observation locations and complete areal coverage of Germany. Changes in four precipitation characteristics are investigated: (1) total amount of seasonal and monthly precipitation, (2) mean and 95 % quantile (q95) of daily precipitation, (3) transition probabilities to quantify wet and dry spells, and (4) precipitation amounts for a 7-day event with return period 100 years. For all parameters, strikingly clear trend patterns in space and time (of the year) emerged. Stations with increasing and decreasing trends are never found in direct neighbourhood, but are well separated from each other. Changes are season and even month specific. These clear spatial and temporal patterns are an expression of the organization of precipitation mechanisms over Germany. These findings add a note of caution in regard to trend analyses: Spatially and temporally aggregated trend studies might not disclose the complete range of changes and might miss important details. Interestingly, the variability of daily precipitation has changed in parallel with the mean behaviour: Those regions and seasons that show an increase in mean show also an increase in standard deviation, leading to a disproportional increase in heavy precipitation. In addition, there is a tendency towards higher persistence, in particular, longer wet spells in winter, spring, and autumn, and longer dry spells in summer. If these trends continue, there will be an increasing potential for floods in winter and spring, and increasing problems for water availability in summer in regions that show signs of water stress today.

Keywords

precipitation change; trend analysis; extreme precipitation; transition probabilities; gamma; Germany

Published as:

Murawski, A., Zimmer, J., and Merz, B. (2016b). "High spatial and temporal organization of changes in precipitation over Germany for 1951–2006". In: *International Journal of Climatology* 36.6, pp. 2582–2597. DOI: 10.1002/joc.4514

2.1 Introduction

Precipitation is one of the most important climate variables. Given the link between temperature and atmospheric water holding capacity, human-induced global warming may already have contributed to changes in precipitation. Changes in extreme precipitation are of particular importance in this respect, and it has been suggested that heavy precipitation events increase with global warming (Min et al., 2011; Trenberth et al., 2007). Against this background, we analyse changes in daily precipitation over Germany during the second half of the 20th century.

Much effort has been spent on detecting trends in precipitation, and in particular, in extreme precipitation, as this can have adverse consequences for society. For Europe, most analyses of observed precipitation found increasing heavy precipitation during the period of extensive data coverage, i.e. from several decades to the last century (Alexander et al., 2006; Groisman et al., 2005; Klein Tank and Können, 2003; Moberg et al., 2006; Zolina, 2014; Zolina et al., 2008, 2005). For example, Moberg et al. (2006) investigated changes in precipitation extremes derived from daily time series for Europe west of 60°E for 1901–2000. They found that winter precipitation totals have increased by approximately 12 % with similar trends in some percentiles (90th, 95th, 98th) of daily winter precipitation (analysed on 121 stations north of 40°N). For summer, they did not find significant trends over the whole area under investigation, but a slight tendency towards more intense but less frequent precipitation. Zolina et al. (2010) analysed the duration of wet spells in Europe over the period 1950–2008 using daily data from 699 rain gauges. They found that wet periods, defined as consecutive days with significant precipitation (more than 1 mm), have become longer by about 15 % to 20 %. Interestingly, the total number of wet days has not increased, pointing to a change in the structure of rainfall events. Moreover, heavy precipitation events have become more intense. A similar study of Zolina et al. (2013) using data for 1950–2009 specified that the changes found in the previous work have mainly occurred in winter. Pauling and Paeth (2007) investigated the changes in winter precipitation anomalies over Europe back to 1700. They found that over Central Europe wet winters were more frequent during 1951–2000 with respect to the past 300 years (except 1701–1750). For Germany, Trömel and Schönwiese (2007) analysed 132 time series of monthly total precipitation covering 1901–2000. For most of the year, they found an increasing probability of exceeding the 95th percentile and a decreasing probability of falling under the 5th percentile for several stations in the south of Germany. The same results were found for the western part of Germany for summer. In winter, both probabilities increased in the west of Germany. The opposite development was found for the east of Germany in summer and autumn (decrease in both probabilities: exceeding the 95th and falling below the 5th percentile). Hence, this study illustrated the large heterogeneity of precipitation behaviour in space and in the annual course, and pointed to the importance of region- and season- or even month-specific analyses. Zolina et al. (2008) analysed a much denser network of stations ($>$ 2000) for the period 1950–2004. They analysed linear trends in extreme and heavy precipitation. As indicator, they used the 95 % and 99 % percentiles of the gamma distribution fitted to daily precipitation values. Regrettably, their analysis was limited to the western and southern parts of Germany. They found positive linear tendencies in heavy precipitation for all seasons except summer where most trends were negative and emphasized the importance of seasonal analysis, because their trend analyses without seasonal breakdown did not show any clear spatial patterns. A subsequent study by Zolina (2014) analysed wet spells over the whole of Germany at 3161 stations for 1950–2008, but was restricted to only two seasons. Similar results were found by Hundecha and Bárdossy (2005) who analysed the evolution of daily extreme precipitation for 1958–2001 in the German parts of the Rhine basin using data of 611 precipitation stations. For the area of east-central Germany, Hänsel et al. (2009) studied trends of monthly rainfall for 1951–2006 based on more than 200 precipitation stations. They found season-specific trends with increasing monthly winter precipitation and decreasing summer precipitation. Although the trend patterns showed similarities across the region, the winter increase was highest in the mountainous south-western part, whereas the summer decrease was most pronounced in the northern lowland. For the same period (1951–2006), Łupikasza et al. (2011) analysed extreme precipitation trends for east-central Germany and southern Poland. They used different indicators based on daily precipitation data at 43 stations for the complete area. For all seasons and for east-central Germany, increasing trends dominated the temporal changes, however, increases were particularly significant in winter.

Although several studies (see Table 2.1 for an overview) have analysed the time development of precipitation for Germany, they either used data of sparse observational networks or analysed only parts of Germany and/or restricted themselves to a very limited choice of precipitation variables that mainly aim at quantifying extremes. In this article, we complement this knowledge by analysing changes in four indicators that describe precipitation characteristics quite extensively: (1) the total amount of seasonal and monthly precipitation, respectively, (2) the mean and 95 % quantiles (q95) of daily precipitation, (3) transition probabilities to quantify wet and dry spells, and (4) precipitation amounts for an extreme event of 7 days with return period 100 years. All analyses are performed on a seasonal or even monthly level and are based on data of more than 2300 precipitation gauges covering the whole area of Germany for the period 1951–2006. Thus, an extended analysis of precipitation on an exceptionally good and homogeneous data base is provided.

The analysis of changes in multi-day, extreme precipitation is of particular interest. Floods are associated with different time scales of the triggering rainfall events. Trans-national and trans-basin floods are typically related to multi-day, heavy precipitation events. The most recent examples are the August 2002 and June 2013 floods in Central Europe. The flood in 2002 has been the most expensive natural disaster in Germany so far, and the 2013 flood has been the most severe flood – in hydrological terms – in Germany since 1951 (Schröter et al., 2015). Each event caused damages in the order of EUR 10 billion for Germany alone (Merz et al., 2014). It is important to understand whether the probability of precipitation events with the potential to trigger large-scale floods has changed in the past decades.

Table 2.1: Overview on available studies on precipitation changes and extremes for Germany, Europe, and the World. The analyses methods used are summed up and for some studies results are also summarized.

Author	Region	Period	No of stations	Precipitation behaviour analysed	Indicators used	Results
Brienen et al. (2013)	west and south Germany	1901–2000	118	Empirical distribution, grouping stations to regions via PCA, assessing stability of trends	• Total precip per season • Wet day frequency • Max no consecutive dry days • Mean wet day intensity • 90th percentile • Precip amount from days exceeding 90th percentile • Max precip during 5 consecutive days • Max daily precip	• Increase in intensity-related indices in summer in W-GER • Max no of consecutive dry days increased in Foothills of the Alps and very south of Germany • In first half no signif. trend in winter, in summer increasing trend in intensity-related indices in central W-GER, increase in max no of consecutive dry days in the south • In second half decrease in summer precip and frequency of wet days, increase in max no of consecutive dry days, for winter increase in intensity-related indices
Hänsel et al. (2009)	central-east Germany	1851–2006, 1951–2006	2, ~200	Monthly rainfall	• Trends of annual, summer, winter and monthly precip	• Increase in winter precip and decrease in summer half year • Decrease in agricultural used lowlands and during first vegetation period • Decrease in extreme precip and frequency in summer • Increase of frequency in high precip classes for winter • Mar, Nov – high precip increase; Apr, May, Oct – decrease

continue next page

Table 2.1 – continued

Author	Region	Period	No of stations	Precipitation behaviour analysed	Indicators used	Results
Hundecha and Bárdossy (2005)	German parts of Rhine basin	1958–2001	611	Daily extremes (annual and seasonal basis)	• 90th percentile of daily precip • Max 5-d-total precip • Daily intensity • Max no of consecutive dry days • Fraction of precip amount from daily events > long-term 90th percentile • No of days with precip > long-term 90th percentile	• Increase in heavy precip in spring • Decrease in extreme precip and frequency in summer • Increases extreme precip in autumn
Łupikasza et al. (2011)	central eastern Germany (and southern Poland)	1951–2006	19 (GER)	Daily extremes (seasonal basis)	• Max 1-day precip • Max 5-day total precip • Precip total for days >90th percentile, >95th percentile • No of days with precip >90th percentile, >95th percentile • Precip intensity for days with precip >90th percentile, >95th percentile	• Winter: clear increases in amount, frequency, intensity • Spring & autumn: overall increase, but less prominent • Summer: increase dominates, but also significant decreases
Trömel and Schönwiese (2007)	Germany	1901–2000	132	Monthly extremes	• 5th, 95th percentiles of monthly precip	• Decrease in extreme precip and frequency in summer • Decreasing probability of precip >95th percentile in autumn, NE-GER
Zolina et al. (2008)	western and southern parts of Germany	1950–2004	2125	Daily extremes, (annual and seasonal basis)	• 95th, 99th percentiles of daily precipitation • Precipitation total • No of wet days • Precip intensity	• Heavy (90th) and extreme (95th) precip increased ~5–13 % per decade in winter, spring, autumn • Heavy (90th) and extreme (95th) precip decreased ~3–9 % per decade in summer • Winter: large precip increasing; weak precip decreasing • Summer: decreases for all classes

continue next page

Table 2.1 – continued

Author	Region	Period	No of stations	Precipitation behaviour analysed	Indicators used	Results
Zolina (2014)	Germany	1950–2008	3161	Wet spells (WP) in warm and cold season	• Length of spells • Trend of mean and extremely long WPs	• average duration of wet spells highest in mountains and coastal areas • Significant changes only in cold season (increasing intensities in long WPs, decreasing in short WPs)
van den Besselaar et al. (2013)	Europe	1951–2010	478	Changes in seasonal extreme precip	• Max 1- and 5-day prec of each 20 y period of the time series (with 10 y overlap) • Return period for these extremes	• Increasing extremes in winter and spring in N-Europe • Summer extremes nearly constant in N-Europe
Klein Tank and Können (2003)	Europe	1946–1999		Daily extremes (annual basis)	• Max 1-day precip • Max 5-day precip • No of days with precip $>$10 mm, $>$20 mm • No of days with precip amount $>$75th percentile, $>$95th • Precip fraction due to very wet days ($>$95th)	• wet extremes increase • disproportionate large change in extremes where annual amount also increases
Moberg et al. (2006)	Europe	1901–2000	223	Seasonal totals and daily precip	• Precip total • Simple daily precip intensity • 90th, 95th, 98th percentile of daily precip	• Increase in winter precip totals • Increase in upper percentiles in winter • No significant overall trend in summer
Pauling and Paeth (2007)	Europe	1700–2000 (recon-structed)	0.5° grid	Changes of return periods of seasonal winter precip extremes	• Fitted Gamma to seasonal sums	• Winter precipitation: more extreme • Dry winters: more often over central Europe during past 300 years • Many other parts of Europe: extremes less frequently during last 300 years compared to 1951–2000

continue next page

Table 2.1 – continued

Author	Region	Period	No of stations	Precipitation behaviour analysed	Indicators used	Results
Zolina et al. (2005)	Europe	1804–2003	295, 96	Heavy precip	• Seasonal totals • Number of seasonal wet days • Seasonal mean precip intensity • Occurrence of exceedance of given threshold, e.g. 95th or 99th • Percentage of seasonal total precip sum obtained during very wet (> 95th) days • 95th, 99th percentiles of Gamma distribution for daily precip	• Increasing frequency and intensity of heavy precip over most Europe • For summer decrease in northern Europe and increase in southern Europe
Zolina et al. (2009)	Europe	1951–2000	116	Heavy and extreme precip, daily data	• fractional contribution of very wet days to precipitation total	• increase in winter, decrease in summer extremes
Zolina et al. (2010)	Europe	1950–2008	699	Wet spells and dry spells	• Duration and intensity	• Longer wet periods over most of Europe, no increase of total number of wet days
Zolina et al. (2013)	Europe	1950–2009	699	Wet spells and dry spells	• Duration	• Duration of wet spells increases over northern Europe and central European Russia, especially pronounced in winter • Summer wet spells shorter over Scandinavia and northern Russia • Duration of dry spells decreases over Scandinavia and southern Europe in winter and summer

2.2 Data

The data used in this study were mainly derived from the precipitation gauge network of the German Weather Service (DWD) and processed by the Potsdam-Institute for Climate Impact Research (PIK). Data processing by Österle et al. (2006b) included the selection of 2342 stations with continuous records in the period 1951–2006 and quality control of the data. Precipitation was monitored at all stations, 270 stations also recorded other climate variables, such as air temperature (daily minimum, maximum, and mean) and wind speed. These variables were interpolated to the precipitation gauge stations, such that a complete set of meteorological variables exists for each of the 2342 stations. Quality control of the data covered checking for physically meaningful values, consistency of air temperatures, plausibility of sequences with identical values, and spatially inconsistent measurements. Erroneous and missing values were filled with the help of correlated neighbouring stations. The data processing is described in detail in Österle et al. (2006b). The resulting gap-free data set of 2342 stations located in and near Germany (Figure 2.1), and covering the period 1951–2006 in daily time steps was available for this study. Other studies such as Zolina (2014) allowed gaps of up to 10 % in their data which allowed the use of even a greater number of stations. Nevertheless, their Figure 1 illustrates nicely that the time span analysed here covers the period with the densest and most complete (in terms of data gaps) network of precipitation stations in Germany – the number of stations was considerably less before 1951 and decreased drastically again in the beginning of the 2000s.

Snowfall has a larger wind drift undercatch error than rainfall for the Hellmann gauges used in Germany. Hence, higher winter temperatures and associated redistribution from snowfall to rainfall could wrongly be interpreted as increasing winter precipitation (Førland and Hanssen-Bauer, 2000). To avoid this misinterpretation, undercatch errors were corrected considering wind speed and aggregation state as proposed by Yang et al. (1999).

Most of the parameters were analysed on a seasonal basis. Statements referring to 'winter' include January and February of the particular year and December of the previous year. This means that the seasonal analyses contain time series from December 1951 to November 2006. 'Winter' (WIN) always refers to December, January, February, 'spring' (SPR) to March, April, May, 'summer' (SUM) to June, July, August, and 'autumn' (AUT) to September, October, November.

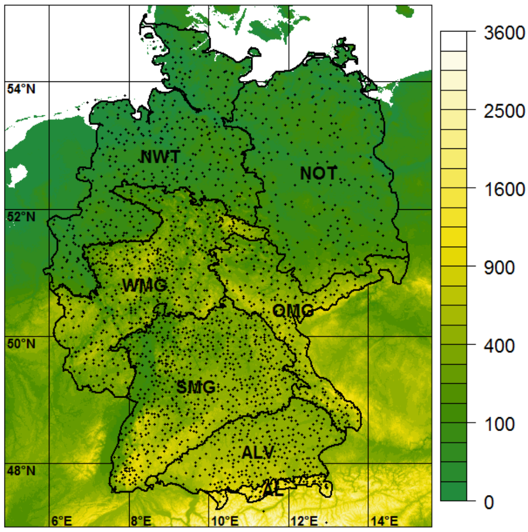

Figure 2.1: Map of Germany including elevation (in m a.s.l.) and locations of precipitation gauges (dots). Bold lines show the regional sub-division into landscapes (abbreviations given in subsection 2.3.3) with similar climate, geomorphology, and topography.

2.3 Methods

2.3.1 Threshold between wet and dry days

A distinction between 'precipitation' and 'no precipitation' (or 'wet' and 'dry') days is necessary to derive transition probabilities and to fit probability density functions (pdf) to the precipitation data. The threshold between these two states was set to 0.5 mm, i.e. only days with precipitation larger or equal to 0.5 mm were considered as wet days. Days with less than 0.5 mm were defined as 'dry' for transition probabilities and were not used when fitting the pdf. This threshold of 0.5 mm (as in Groisman et al., 2005; Kundzewicz et al., 2006) was established to avoid that measurement errors were taken as rain and to ignore amounts of precipitation that were not discernible and not meteorologically relevant.

To quantify the amount of light precipitation which we neglected in our analyses, the mean annual amount of precipitation contributed by events of less than 0.5 mm d^{-1} was examined. The average amount of light precipitation is around 7 mm $year^{-1}$ with up to 14 mm $year^{-1}$ in very few places in the northern half of Germany and less than 4 mm $year^{-1}$ at some stations in the south of Germany. Monthly mean light precipitation was always less than 2 mm, averaging around 0.6 mm. Hence, we conclude that the contribution of light precipitation to the total amount of precipitation is negligible even for those parts in the east of Germany with annual precipitation of less than 600 mm.

2.3.2 Derivation of time series of precipitation characteristics

Total precipitation

Seasonal and monthly precipitation totals were analysed. The total precipitation of a particular time period is the sum of all precipitation values within this time period without any distinction between 'precipitation' and 'no precipitation'.

Mean, variability, and heavy precipitation indicators for daily precipitation

For each station, a pdf of daily precipitation amount was derived by fitting a gamma pdf to the observations (only days with precipitation $\geq$0.5 mm) of each season and year. The gamma distribution is typically used for describing daily precipitation amounts (e.g. Furrer and Katz, 2008; Wilks and Wilby, 1999). We calculated the mean and standard deviation (SD) of the data and derived the shape and scale of the gamma pdf by:

$$\text{Scale} = \text{SD}^2/\text{Mean} \tag{2.1}$$

$$\text{Shape} = \text{Mean}^2/\text{SD}^2 \tag{2.2}$$

Finally, the 95 % quantile (q95) was obtained from the fitted pdf. The time series of mean, SD (not shown here), and upper quantile were further analysed for trends on a seasonal level.

Heavy precipitation indicators (e.g. q95) can be derived from fitted gamma pdf (e.g. Groisman et al., 1999; Zolina et al., 2008, 2005) or directly from the empirical distribution (e.g. Brienen et al., 2013; Hundecha and Bárdossy, 2005; Zolina et al., 2005). (Zolina et al., 2005) compared both approaches and concluded that the gamma distribution-based indices were more robust to sampling uncertainty. Another advantage of the distribution-based approach is that the fitted distributions can be used to derive multi-day precipitation indicators.

It has been shown that the gamma distribution may not well represent the upper tail of observational data (Furrer and Katz, 2008; Panorska et al., 2007). Hundecha et al. (2009) used a mixture of gamma and generalized Pareto distributions with dynamically varying weights and obtained a much better representation of daily precipitation variability. However, because of the large number of fitting parameters, such an approach is not feasible in our application which is based on samples of approximately 37 values (average number of wet days per season).

To check the suitability of the gamma distribution, we applied the Kolmogorov–Smirnov test (Wang et al., 2003) with significance level $\alpha = 0.1$ to every sample to which the gamma pdf was fitted. For the large majority of stations and seasons, the test revealed no significant difference between the data and the fitted pdf. The number of samples (i.e. years) that were not well represented by the gamma pdf were counted for each station and season. If a station had less than 40 (of 55) years that could reasonably be described by the gamma distribution in a particular season, no trend test was performed and hence no trend would be detected. In total, 12 stations were eliminated in winter, 27 in spring, 50 in summer, and 18 in autumn, i.e. between 0.5 and 2.1 % of the stations were eliminated. Most of them were situated in central-east Germany (northern part of region OMG – East Central Uplands, see subsection 2.3.3 for abbreviations) and, especially for summer, in the region NOT – Northeast German Plain.

Transition probabilities

The occurrence of precipitation, or the absence of precipitation, is not completely random over time. Because of the tendency for persistence at the daily time scale, the occurrence of wet or dry spells (periods of consecutive days with or without rain) is likely. This characteristic is frequently described by a two-state, first-order Markov model with two states (1: wet day, i.e. precipitation $\geq$0.5 mm; 0: dry day, i.e. precipitation $<$0.5 mm). The occurrence of precipitation is modelled as a binary-valued discrete random variable (Wilks and Wilby, 1999). The transition probabilities of all possible transitions between dry and wet are given as: P_{00}, dry day is followed by another dry day; P_{01}, dry day is followed by wet day; P_{10}, wet day is followed by dry day; P_{11}, wet day is followed by another wet day. There are only two possibilities for the state of day $t + 1$. Therefore, the probabilities of two complementary transitions add up to 1: $P_{00} + P_{01} = 1$; $P_{10} + P_{11} = 1$, so only transitions P_{00} and P_{11} are examined. These probabilities were derived from the observed daily time series by calculating the relative frequency of each transition of each season and year.

Multi-day precipitation amount of given return period

Changes in the pdf of daily precipitation and in the transition probabilities may lead to changes in the exceedance probability of extreme events with duration longer than 1 day. To investigate changes in such extreme, multi-day precipitation events, time series of precipitation amount for selected multi-day precipitation events, and selected return periods were derived for each station and tested for trends. In this way, the joint effect of temporal changes in the pdf and in the transition probabilities could be assessed. The following Monte Carlo procedure is set up for each season and year and given station:

1. By randomly drawing from the transition probabilities P_{00} and P_{11} derived from the observations, a new time series of wet and dry days is created (90 days for a season).

2. Precipitation amounts are randomly drawn from the gamma pdf fitted to the station data for each season and year, and assigned to 'wet' days of step 1. In this way, a synthetic daily precipitation time series is generated for the period 1951–2006.
3. The maximum precipitation amount occurring within n consecutive days is selected.
4. By repeating steps 1–3 10 000 times, 10 000 synthetic times series of maximum n-day precipitation are derived.
5. A generalized extreme value distribution (GEV) is fitted to these 10 000 values, and the precipitation amount corresponding to a given return period is derived. For each season and station, this results in one time series of n-day, m-year return period precipitation amount. The assessment of multi-day precipitation was performed only for stations that passed the Kolmogorov–Smirnov test in at least 40 years of 55 (for number of stations being removed, see above).

2.3.3 Trend analyses under consideration of temporal and spatial correlation

Trends were analysed by means of the non-parametric Mann–Kendall trend test which calculates a rank correlation coefficient (Kendall, 1938). Trends were judged to be significant if the associated two-sided p-value was less or equal to 0.1 (significance level 10 %). The Mann–Kendall trend test was applied to time series of annual values of the respective parameters. For example, trends in the 95 % quantile of daily summer precipitation were based on, firstly, estimating the 95 % quantile for each year given the daily precipitation values ≥0.5 mm of this year's summer, and secondly, analysing the resulting time series of annual values of the 95 % quantile.

To quantify the magnitude of change, the slope of the trend was calculated using the non-parametric trend slope estimator proposed by (Sen, 1968):

$$\beta = \text{median}\left(\frac{x_n - x_m}{n - m}\right) \quad ;\text{for all } n > m; x_n, x_m = \text{respective parameter in years n, m} \tag{2.3}$$

Because persistence in the time series may distort the results of the Mann–Kendall trend test, all (annual) time series were checked for autocorrelation. Most of them were free of any autocorrelation, but a few showed significant correlation at some time lags. To account for the bias in trend results for autocorrelated time series, a block bootstrap approach as proposed by Khaliq et al. (2009) was used. The underlying idea is to resample the autocorrelated time series in away that preserves the correlation structure. Then the test statistic is obtained from the resampled time series. By doing this for a large number of times (10 000), a simulated distribution of the test statistic was obtained. If the test statistic of the original time series lies in the tails of the simulated distribution – i.e. it is unlikely to get the same test result from a time series that contains a similar autocorrelation structure as the original series but no temporal trend – the test result of the original time series is judged to be unaffected by autocorrelation. To preserve the autocorrelation structure while resampling, the resampling is done in blocks of determined length. Following the approach of Khaliq et al. (2009), the block length is the number of significant (at significance level $\alpha = 0.1$) contiguous serial correlations plus 1. The block bootstrap approach was employed on Kendall's tau statistic for time series that showed an apparently significant trend. Only if the result of the block bootstrap approach confirmed the presence of a trend, this was considered to be justified.

The results of our trend analyses show spatial clustering of stations with significant trends. Obviously, neighbouring stations may experience similar changes in rainfall characteristics, and thus a station is likely to show a trend if the neighbouring station does. In trend detection studies with many sites within a region, it is advisable to evaluate the field significance, i.e. the significance of trends across the region. This is done by comparing the number of observed significant trends with the number expected within the region. It has been found that spatial correlation between sites may inflate the results of trend tests (Douglas et al., 2000). Hence, we apply the field significance test as given in Yue et al. (2003). This test accounts for spatial correlation by a bootstrapping procedure which preserves the cross-correlation among sites. Field significance was calculated for seven regions in Germany. The spatial extent of these regions is given in Figure 2.1 and was chosen according to the Federal Agency of

Nature Conservation (BfN). These regions represent landscapes with similarities in climate, geomorphology, and topography. The abbreviations used in Figure 2.1 and in the following are AL, Alps; ALV, Alpine Foreland; NOT, Northeast German Plain; NWT, Northwest German Plain; OMG, East Central Uplands; SMG, Southwest Uplands/Scarplands; and WMG, West Central Uplands.

2.3.4 Visualization of results

All trend analyses are performed directly on station data. To better visualize the findings, the results obtained at every station are interpolated to a grid covering Germany by means of inverse distance interpolation. This kind of visualization is useful to show spatial characteristics of average values for transition probabilities and multi-day precipitation. For the display of trend results, the magnitude of trends (absolute change derived from Sen's slope over the study period) is interpolated to the whole area. Stations with significant trends are marked with dots.

2.4 Results and discussion

2.4.1 Changes in total precipitation

When applying the Mann–Kendall trend test to time series of monthly and seasonal precipitation, very distinct patterns emerge (Figure 2.2 and 2.3). Most obvious is that all seasons except summer show almost only positive trends, i.e. trends towards higher precipitation. Table 2.2 gives the number of stations showing trends in seasonal and monthly total precipitation. Winter precipitation increased significantly in the Northwest German Plain and East Central Uplands. Many stations experienced a total increase of winter precipitation of 40 mm to 80 mm (i.e. 10 % to 30 %, in some places 40 %), others, especially in the east of Germany, showed a total increase of less than 40 mm (around 20 %). Spring precipitation increased significantly in western regions (NWT, WMG, SMG) with a magnitude of 20 mm to 60 mm (i.e. 10 % to 30 %) and a higher increase in mountainous regions of the Black Forest and the Sauerland. Summer precipitation showed a distinct decrease of 20 mm to 100 mm (10 % to 30 %) in many parts of Germany with field significance being observed for regions ALV, NOT, SMG, and WMG. In some places, e.g. in the Black Forest, summer precipitation decreased even by more than 100 mm. Autumn precipitation increased mainly in the southern parts (regions AL, ALV, OMG, SMG) by up to 140 mm (30 % to 50 %) in the mountain ranges. Patterns that can be found in seasonal precipitation totals are quite differently pronounced in the associated months. Although January, February, and December show only rather few stations with significant trends that are not field significant for any region, winter precipitation trends are much more distinctive. The same conclusion, i.e. single months do not necessarily show the same spatial pattern of trends as the season to which they belong, can be drawn for almost all months. Seasonal results rather seem to be a composition of the three contributing months: trend patterns that

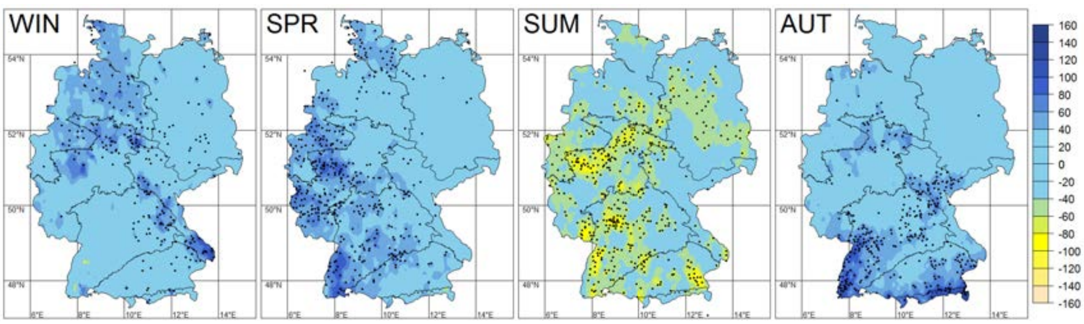

Figure 2.2: Change of seasonal total precipitation (in mm per season for 1952–2006). Dots indicate stations with significant trend (α = 0.1) in the respective season. The background is coloured according to interpolated values of the magnitude of trends at all stations (derived from Sen's slope). Black lines show the regional sub-division into landscapes as given in Figure 2.1.

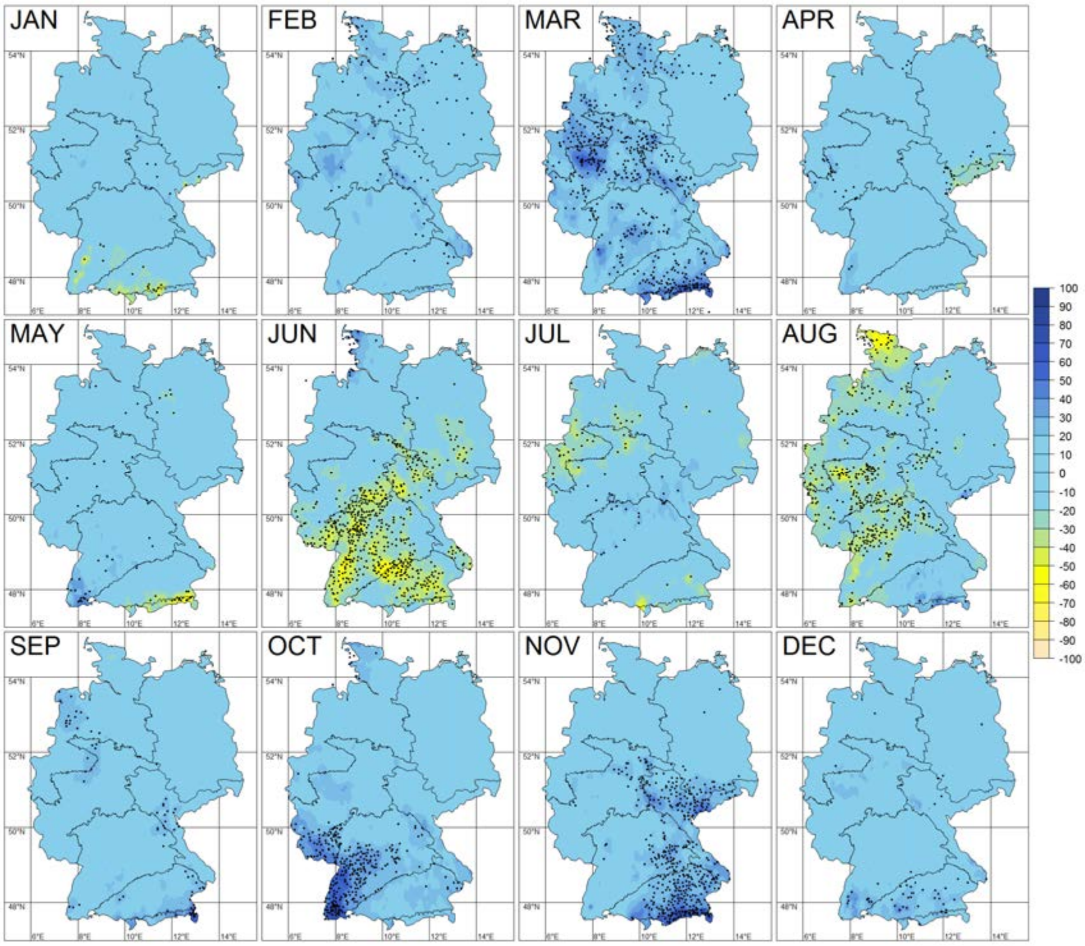

Figure 2.3: Change of monthly total precipitation (in mm per month for 1951–2006). Plot as in Figure 2.2.

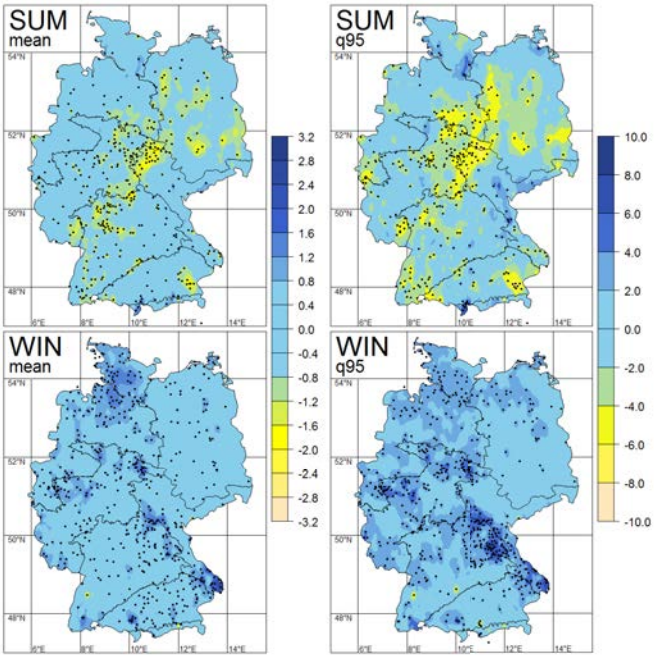

Figure 2.4: Change of mean and upper quantile of the gamma distribution of daily precipitation for summer and winter (in mm for 1952–2006). Plot as in Figure 2.2.

are well pronounced in a single month or are similar in different months are expressed in the seasonal result as well (e.g. compare the superposition of positive trends for March, April, and May, leading to pronounced positive trends in spring for the Southwest of Germany, east of the Rhine). Contradicting trend directions in 2 months cancel out each other, leading to insignificant change in the respective season (e.g. compare March and May with spring for the very South of Germany). This result should serve as a note of caution for previous studies (as in section 2.1 and Table 2.1): trend results obtained on a seasonal basis might not be valid for single months. Several months showed interesting spatial patterns of significant trends. March revealed significantly increasing precipitation in five of seven regions and for 24 % of all stations, whereas April and May showed only weak changes (except May where a decrease of precipitation in the Alps was found). Thus, the change in spring precipitation was mainly influenced by changing March precipitation. June showed significantly decreasing precipitation of up to 60 mm for 24 % of all stations and for all regions except the Alps and the Northwest German Plain. July precipitation revealed only very few and weak trends, and the change of August precipitation is rather located in the west. The increase in autumn precipitation in the southern half of Germany arose from quite distinct patterns in the respective months: in October strong spatial clustering of positive trends was found in the Black Forest (southwest) and surroundings whereas the increase in November precipitation was manifested mainly in the southeast and central-east. It can be summarized that strikingly clear spatial patterns of trends in seasonal and monthly precipitation totals emerged. Stations showing significant trends are not erratically located but tend to be strongly spatially clustered. Increasing and decreasing trends are never found in direct neighbourhood, but are well separated from each other. It is also worthwhile to notice that the trend patterns of succeeding months are quite distinct from each other and that seasonal trend patterns are hardly found in the respective months. Therefore, trend studies should not be limited to seasonal analyses only, but should also check single month (if an appropriate data base is available).

2.4.2 Changes in mean, variability, and heavy precipitation indicators

Figure 2.4 shows the trend results for the mean and the 95 % quantile of the daily precipitation amounts for winter and summer. A remarkable attribute of these results is that, for a given

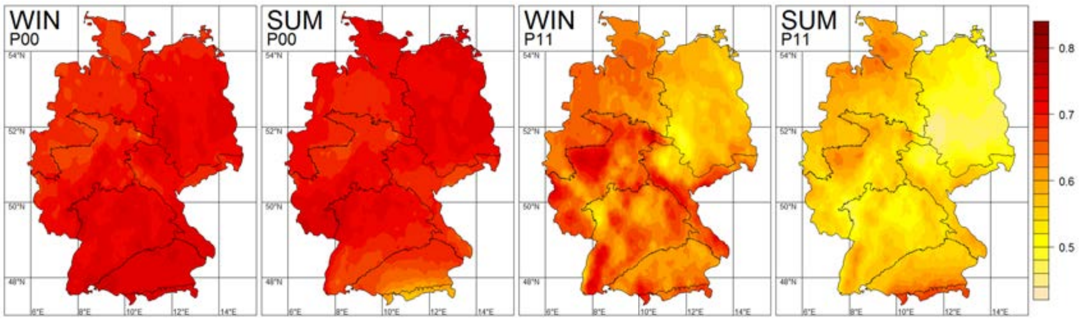

Figure 2.5: Transition probabilities P_{00} and P_{11} (as fraction) for summer and winter, mean value for 1951–2006.

season, the spatial patterns are very similar. This means the SD (not shown here) increases (or decreases) in accordance with the mean, and hence, the upper quantile increases (or decreases) with a similar pattern. To better understand the patterns of change in mean precipitation, we analysed various empirical quantiles of the data as well (not shown here). We found that in winter increasing mean precipitation in the North is caused by changes over the complete distribution whereas in the Southeast only upper quantiles increase resulting only in small changes of the mean. In summer, the patterns of trends are solely influenced by the upper quantiles, and lower quantiles do not show any spatial pattern but are very heterogeneous. Another striking characteristic is the direction of trends (Figure 2.4 and Table 2.2). Whereas almost all significant trends in winter are positive, the great majority of trends in summer is negative. In winter, stations showing significant trends are focussed in the north, west, and southeast with regions NOT, NWT, WMG, and OMG being field significant for both indicators. In contrast to that, summer exhibits a pattern of negative trends that is field significant for all indicators in the West Central Uplands, and significant only for the mean in the Northeast German Plain, Southwest Uplands, and East Central Uplands. The results for spring and autumn are not shown here. However, it can be summarized that an increase of up to 7 mm (for 1952–2006) in spring and 13 mm in autumn for the 95 % quantile was found with significant changes in regions NWT, SMG, WMG, and ALV for spring, and NWT, SMG, and WMG for autumn.

2.4.3 Transition probabilities

Spatial pattern

Figure 2.5 shows the spatial pattern, averaged over 1951–2006, of transition probabilities P_{00} and P_{11} for winter and summer. Transition probability P_{00} is always greater than 0.5, which means there is a higher probability that a dry day follows after another dry day compared to a change from dry to wet. In contrast, transition probability P_{11} could fall below 0.5 in some regions and seasons. The probability for transition P_{00} is quite high in winter (approximately 0.66–0.76). However, it has to be taken into account that the transition probabilities are influenced by the chosen threshold (0.5 mm) for assigning a day as wet or dry. Further, P_{00} is rather homogeneously distributed over Germany with slightly lower probabilities in the northwest of Germany and some low mountain ranges of east-central Germany. In contrast to that, P_{11} shows a marked spatial pattern which has large similarities to the spatial pattern of total precipitation (not shown here) – mountainous parts of the west and south (except the Alps) have highest transition probability P_{11} with values around 0.66–0.84. Lowest probabilities were found on the lee side of the Harz Mountains in central-east Germany. This result can be explained by the fact that lee sides and the east get relatively low precipitation in winter, and thus, the probability for two wet days in a row is quite small. In summer, the spatial pattern of P_{11} has some similarities to winter, however, the values are lower. In contrast, the values of P_{00} are somewhat higher in summer compared to winter for most parts in the north and west, whereas the south and south eastern mountain ranges show lower values of P_{00} with probabilities as low as 0.56 in the Alps, exhibiting a similar pattern as total summer precipitation (not shown here). The patterns

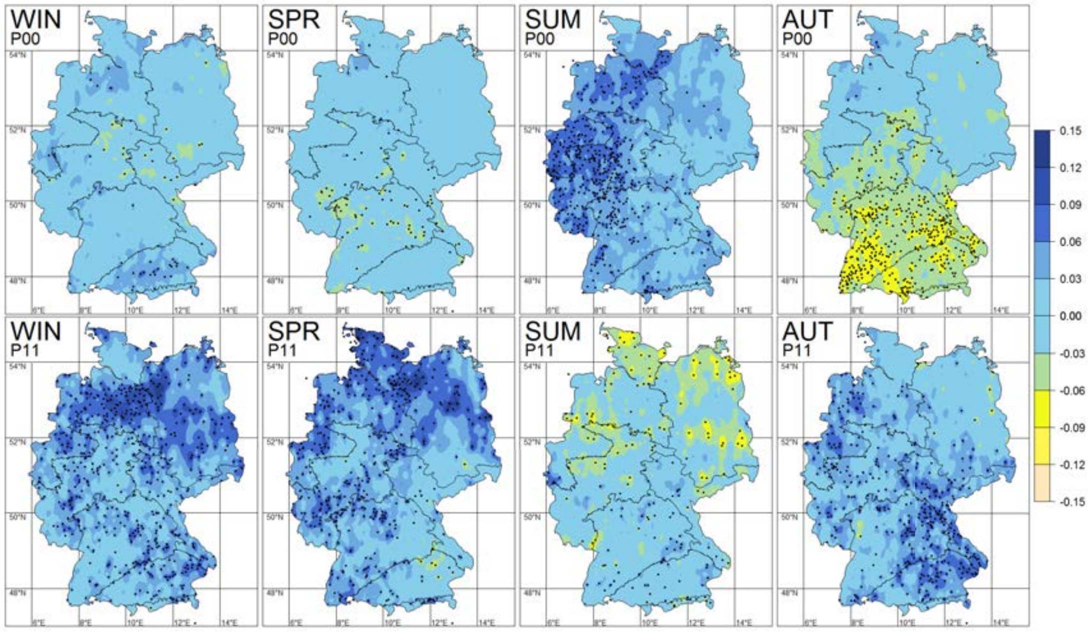

Figure 2.6: Change of transition probabilities P_{00} and P_{11} (as fraction for 1952–2006) for all seasons. Plot as in Figure 2.2.

of spring and autumn transition probabilities (not shown) are similar to those of summer and winter with intermediate values.

Trends in transition probabilities

The trend results for transition probabilities are given in Figure 2.6. P_{00} (dry-dry) shows no particular trends in winter and spring, but an increase in the west in summer and a decrease in the south in autumn, which denotes a tendency for longer dry spells during summer in the west and shorter dry periods in autumn in the south of Germany. This supports the observed trends in seasonal total precipitation. As summer tended to become drier, longer dry periods might occur and P_{00} increased. For autumn, decreasing P_{00} means that dry periods were more often interrupted by rainfall which resulted in higher total precipitation, mainly in the south for which a trend towards higher precipitation was observed. The absolute change of P_{00} is in the range of 0.03 to 0.09 in summer and -0.03 to -0.09 in autumn. For transition P_{11} (wet-wet), an upward trend of the probability in the range of 5 % to 15 % was observed in winter in all regions of Germany except the Alps. Thus, wet spells tend to last longer which is in line with observed increasing winter precipitation. In the west and north and in the Alps, P_{11} increased also in spring (5 % to 15 %); in the south and west, P_{11} increased in autumn (5 % to 10 %).

2.4.4 Seven-day precipitation amount with return period 100 years

Spatial pattern, average over 1952–2006

Figure 2.7 shows the 7-day amount of precipitation with a return period of 100 years for each season. The patterns of each season are again very similar to those of total precipitation (not shown here). Salient features of these patterns are the strong control by orography, low values in the east for winter, rather homogeneous values all over Germany and highest values in the Alps for summer, and intermediate values for spring and autumn. These patterns should not be surprising as the parameters that entered our Monte Carlo procedure [pdf (annually averaged results not shown here) and transition probabilities] follow similar patterns. Far more interesting are the huge differences of multi-day precipitation amounts. For instance, an event that has a return period of 100 years in the east of Germany might occur at least once a year in the Alps. For winter, the precipitation depth of the 100-year/7-day event varies from 50 mm to 70 mm in the eastern lowlands, 70 mm to 100 mm in the western and southern lowlands, and

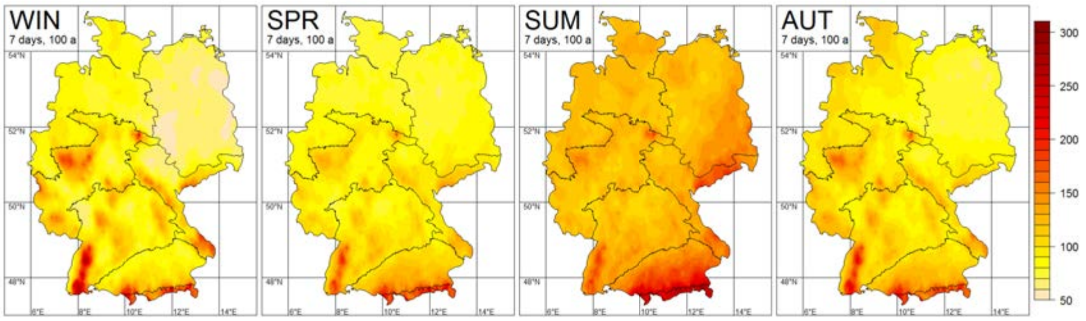

Figure 2.7: Seven-day precipitation amount with return period 100 years (in mm) for all seasons, mean value for 1952–2006.

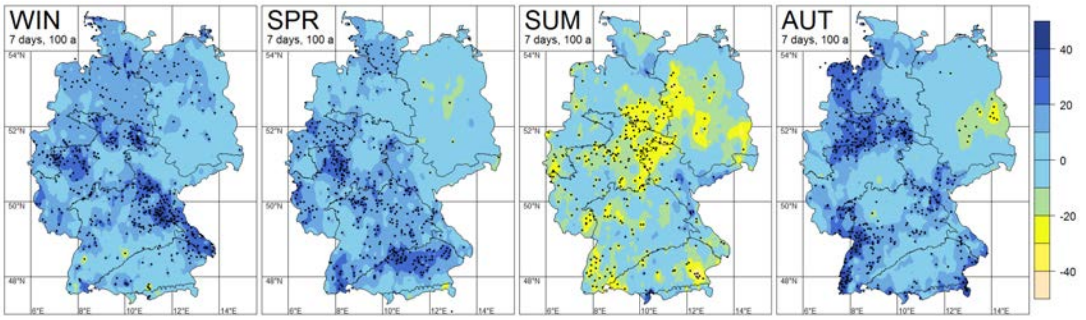

Figure 2.8: Change of 7-day precipitation amount with return period 100 years (in mm for 1952–2006) for all seasons. Plot as in Figure 2.2.

up to 260 mm in the mountains. In summer the range extends from 90 mm to 160 mm for most regions of Germany to 310 mm in the Alps.

Trends in extreme, multi-day precipitation

In Figure 2.8, the change of the precipitation amount of the 100-year/7-day event during 1952–2006 is shown. In winter, we detected an increase by around 10 % to 40 % in all regions except the Alps and the Alpine Foreland with the highest increase in the East Central Uplands (up to 60 %). In spring, there is an increase of up to 40 % in the west (regions NWT, SMG, WMG) and the Alpine Foreland. For summer, a field significant downward trend of up to -30 mm was found in the West Central Uplands. Autumn showed increasing extreme precipitation in the west. Interestingly, the spatial patterns of all seasons are very similar to the results of the trend analyses for the parameters of the gamma distribution, whereas the patterns of the changes in transition probabilities cannot be identified. This shows that the observed changes in the pdf dominate the changes in the 100-year/7-day precipitation event. The changes in transition probabilities are mostly below 15 %, and are comparatively small.

Table 2.2: Trend results for all precipitation characteristics analysed: monthly and seasonal total precipitation; seasonal mean, 95 % quantile (q95); seasonal transition probabilities and seasonal multi-day precipitation.

	JAN	FEB	MAR	APR	MAY	JUN	JUL	AUG	SEP	OCT	NOV	DEC	WIN	SPR	SUM	AUT
	total precipitation															
up	6 (0%)	123 (5%)	559 (24%)	27 (1%)	31 (1%)	23 (1%)	25 (1%)	9 (0%)	76 (3%)	304 (13%)	429 (18%)	50 (2%)	249 (11%)	430 (18%)	2 (0%)	348 (15%)
down	25 (1%)	2 (0%)	0 (0%)	33 (1%)	29 (1%)	562 (24%)	42 (2%)	383 (16%)	0 (0%)	0 (0%)	1 (0%)	0 (0%)	6 (0%)	1 (0%)	445 (19%)	1 (0%)
AL			+		−				+		+					+
ALV			+			−					+				−	+
NOT						−									−	
NWT			+					−					+	+		
OMG			+			−					+		+			+
SMG						−		−		+	+			+	−	+
WMG			+			−		−						+	−	

	WIN		SUM		WIN	SPR	SUM	AUT	WIN	SPR	SUM	AUT	WIN	SPR	SUM	AUT
	mean	q95	mean	q95	P00				P11				7d/100a precipitation			
up	513 (22%)	522 (22%)	38 (2%)	39 (2%)	38 (2%)	10 (0%)	487 (21%)	7 (0%)	520 (22%)	415 (18%)	54 (2%)	360 (15%)	513 (22%)	438 (19%)	25 (1%)	472 (20%)
down	26 (1%)	11 (0%)	314 (13%)	257 (11%)	22 (1%)	78 (3%)	1 (0%)	440 (19%)	8 (0%)	14 (1%)	120 (5%)	14 (1%)	11 (0%)	9 (0%)	261 (11%)	19 (1%)
AL								−		+						+
ALV	+							−	+			+		+		
NOT	+	+	−						+	+			+			
NWT	+	+					+		+	+		+	+	+		+
OMG	+	+	−					−	+			+	+			
SMG		+	−				+	−	+				+	+		+
WMG	+	+	−	−			+		+	+			+	+	−	+

Number and percentage of stations with significant upward or downward trend, respectively. Plus signs (minus signs) indicate field significance in upward (downward) trends for the region as described in subsection 2.3.2. Significance level: 10%.

2.5 Conclusions

This article used a quality-controlled data set of a very dense network of 2342 precipitation stations with an average distance of 12 km between stations for the period 1951–2006 for Germany. The data base allowed a comprehensive analyses of spatio-temporal precipitation patterns. The time series of daily precipitation values for each station were used to derive an indicator set describing different characteristics of precipitation: (1) precipitation totals to capture the changes at the monthly and seasonal time scale, (2) mean and 95 % quantile to represent the daily precipitation behaviour, (3) transition probabilities to describe persistence of daily precipitation, and (4) 7-day precipitation amount with return period 100 years to exemplify the combined effect of changes in persistence and in the pdf of daily precipitation on multi-day, heavy precipitation.

For all indicators, strikingly clear spatial trend patterns emerged. Stations showing significant trends are not erratically located but tend to be strongly spatially clustered. Increasing and decreasing trends are never found in direct neighbourhood, but are well separated from each other. These clear spatial patterns are an expression of the spatial organization of precipitation mechanisms over Germany.

The trends in monthly and seasonal precipitation totals show not only clear spatial patterns but also very distinct seasonality. The trends can be roughly summarized as getting wetter in winter, spring, and autumn, and getting drier in summer. However, it has to be noted that these trends are composed of different spatial patterns, for instance, the increase in winter is particularly pronounced in the southeast and northwest, whereas the spring increase is especially distinct in the west. Interestingly, the further stratification of seasonal totals in monthly totals yielded different trend patterns, i.e. trend patterns of succeeding months are quite distinct from each other, and the trend patterns of individual months can significantly depart from their seasonal value. Hence, trend analyses at the seasonal scale may not disclose the complete range of changes.

The overall patterns of trends detected at the seasonal time scale can also be seen at the daily scale: Whereas almost all significant trends of daily precipitation indicators are positive in winter, the great majority of trends in summer is negative, and moreover, the clusters of increasing or decreasing stations are similar in both cases. Our analyses show increasing heavy precipitation for winter, spring, and autumn, but show the opposite trend for summer precipitation.

In order to complete the description of changes in daily precipitation, we analysed the spatio-temporal behaviour of transition probabilities. P_{00}, the probability of two dry days in sequence, is rather homogeneously distributed over Germany. In contrast, P_{11}, the probability of two wet days in sequence, shows a clear spatial heterogeneity with highest probabilities in the mountainous parts of the west and south (except the Alps) and the lowest values in lee zones (especially east of the Harz Mountains). There is also a clear seasonal effect: lower P_{11} values and higher P_{00} values in summer, respectively, compared to winter transition probabilities. Trends of transition probabilities show an overall increasing persistence for wet spells in winter, spring, and autumn. However, this increase is region specific. For example, the increase in spring is particularly marked in parts of north and northeast Germany, and there are regions, e.g. Saxony and Bavaria, which do not show any change. Increased persistence (higher P_{00} and higher P_{11}, see Figure 2.6) is found especially in the Northwest German Plain (except summer), but also for many regions in winter and spring; in contrast to that, autumn shows strong signals towards longer wet spells and shorter dry spells in all regions except the NWT. The contrary behaviour is found for summer in the northern half of Germany: longer dry spells and shorter wet spells.

The overall result of increasing persistence is in accordance with results of Petrow et al. (2009) who analysed flood trends and their potential climatic causes across Germany for the same period. They found a tendency for increasing persistence of rainfall-causing atmospheric circulation patterns, especially for the winter half year (November–April). Changes in the persistence of dry spells are less distinct. However, there is a clear tendency for longer dry spells during summer in the west and shorter dry periods in autumn in the south of Germany. This increase in persistence might be linked to global warming, because reduced meridional temperature gradients tend to lower the steering velocity of weather patterns and seem to favour amplified waves with increased meridional wind components (e.g. Francis and Vavrus, 2012).

The combined effect of daily precipitation amount and persistence on multi-day heavy precipitation was exemplarily analysed for the 100-year/7-day event. The spatial pattern, averaged over the complete period, shows huge differences, from 50 mm to 70 mm in the eastern lowlands up to more than 300 mm in the Alps. The differences within a season and between seasons can be explained by different precipitation formation processes: areal frontal precipitation plus localized, but stationary orographic upslope enhancement in winter; much more localized convective precipitation in summer, being pronounced in certain regions (low mountain ranges and Alpine Foreland due to Alpine pumping). The footprint of the cyclone track Vb (van Bebber, 1892) is clearly visible in summer in Saxony, Brandenburg, and in the south and east of Bavaria.

The results of the trend analyses show that, overall, the 100-year/7-day precipitation amount increased during winter, spring, and autumn. Strong increase is confined to parts of Germany, differently for different seasons. For some regions, the increase is remarkable, e.g. an increase in the order of up to 50 mm in the southeast and central-west in winter. The overall tendency for summer is downward with the highest decrease of up to -30 mm in central Germany.

Multi-day, heavy precipitation is closely connected to the occurrence of regional flooding, especially on time scales of a few days. Recent experience, e.g. the May/June 2013 flood in the Elbe and Danube catchments in Central Europe, underlines that multi-day rainfall accumulations may lead to disastrous flooding. Such extreme precipitation events are becoming more likely with increased persistence. However, the cyclone track across the catchment areas and the timing play an important role, too.

In summary, remarkable changes in daily precipitation are observed during the second half of the 20th century. Based on a very high density of stations, it is shown that temporal changes are spatially well structured. In case the observed trends continue, there will be an increasing potential for floods in winter and spring, e.g. in parts of northwest and southeast Germany, and at the same time, increasing probabilities for water stress in summer in regions that show signs of water stress today.

Acknowledgements

We gratefully appreciate the provision of data by the German Weather Service, kindly provided by PIK. A. Murawski acknowledges funding by Climate KIC.

3. Can local climate variability be explained by weather patterns? A multi-station evaluation for the Rhine basin

Abstract

To understand past flood changes in the Rhine catchment and in particular the role of anthropogenic climate change in extreme flows, an attribution study relying on a proper GCM (general circulation model) downscaling is needed. A downscaling based on conditioning a stochastic weather generator on weather patterns is a promising approach. This approach assumes a strong link between weather patterns and local climate, and sufficient GCM skill in reproducing weather pattern climatology. These presuppositions are unprecedentedly evaluated here using 111 years of daily climate data from 490 stations in the Rhine basin and comprehensively testing the number of classification parameters and GCM weather pattern characteristics. A classification based on a combination of mean sea level pressure, temperature, and humidity from the ERA20C reanalysis of atmospheric fields over central Europe with 40 weather types was found to be the most appropriate for stratifying six local climate variables. The corresponding skill is quite diverse though, ranging from good for radiation to poor for precipitation. Especially for the latter it was apparent that pressure fields alone cannot sufficiently stratify local variability. To test the skill of the latest generation of GCMs from the CMIP5 ensemble in reproducing the frequency, seasonality, and persistence of the derived weather patterns, output from 15 GCMs is evaluated. Most GCMs are able to capture these characteristics well, but some models showed consistent deviations in all three evaluation criteria and should be excluded from further attribution analysis.

Published as:

Murawski, A., Bürger, G., Vorogushyn, S., and Merz, B. (2016a). "Can local climate variability be explained by weather patterns? A multi-station evaluation for the Rhine basin". In: *Hydrology and Earth System Sciences* 20.10, pp. 4283–4306. DOI: 10.5194/hess-20-4283-2016

3.1 Introduction

The Rhine River is a trans-boundary river with a catchment area of 185 000 km^2 and significant flood risk. Along the main river reach from Karlsruhe in south-western Germany to Rees at the Dutch–German border, an area of 14 600 km^2 is at risk of being flooded for an extreme scenario with a return period of 200 to 500 years (Thieken et al., 2015). This enormous economic exposure to floods is accompanied by expectations that flood magnitudes will increase due to climate change e.g. Bosshard et al., 2014; Dankers and Feyen, 2009; te Linde et al., 2010. Further, the Rhine catchment has experienced increasing flood trends during the second half of the 20th century (Petrow and Merz, 2009). It has been argued that climatic drivers, land use changes and river training may have contributed to the observed trends (Petrow et al., 2009; Pinter et al., 2006; Villarini et al., 2011; Vorogushyn and Merz, 2013). Whereas the role of river training in the main Rhine channel has been quantified (Lammersen et al., 2002; Vorogushyn and Merz, 2013), the effect of climatic and land use changes remains unclear. In particular, the contribution of anthropogenic climate change to flood trends is an open question. To understand the role of climatic drivers in past changes in river flooding, rigorous attribution studies are needed (Merz et al., 2012).

Several studies tried to quantify the role of changes in meteorological variables in river flows using hydrological models with alternative sets of climate drivers (Duethmann et al., 2015; Hamlet and Lettenmaier, 2007; Hamlet et al., 2007; Hundecha and Merz, 2012). If an attribution of hydrological changes to changes in the atmospheric composition such as greenhouse gas concentration is attempted, output from GCMs (general circulation models), representing two different “worlds” with and without anthropogenically induced climate change, are to be compared (Min et al., 2011). This requires that output of GCMs is properly downscaled to a resolution compatible with hydrological models.

Different approaches are applied in the hydrological community for statistical downscaling (for a review, see Fowler et al., 2007; Maraun et al., 2010). Statistical downscaling approaches using weather generators offer the possibility of generating multiple realizations of long synthetic time series, e.g. 100 years of daily values, and are considered to have similar skills compared to regional climate models (RCMs) (Hewitson and Crane, 2006). This provides a basis for a more robust estimation of changes in hydrological variables and moments of their distributions. They are particularly suited for quantifying rare floods and their impacts (e.g. Falter et al., 2015), in case they are capable of representing the statistical behaviour of extreme events. Examples of using weather generators to bridge the spatial gap between GCMs and hydrological impacts are widespread (e.g. Elshamy et al., 2006; Fatichi et al., 2011; Fowler et al., 2000, 2005; Hewitson and Crane, 2006; Katz, 1996; Kilsby et al., 2007; Kim et al., 2015; te Linde et al., 2010; Lu et al., 2015; Semenov and Barrow, 1997; Wilks, 1992).

In order to represent different climate states, parameters of a weather generator can be conditioned on the climate model output by applying a change factor (Kilsby et al., 2007) or on covariates such as weather patterns. The latter approach is expected to better capture change in variability of the changing climate state. Weather patterns are classifications of atmospheric circulation fields or other synoptic fields (Huth et al., 2008). The underlying assumption of the downscaling based on weather patterns is that the regional or local behaviour of climate variables is partly a response to the larger-scale, synoptic forcing. The weather generator is then parameterized separately for each class of weather patterns (e.g. Bárdossy and Plate, 1991, 1992; Corte-Real et al., 1999; Fowler et al., 2005; Haberlandt et al., 2015). Statistical downscaling tends to underestimate the variance of regional or local climate if the contribution of local processes is not considered, and may poorly represent extremes. Different methods have been proposed to rectify this problem: variable inflation (Karl et al., 1990), expanded downscaling (Bürger, 1996), and randomization (Kilsby et al., 1998). This problem typically occurs in downscaling approaches that are based on regression models and weather patterns. It is circumvented when a weather generator is conditioned on weather patterns, provided that the weather generator is able to adequately capture the tail behaviour of the surface climate variables.

A downscaling approach based on weather pattern classification builds on four assumptions. Firstly, local climate needs to be sufficiently explained by the classification of the large-scale synoptic situation. Bárdossy et al. (2002) summarize that many studies have shown that there is a strong link between atmospheric circulation types derived from CTCs (circulation-type classifications) and surface variables such as near-surface temperature and precipitation. Even when the small-scale climate is governed by mesoscale events such as convective systems, these are, in turn, conditional on the synoptic state (Goodess and Jones, 2002). On the other hand, weather patterns can only be a proxy for local weather, due to the categorization of continuous data by the discrete classification, and more importantly, due to the fact that the large-scale situations do not fully represent smaller-scale features. This so-called within-type variability (e.g. Huth et al., 2008) is caused, for instance, by small-scale processes, such as orography-enhanced rainfall, or by variations in dynamic properties (pressure gradient, vorticity, intensity) of weather patterns (Beck et al., 2007).

Secondly, the linkage between weather patterns and regional and local climate is assumed to be stationary. This means that climate change will mainly manifest itself as a change in the frequency, persistence, and seasonality of these weather patterns. The transfer function between synoptic state and regional and local climate thus remains constant. Land use and land cover change, for example, could introduce a variable forcing on local climates (Hewitson and Crane, 2006). Using long observational time series, it has been argued that the linkages between large-scale weather patterns and regional climates are characterized by distinct variabilities (Beck et al., 2007).

The third assumption is that GCMs are able to properly reproduce weather patterns. GCMs are often strongly biased in variables such as precipitation (e.g. Sunyer et al., 2015), but are expected to reflect large-scale circulations well. This skill in representing the synoptic situations compared to the poor skill in representing surface variables is utilized for statistical downscaling. For example, Hewitson and Crane (2006) conclude that much of the discrepancy between GCM projections of precipitation over South Africa may result from differences in their precipitation parameterization schemes, whereas the synoptic dynamics are well simulated. It has been shown, however, that the skill of GCMs in reproducing weather pattern characteristics such as geopotential height and sea level pressure varies strongly (Brands et al., 2013; Wójcik, 2015).

Finally, to obtain meaningful input for the hydrological model, a weather generator has to adequately represent the space–time dynamics of the catchment meteorology. This is a particular challenge for large river basins, where the correlation structure of e.g. precipitation becomes difficult to capture over large distances.

In the presented paper we evaluate the assumptions for weather pattern based downscaling for the Rhine catchment. This is a prerequisite for conditioning a weather generator on circulation patterns for understanding the role of climatic drivers in past and future flood changes in the Rhine basin. We focus on the first and third assumptions here. The assumption of stationarity of the linkage between weather patterns and local climate and the skill of the weather generator itself will be investigated separately. In the future we intend to use a multi-site, multi-variate weather generator (Hundecha and Merz, 2012; Hundecha et al., 2009) for downscaling GCM output to drive a regional hydrological model. An extreme value statistic on the simulated streamflow will then allow us to quantify the role of climatic change in flood flows.

To underpin the first and third assumptions, we derive an “optimal” weather pattern classification and investigate (1) to which extent weather patterns are able to stratify local climate variables, and (2) the skill of the GCMs in reproducing these weather patterns. It has been argued that there is no “best” statistical downscaling approach, but that the optimal classification depends on the application and region (Hewitson and Crane, 2006; Huth et al., 2008). We look specifically from the perspective of a hydrological impact study for the Rhine catchment.

There is a significant body of literature on weather pattern classification. Our work extends these studies in several aspects. Firstly, we test the skill of several classification variables. Often classifications are based on msl (mean sea level pressure) only. We use, in addition, the synoptic temperature and humidity fields to classify weather patterns. Considering temperature as a classification variable has the advantage that one classification can be used throughout the year. Secondly, we test the ability of weather pattern classifications to stratify a comparatively large number of climate variables with daily resolution: precipitation, minimum, mean, and maximum temperature, radiation, and relative humidity. Other studies often consider only one or two variables (e.g. Anagnostopoulou et al., 2008; Beck et al., 2007; Beck and Philipp, 2010;

Haberlandt et al., 2015; Kyselý, 2007; Łupikasza, 2010) and only a few studies are available with an extended list of up to eight variables (e.g. Cahynová and Huth, 2010; Enke et al., 2005b; Kidson, 1994). We use a comparatively long time period of 111 years. The periods of other studies are typically much shorter, e.g. 11 to 50 years (Anagnostopoulou et al., 2008; Beck and Philipp, 2010; Bettolli and Penalba, 2012; Brinkmann, 1999, 2000; Brisson et al., 2010; Cahynová and Huth, 2010; Goodess and Jones, 2002; Hewitson and Crane, 2006; Kidson, 1994; Łupikasza, 2010) or 100 years (Kyselý, 2007). Beck et al. (2007) cover a longer period, going back to 1780, however, using only monthly resolution. Fourthly, our analysis covers a large, transboundary area of around 160 000 km^2 and a very large number of climate stations (490). Weather pattern classifications typically work with a comparatively low number of stations, ranging from e.g. 1 station for Prague (Kyselý, 2007) to 84 stations for New Zealand (Kidson, 1994).

Further, we analyse the newest generation of climate models from the Coupled Model Intercomparison Project Phase 5 (CMIP5). We investigate their ability to reproduce frequency, persistence, and seasonality of weather patterns. Wójcik (2015) emphasizes the need to assess the reliability of GCMs prior to any statistical downscaling approach. Whereas Perez et al. (2014) analysed the frequency of patterns over the north-eastern Atlantic and Belleflamme et al. (2013) examined the frequency and persistence of patterns over Greenland, so far no other study analysed seasonality as done here. Particularly for understanding the role of climate change in flood flows, matching the seasonality is essential.

3.2 Data

For the workflow proposed here, three different sets of climate data are needed: (1) data on which to establish the weather pattern classification, (2) compatible output of climate models with different greenhouse gas (GHG) forcings, i.e. the same variables and spatial coverage as (1), and (3) observations from local climate stations in the investigated area (Rhine catchment) for all meteorological variables of interest, preferably covering the same time period as (1).

To investigate the suitability of different climate variables to establish the weather pattern classification, long-term reanalysis fields can be used. We utilized the newly available ERA-20C – a gridded reanalysis data set from the ERA-CLIM project (Poli et al., 2013). This data set is a pilot reanalysis of the 20th-century assimilating surface observations only and is forced by a HadISST2.1.0.0 ensemble of sea surface temperature and sea ice conditions, available for the period 1900–2010. The 3- or 6-hourly data, depending on the variable, were aggregated to daily averages for this study. The spatial resolution of $1° \times 1°$ was chosen. There are finer resolutions available for ERA-20C, but the resolution of GCMs is not finer than $1.25° \times 0.94°$.

The skill of different weather pattern classifications was assessed according to their ability to stratify climate station data located in the Rhine catchment (Figure 3.1). Sets of daily precipitation, temperature (mean, min, max), relative humidity, and global radiation data for the period 1901–2010 were available from the national meteorological services and kindly processed and quality controlled by the Potsdam Institute for Climate Impact Research (PIK) (Österle et al., 2006a). For the German part of the catchment 432 stations were available, 9 stations for the Austrian part, and 49 stations for Switzerland and Liechtenstein. To date no data from meteorological stations in France were available. This set of 490 climate stations allows for the classification results to be compared to a large and dense station network.

For the assessment of the effect of anthropogenic GHG emissions on changes in floods, data from modelling experiments with two different GHG forcings representing (a) the historical (natural + anthropogenic) GHG concentrations (All-Hist) and (b) only natural GHG concentrations (Nat-Hist) are required. These experiments are available from a number of GCMs of the CMIP5 project (Taylor et al., 2012). An overview of the models and the number of runs available for the All-Hist experiment used here are given in Table 3.1. The model output is available in daily time steps, mostly starting as early as the mid-19th century. All available runs were analysed in relation to the ability of different GCMs to replicate the frequency, persistence, and seasonality of weather patterns.

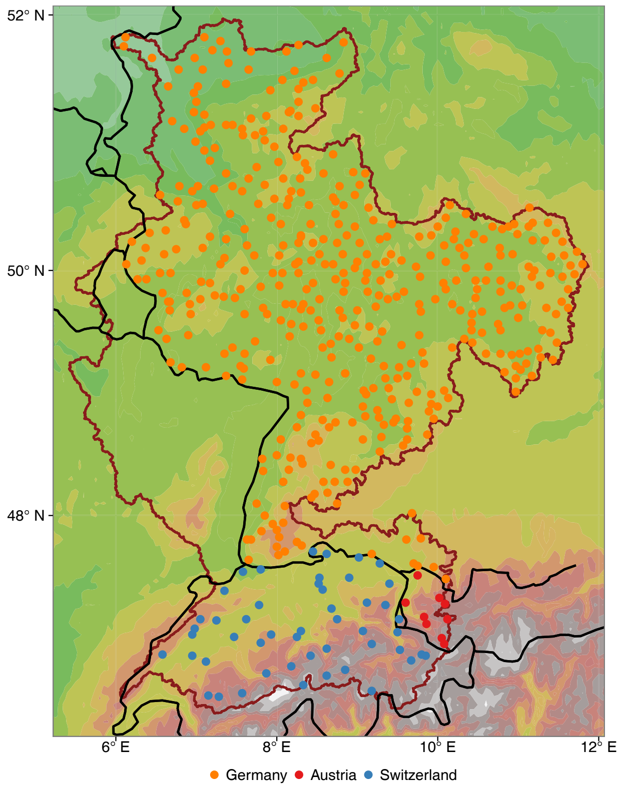

Figure 3.1: Locations of the climate data stations used. See text for more details on single data sets. The dark red line shows the Rhine catchment; the black lines denote state borders.

Table 3.1: Overview of GCMs used (`http://esgf-data.dkrz.de/`).

Model	Institute ID	Country	Period	Resolution Lon × Lat	Runs
BCC-CSM1.1	BCC	China	1850–2012	2.8 × 2.8	3
BNU-ESM	GCESS	China	1950–2005	2.8 × 2.8	1
CanESM2	CCCMA	Canada	1850–2005	2.8 × 2.8	5
CESM1-CAM5	NSF-DOE-NCAR	USA	1850–2005	1.2 × 0.9	1
CNRM-CM5	CNRM-CERFACS	France	1850–2005	1.4 × 1.4	10
CSIRO-Mk3.6.0	CSIRO-QCCCE	Australia	1850–2005	1.9 × 1.9	10
GFDL-CM3	NOAA-GFDL	USA	1860–2005	2.5 × 2.0	3
GFDL-ESM2 M	NOAA-GFDL	USA	1861–2005	2.5 × 2.0	1
HadGEM2-ES	MOHC	UK	1859–2005	1.9 × 1.2	4
IPSL-CM5A-LR	IPSL	France	1850–2005	3.8 × 1.9	6
IPSL-CM5A-MR	IPSL	France	1850–2005	2.5 × 1.3	3
MIROC-ESM	MIROC	Japan	1850–2005	2.8 × 2.8	3
MIROC-ESM-CHEM	MIROC	Japan	1850–2005	2.8 × 2.8	1
MRI-CGCM3	MRI	Japan	1850–2005	1.1 × 1.1	5
NorESM1-M	NCC	Norway	1850–2005	2.5 × 1.9	3

3.3 Methods

3.3.1 Weather pattern classification

Within COST Action 733 “Harmonisation and Applications of Weather Type Classifications of European Regions” a collection of circulation-type classification approaches was compiled and made available (COST733CLASS software: `http://cost733.geo.uni-augsburg.de/cost733class-1.2/`, Philipp et al., 2016). Included, among others, is the SANDRA classification method (simulated annealing and diversified randomization), which is “a non-hierarchical technique for minimizing the sum of Euclidean Distances within the classes” (Philipp, 2009). The method is similar to k-means clustering, but is able to get closer to the global optimum instead of getting trapped in a local one. A detailed description of the method can be found in Philipp et al. (2007). Several studies found a good or even superior performance of SANDRA compared to other classification methods (e.g. Beck and Philipp, 2010; Huth, 2010; Huth et al., 2008; Philipp et al., 2007; Philipp, 2009; Philipp et al., 2016).

Methods for assigning new data to an already existing classification are also available in the COST733CLASS software. This was used to apply the selected classification to GCM data. The method takes data of the same spatial domain and resolution and compares every case, i.e. day, to the centroids of the existing classification. The class with the smallest Euclidean distance to the respective case is assigned. In this way a catalogue (i.e. time series) of weather patterns can be obtained for every GCM data set, which can then be analysed and compared to the catalogue derived from reanalysis data (see subsection 3.4.2). Since the GCMs do not necessarily have the same spatial resolution as the classification input, they were first linearly re-interpolated to the same grid as the ERA-20C data.

By employing a weather pattern classification we are aiming towards providing a stratification of observed weather variables such as precipitation, temperature, relative humidity, and solar radiation (as required for the hydrological model). For use with the weather generator, it is desirable to obtain a classification that provides patterns that are preferably as distinct as possible from each other in terms of local weather characteristics. To derive an optimal classification, different characteristic variables, e.g. msl, geopotential height, temperature, humidity, different spatial domains, and different numbers of weather-type classes, can be tested. Historically, the first classifications were based on sea level pressure. An improvement of classifications and variable stratification can be achieved by additionally considering geopotential height (Nied et al., 2014; Spekat et al., 2010). Given the further aim of this classification to be used for downscaling of historical runs of CMIP5 models, geopotential height is available only in a few runs and is thus excluded from our consideration.

Note that the term “weather (pattern) classification” is used to contrast the difference to air mass classifications, since surface weather variables are used here instead of variables defined at different tropospheric levels (Huth et al., 2008).

3.3.2 Finding optimal classification parameters

Here we tested different combinations of variables for weather-type classification. Classifications on mean sea level pressure (msl) are commonly applied (e.g. Masson and Frei, 2014; Philipp, 2009; Wilby and Quinn, 2013). Other frequently used variables include geopotential height of different levels, thickness between different levels, vorticity and temperature at certain levels, or total column water vapour (e.g. Anagnostopoulou et al., 2008; Bárdossy et al., 2002; Nied et al., 2014; Philipp et al., 2016). However, our selection was restricted to variables that are also available from the GCM outputs. Goodess and Jones (2002) state that temperature and humidity are the two most important variables to be included when using a circulation-type approach for downscaling of rainfall. Thus we included temperature in 2 m (temp) (used, among other variables, in e.g. Kalkstein et al., 1987) and specific humidity (hus, as e.g. in Hewitson and Crane, 2006). This led to four combinations of variables: msl, temp, msl + temp, and msl + temp + hus.

Different options for the selection of a spatial domain were tested here: one covering the whole of Europe, others being considerably smaller, and partly focussing on the Rhine catchment; see Figure 3.2. One domain is identical to domain D07 in Philipp et al. (2010);

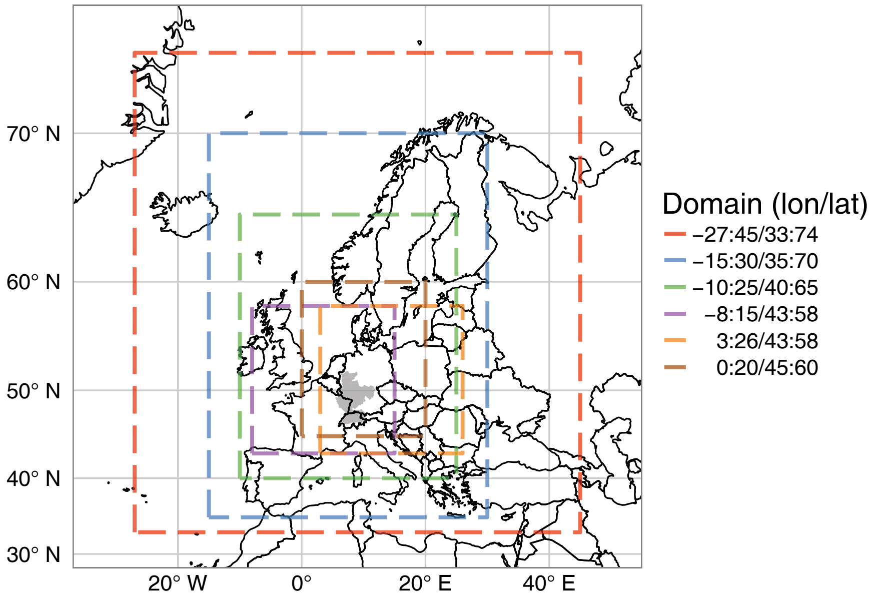

Figure 3.2: Spatial domains of weather pattern classifications in degree of geographic longitude/latitude. The dark grey polygon shows the location of the Rhine catchment. Domain 3 : 26 / 43 : 58 as in Philipp et al. (2010), region D07; −15 : 30 / 35 : 70 as in Nied et al. (2014).

another one is a westward shifted version of it. The domain from Nied et al. (2014) was included as well.

A wide range of numbers of classes was tested to assess the power of classification: 9, 18, 27 (all frequently used, e.g. in Huth et al., 2016; Philipp et al., 2010), and 40 (as in Bissolli and Dittmann, 2001; Nied et al., 2014; Philipp, 2009). Many authors (e.g. Huth, 2010) consider 40 already a very large number, but e.g. Jones and Lister (2009) use 6–11 patterns per season in a total of 34. Thus, when establishing a classification for the whole year, a greater number of classes can be useful.

These different parameter sets allow for 120 possible combinations, which poses an intractable computational problem. To break this number down in a reasonable way that still yields reliable results, firstly, some parameter values were prioritized (domains (long/lat in degrees) −27 : 45 / 33 : 74 and −8 : 15 / 43 : 58, 18 and 40 classes). Secondly, four classification variables were combined with four prioritized parameters and the best-performing variable (combination) was selected. This variable was then combined with all spatial domains finding the optimal one. Finally, all numbers of classes were evaluated with the best variable and domain. This reduces the number of combinations to 26, which is still a rather large computational effort.

3.3.3 Evaluation of classifications

First of all it has to be clear whether the classification itself should be evaluated (i.e. stratification of the input variables, such as msl) or whether the stratification of other variables, such as precipitation, that were observed on days with certain weather patterns, should be evaluated based on the developed classification. The latter is needed here. Hence, given a certain classification catalogue, data from weather stations can be assigned to the patterns that occurred on the same day, resulting in a distribution of values associated with each pattern. The distribution of values linked to a pattern can then be compared to the original (complete) population of values.

The quality of a given classification can be evaluated using different statistical metrics. For example, Huth et al. (2008) and Beck and Philipp (2010) give various quality measures, among them the explained variation (EV) and the so-called Pseudo-F statistic (PF). These are chosen because EV is frequently used in similar applications and is easily understood, while PF has the advantage of considering the number of classes and cases per class.

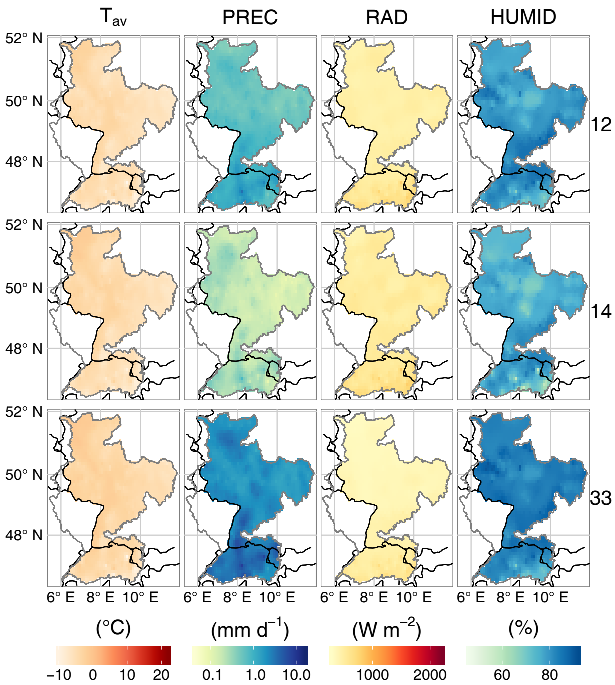

Figure 3.3: Average daily values of meteorological variables for example patterns 12, 14, and 33 to emphasize the need for multi-variate evaluation of weather pattern classifications (T_{av} – average temperature; PREC – precipitation; RAD – global radiation; HUMID – relative humidity). The black lines show state borders; the grey outline denotes the Rhine catchment.

The explained variation (Equation 3.1) is defined as the ratio of the sum of squared deviations from the mean within classes (WSS) and the total sum of squared deviations from the overall mean (TSS). In Equation 3.3 and Equation 3.4 k denotes the number of classes (i.e. patterns), m is the number of dimensions (i.e. variables), n is the number of cases (i.e. days), and C_j denotes class/pattern j. Thus EV ranges between zero (poor) and one (perfect stratification).

The Pseudo-F statistic (PF, Equation 3.2) of Caliński and Harabasz (1974) is the ratio between the sum of squared deviations between means of classes (BSS, Equation 3.5) and the sum of squared deviations within classes (WSS, Equation 3.4), weighted by the number of classes and cases. A minimum of within-type variation (and a maximum of distinction between types/classes) is achieved by large values of PF; poor clustering is denoted by values close to zero.

Both indices are usually applied to one meteorological variable at a time, thus evaluating the skill of the classification in stratifying e.g. temperature or precipitation (Huth et al., 2016). When mapping each variable per weather pattern, it becomes evident that some patterns might be very similar with regards to one (or more) variable(s), while being substantially different in other variables. For example in Figure 3.3, the selected pattern nos. 12, 14, and 33 have a very similar mean temperature for the whole area but very different precipitation. A classification focussing only on one variable would neglect the variability of the others. We therefore evaluate the stratification with respect to both single- and multi-variate performance.

Each evaluation metric is applied to normalized climate data, derived separately for each station and aggregated as an area-weighted average over the complete Rhine catchment.

$$\mathrm{EV} = 1 - \frac{\mathrm{WSS}}{\mathrm{TSS}} = \frac{\mathrm{BSS}}{\mathrm{TSS}} \tag{3.1}$$

$$\mathrm{PF} = \frac{\mathrm{BSS}/(k-1)}{\mathrm{WSS}/(n-1)} \tag{3.2}$$

$$\mathrm{TSS} = \sum_{i=1}^{n}\sum_{l=1}^{m}(x_{il} - \bar{x}_l)^2 \tag{3.3}$$

$$\mathrm{WSS} = \sum_{j=1}^{k}\sum_{i\in C_j}\sum_{l=1}^{m}(x_{il} - \bar{x}_{jl})^2 \tag{3.4}$$

$$\mathrm{BSS} = \sum_{j=1}^{k} n_j \sum_{l=1}^{m}(\bar{x}_{jl} - \bar{x}_l)^2 \tag{3.5}$$

3.4 Results

3.4.1 Stratification of local climate variables

Selection of classification variables

To select the classification variables, both evaluation metrics (EV and PF) point to the same choice (see Figure 3.4). The multi-variate evaluation clearly suggests a classification including temperature (EV around 0.5). This preference is even stronger for single-variate evaluations of temperature (T_{av}, T_{min}, T_{max}), with explained variation (EV) around 0.75. For precipitation (PREC) the temp-only classification performs worst, though EV values are low for all classifications (EV $<$ 0.2). From the literature there is no evidence that other studies acquire considerably better results in similar analyses, but surprisingly the exact values of their evaluation criteria are typically not given. Nevertheless this low skill needs to be discussed further (see also section 3.4.1 and 3.5). Any classification including msl improves the stratification of precipitation compared to the classification based on temperature only. Thus a classification including both temperature and mean sea level pressure should be chosen to obtain a reasonably good stratification of all variables.

For relative humidity (HUMID) and global radiation (RAD) the same relation between classifications as for temperature was found (classification including temp better than msl only), although the differences between classifications for HUMID are small. Including specific humidity as a classification variable slightly improves the stratification of all variables. Thus the classification on msl + temp + hus was finally selected. This selection holds the additional advantage of a strong seasonal restriction of pattern occurrence. While patterns from an msl-only classification show only weak seasonality (i.e. each pattern might occur in any month throughout the year), the use of raw values (i.e. no anomalies) of temperature and specific humidity confines each pattern to a specific season with a clear peak of occurrence in a certain month. This allows us to use one classification for the whole year instead of using separate classifications for each season, as is frequently done in other studies.

For both metrics and all meteorological variables the smaller spatial domains deliver better results (Figure 3.5). The three smallest domains (coloured in purple, orange, and yellow) differ only in their exact location, but are of roughly the same size. The orange domain gives slightly better results for all variables and was chosen for further analysis.

The choice of an optimal number of classes is less obvious (Figure 3.5). The analysis of the EV shows a slight tendency towards a greater number of classes, whereas PF prefers a lower number. However, for the use with a weather generator, a high number of classes with consequently narrow distributions for each class are preferred. At the same time a sufficient amount of observations per class are needed for fitting the distributions. Considering this tradeoff, a classification with 40 classes was selected here.

Average values of meteorological variables per pattern of the final classification are shown in Appendix 3.A, Figure 3.A1–3.A6.

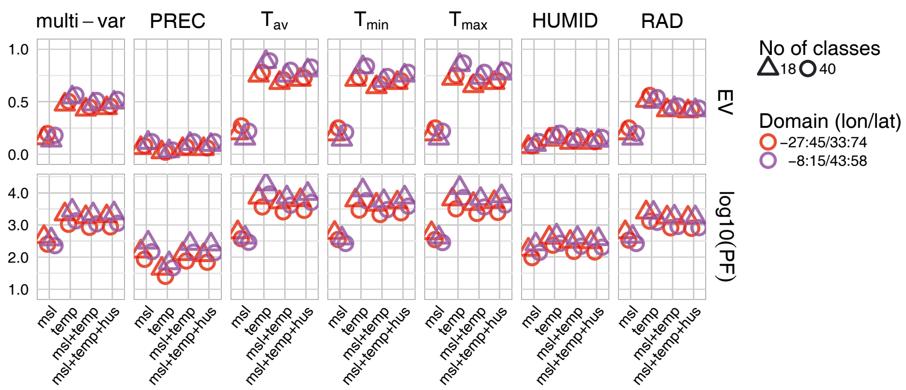

Figure 3.4: Evaluation metrics for the selection of classification variables (*x* axis). Weather variables from station data in columns. Note the log scaling of PF.

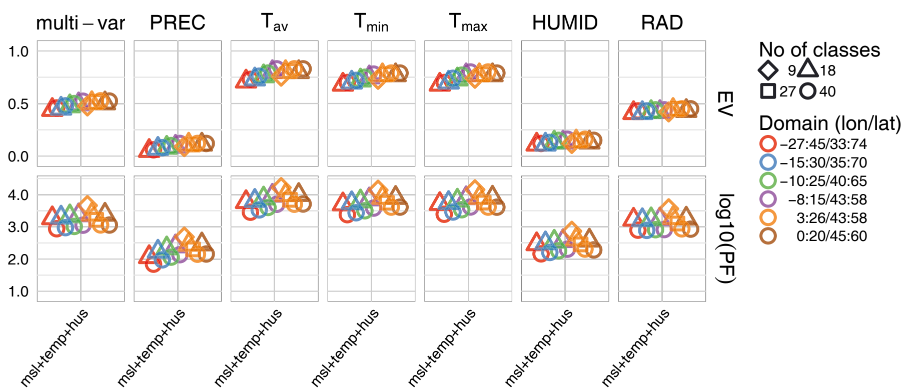

Figure 3.5: Evaluation metrics for the chosen classification variables, combining results of selection steps 2 and 3. It aims at selecting (a) the best spatial domain (colour scale), and then (b) selecting the best number of classes (point shapes).

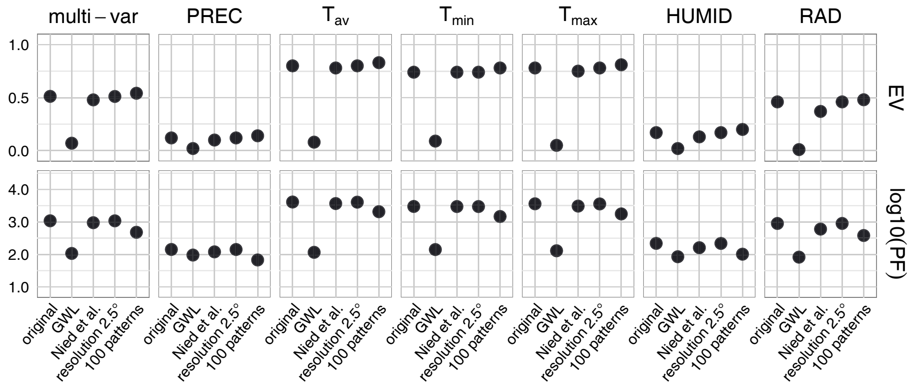

Figure 3.6: Comparison of selected classification from section 3.4.1 (original) and other classifications: Hess–Brezowsky Grosswetterlagen (GWL), classification variables as in Nied et al. (2014), a classification on a coarse grid, and one with 100 classes.

Comparison to other classifications

The selected classification was compared with the Hess–Brezowsky Grosswetterlagen (GWL) catalogue of circulation patterns, to the classification after Nied et al. (2014), and to two experiments where only one parameter of the selected classification was modified (Figure 3.6): a classification based on a coarse grid ($2.5° \times 2.5°$ instead of $1° \times 1°$), and one using 100 classes (as in Perez et al., 2014). A comparison to the well-established Hess–Brezowsky Grosswetterlagen (applied in e.g. Fleig et al., 2015; Kyselý, 2007) shows that GWL is inferior to our classification, with EV values not exceeding 0.1. The stratification skill obtained by GWL is best comparable to a classification based on msl only, but is inferior when including other variables in the classification scheme. The classification based on 500 hPa geopotential height, 500 hPa temperature, and total column water vapour as used by Nied et al. (2014) performs equally well as the selected classification with only slightly lower skill values.

ERA-20C data were originally used with $1° \times 1°$ resolution. A coarser resolution of $2.5° \times 2.5°$ results in an identically good stratification. Hence small-scale features that might be present in a high-resolution reanalysis data set do not distort the results, which is also true for a classification extent covering all of Europe (not shown here).

A last test was dedicated to the number of patterns: 100 patterns as in Perez et al., 2014 were tested, confirming the general tendency (increasing EV, decreasing PF values for an increasing number of classes), although the improvement of EV seems to level off for a high number of classes, meaning that the gain in stratification skill is only minimal.

Stratification skill for precipitation

The stratification skill (i.e. EV and PF values) is rather low for precipitation, but maps of mean pattern precipitation (Figure 3.A2) indicate distinct precipitation patterns. Therefore a more detailed investigation of explained variance for individual patterns was done. EV can be expressed as the sum of EV values for individual patterns weighted by the respective relative frequency of the pattern (n_j/n)

$$\mathrm{EV} = \sum_{j=1}^{k} \frac{n_j}{n} \cdot \mathrm{EV}_j \text{ with} \tag{3.6}$$

$$\mathrm{EV}_j = \frac{(\bar{x}_j - \bar{x})^2}{\mathrm{TSS}/n}. \tag{3.7}$$

This allows one to analyse the contribution of each pattern to the overall EV value. Figure 3.7 shows the cumulated $\mathrm{EV_j}$ values of each pattern. In an idealized case where mean precipitation and frequency of occurrence are uniformly distributed among all types, Equation 3.6 describes (as an integral over a square) a cubic function with a saddle point at the overall mean precipita-

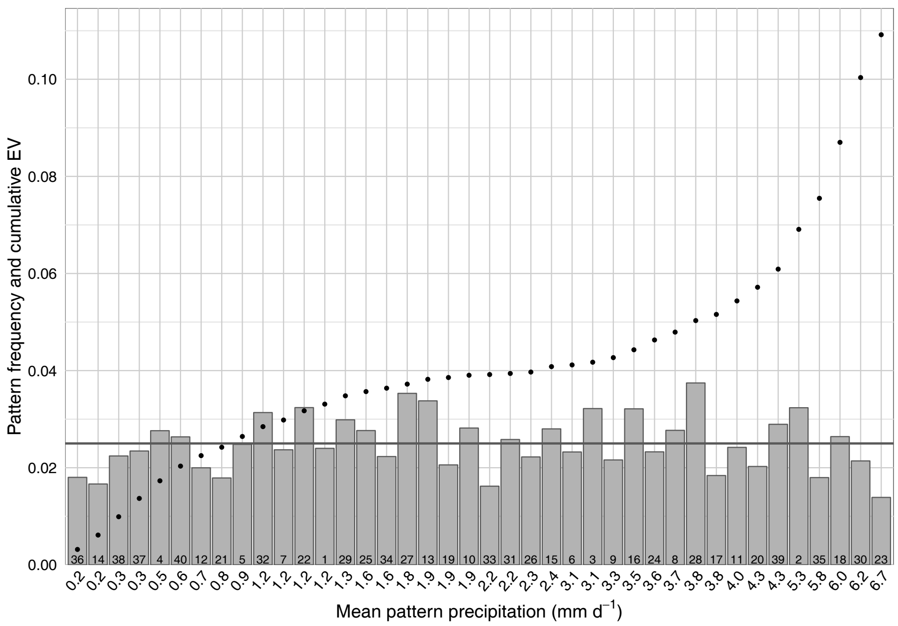

Figure 3.7: Precipitation intensity of patterns in relation to pattern frequency (bars) and cumulated explained variation per pattern (dots). The pattern number is given at the bottom of the bars. The grey horizontal line denotes the average frequency to aid distinction of rare and frequent patterns.

tion. Patterns associated with the tails of the distribution would contribute most to the overall EV, while average types have contributions close to zero (because their mean is close to the overall mean; thus, the deviation between both is small, resulting in near-zero EV_j).

However, in the case of precipitation, patterns with below-average mean precipitation contribute only little to the overall EV, because the overall mean is rather small (2.4 mm) and hence the deviation between the mean of low-precipitation patterns and the overall mean is small. This applies to more than half of all the patterns (24 out of 40). Most EV contribution is gained by patterns with very high precipitation – 50 % of total EV is contributed by the seven patterns with the highest precipitation. This behaviour clearly originates from the strongly right skewed distribution of precipitation. Thus, the small skill values can be considered inherent to precipitation.

Additionally, analysing precipitation frequency and intensity per pattern (not shown) reveals that the variations in Figure 3.A2 are mainly caused by pattern-specific precipitation frequency.

3.4.2 Performance of GCMs

After selecting the most appropriate classification, all GCMs (15 models with up to 10 runs for experiment All-Hist) were assigned to the centroids of the final classification, resulting in a catalogue (i.e. time series) of patterns for each GCM run. These time series were compared to the catalogue derived from the reanalysis data to assess the ability of GCMs to reproduce the weather pattern climatology in terms of frequency, seasonality, and persistence as suggested e.g. by Bárdossy et al. (2002). Seasonality is evaluated by the first, last, and peak months of pattern occurrence. All patterns show a distinct seasonality. Each season is characterized by a limited number of consecutive months in which a pattern occurs. We evaluate the beginning (i.e. first month) and end (i.e. last month) of pattern occurrence. The peak month is defined as the month with the highest number of days with pattern occurrence. Some patterns show two distinct seasons. In this case both seasons are evaluated separately. Results from different runs of each GCM are averaged.

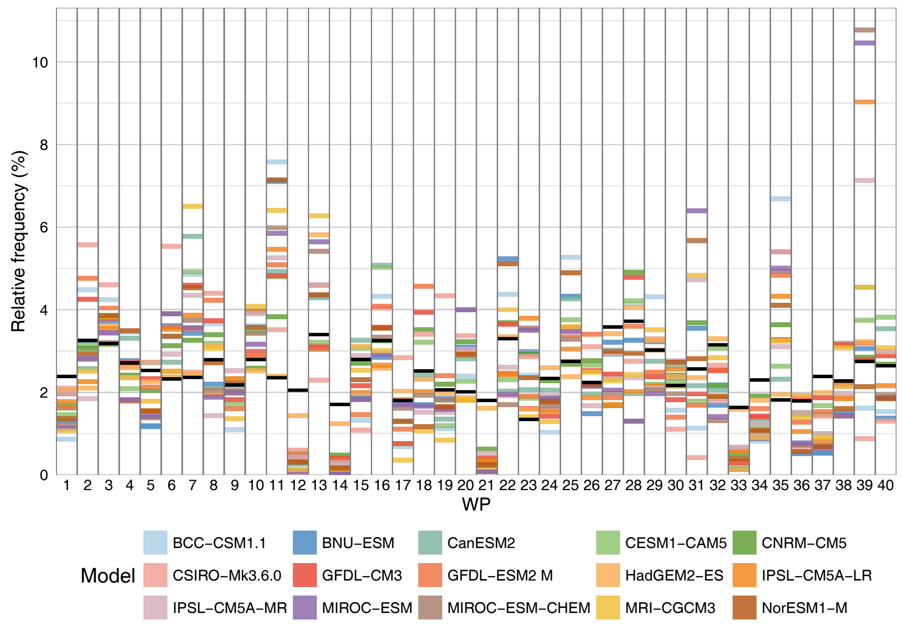

Figure 3.8: Relative frequency of patterns in GCMs (coloured dashes) compared to frequency in reanalysis data (black dashes).

Frequency of patterns

The frequency of patterns as obtained from each GCM run was compared to pattern frequencies in the reanalysis data (Figure 3.8). The time series are compared for the whole period, i.e. no separation by seasons or individual years was done. Especially for patterns with high mean daily precipitation, a good agreement between reanalysis and GCMs (All-Hist) would be desirable (maps of average daily values in the Appendix 3.A, Figure 3.A1–3.A6). Frequencies for different runs of one GCM were averaged, but differences between runs are much smaller (usually less than 0.5 %) than between GCMs. The deviations between reanalyses and GCM frequencies are highly diverse for different patterns, e.g. pattern 30 – a high-precipitation pattern with more than 6 mm per day on average (see Appendix 3.A, Figure 3.A2) – is well reproduced, while some GCMs have difficulties in matching e.g. patterns 11 or 39. No clear season-specific deviations were found – some models have higher deviations in winter, others in summer (not shown). For eight patterns all GCMs underestimate the frequency found in the reanalysis and for another seven patterns all GCMs overestimate the frequency. By having a closer look at this behaviour, it becomes apparent that particularly cold weather patterns (1, 12, 14, 21, 33, 34, 37) are underestimated, although the warm pattern 27 is also underestimated. Apparently, all GCMs have difficulties in reproducing these weather patterns. However, it goes beyond the scope of this paper to analyse the genesis of these weather patterns and why GCMs are not capable of capturing them well. With regards to the overestimated patterns (3, 6, 7, 11, 20, 23, 35), they show a tendency towards average to above-average precipitation, but other, high-precipitation patterns seem to be well captured. The remaining 25 patterns enclose the reanalysis values in their range. Among the models with an overall good performance in terms of frequency are CNRM-CM5, GFDL-CM3, and HadGEM2-ES, while the models BCC-CSM1.1, CCSM4, IPSL-CM5A-LR, MIROC-ESM, and MIROC-ESM-CHEM show the highest deviations from the reanalyses. In the work of Belleflamme et al., 2014, which uses a similar set of GCMs, three of these badly performing models were found to have the best rankings in reproducing pattern frequency (in summer), which shows that statements about GCM performance are somewhat dependent on the actual application and its geographic focus.

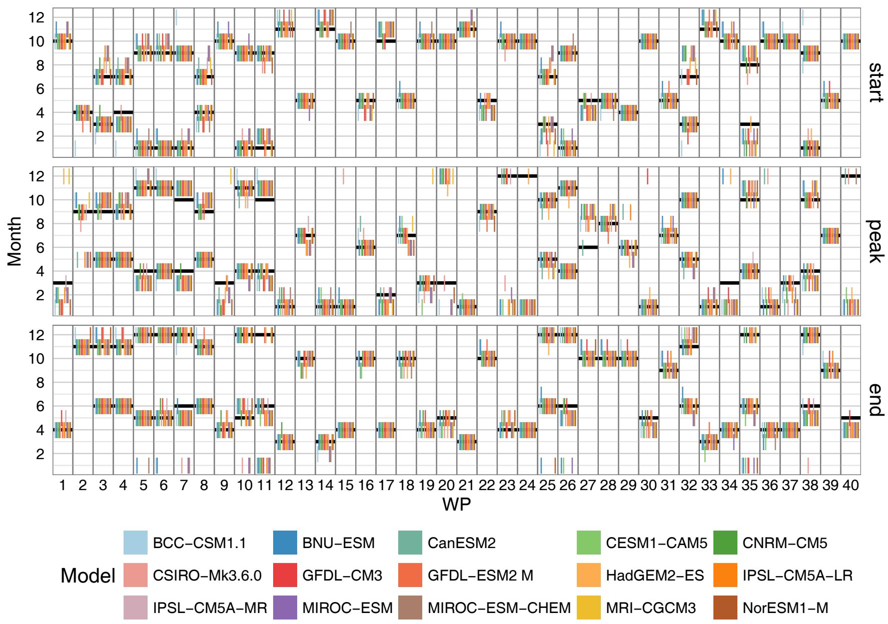

Figure 3.9: Comparison of seasonality of patterns in GCMs (coloured vertical dashes) and reanalysis data (black horizontal dashes). Seasonality is presented as start month(s) (upper panel), peak month(s) (middle panel), and end month(s) (lower panel) of occurrence of patterns. Dashes for GCMs are only vertical to avoid overlapping – each symbol denotes 1 distinct month. If a pattern occurs in two distinct seasons, both are shown.

Seasonality

The seasonality of patterns in terms of the earliest and last months of occurrence in the course of the year, and the most frequent month of occurrence, is generally well reproduced, even for patterns with two peaks (Figure 3.9). While start and end are often matched perfectly, the peak months deviate more often, but usually by not more than 1 or 2 months. A deviation of 1 month is considered an acceptably good performance. This good reproduction of pattern seasonality is certainly due to the use of variables with a strong seasonal cycle (temperature and specific humidity) for classification – near-surface temperature and its gradient between continent and sea give very season-specific patterns that are beneficial for the seasonal stratification of weather patterns.

Most GCMs are able to reproduce the correct start months in 16 to 34 patterns; the highest number of mismatched patterns (20 or more) are found in BCC-CSM1.1, BNU-ESM, MIROC-ESM, and MIROC-ESM-CHEM. The correct end months are reproduced in 18 to 32 patterns. Only one GCM with more than 20 mismatched patterns was found (BCC-CSM1.1), and 15 or more mismatches occurred in BNU-ESM and CESM1-CAM5. Models BCC-CSM1.1, BNU-ESM, IPSL-CM5A-LR, MIROC-ESM, MIROC-ESM-CHEM, and MRI-CGCM3 fail in more than half of all patterns to match the peak months. All GCMs are generally slightly better in capturing the correct start and end months of summer or winter patterns compared to spring/autumn patterns.

Persistence

Finally the persistence of patterns is assessed as the number of consecutive days with the same weather pattern. In Figure 3.10 the average duration in reanalysis data is compared to the duration in GCMs. The mean duration of patterns is mainly around 2 days, which is usually well represented by the GCMs. Deviations from the persistence of reanalysis data that are greater than 1 day were only found in very few patterns (14, 39); usually mean persistence deviates by less than 1 day.

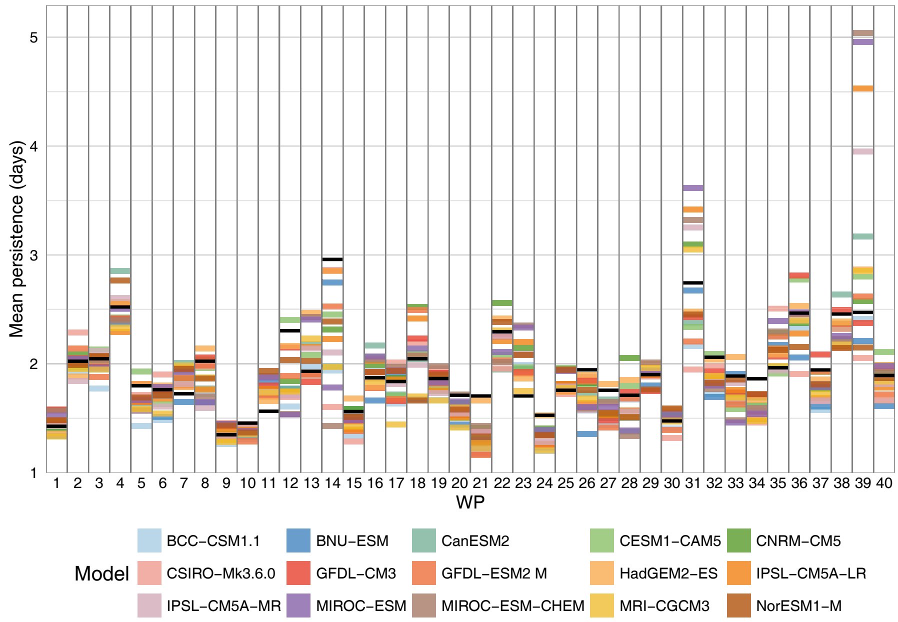

Figure 3.10: Persistence of patterns (mean number of consecutive days with the same pattern) in GCMs (coloured dashes) compared to persistence on reanalysis data (black dashes).

The best agreement between reanalyses and GCMs was found for CESM1-CAM5, CNRM-CM5, GFDL-CM3, and HadGEM2-ES, while the greatest deviations occurred for BCC-CSM1.1, CSIRO-Mk3.6.0, IPSL-CM5A-LR, MIROC-ESM, and MIROC-ESM-CHEM. There is no general difference in deviation from reanalysis for different seasons, though most GCMs match the persistence of spring or autumn patterns slightly better than the persistence of summer or winter patterns. Other studies found patterns to last longer than in our case (e.g. Kyselý, 2007, who found a mean persistence for Hess–Brezowsky Grosswetterlagen of 4.3–5.2 (and up to 6.2) days), which might be due to our comparatively large number of patterns.

3.5 Discussion

3.5.1 On the optimal classification

This study derives an “optimal” weather pattern classification for the Rhine catchment and investigates to which extent weather patterns are able to stratify local climate variables. Furthermore, the ability of the latest GCM generation to reproduce these weather patterns is evaluated in terms of frequency, seasonality, and persistence. The particularities of this study, compared to past studies on weather pattern classifications, include (1) the investigation of the skill of several classification variables, (2) the large number of local weather variables used for classification evaluation, (3) the large study area (160 000 km^2) and the very high number of climate stations (490), and (4) the use of long time series (111 years).

It has been argued that there is no “best” classification and that the optimal solution depends on the specific application and region. The best classification for the Rhine catchment was achieved with a combination of mean sea level pressure, temperature, and specific humidity as classification variables. Often, weather patterns are classified on pressure fields only. Our results suggest that adding humidity and temperature, which exhibit a distinct seasonal cycle, as classification variables improves the stratification of local climate variables considerably and support the findings of Goodess and Jones (2002). Including temperature as a classification variable yields a very good stratification of weather patterns throughout the year, i.e. weather patterns also show a distinct seasonality. In this way a single classification can be used for the whole year, and there is no need to provide different classifications for each season separately, contrary to classifications based solely on mean sea level pressure.

Concerning the number of classes, our results do not give a clear indication about the optimal number. We have selected a comparatively large number, i.e. 40 patterns. This selection is in line with other studies that compared classifications. Philipp (2009) found for SANDRA classifications that best skills are reached for class numbers greater than 30. Tveito (2010) compared 73 classifications from the COST733 collection of classifications catalogues and found the best performances for high numbers of classes; generally for the same classification method a solution with more types performed better. The 10 best classifications had at least 26 classes and the best 3 classifications had 30, 40, and 29 types, respectively. Of course, the decision about the number of classes is guided by the purpose of the classification and the data availability. The stratification of local climate variables into a large number of classes requires a sufficient amount of data. Our sensitivity analysis with 100 weather patterns clearly indicated worse performance compared to the classification based on 40 patterns, but in general, a larger number of classes is advisable if not limited by the amount of available data.

In terms of spatial domain, the best results are obtained for rather small classification areas covering the target area. Increasing the classification domain covering the whole of Europe slightly aggravates the stratification of local variables, particularly of temperature. It is however difficult to make generalizations with regards to the selection of the spatial domain given our results.

The "optimal" classification is only partially able to stratify local climate variables, i.e. the classification explains a modest share of the local climate variability. EV values, averaged across all 490 stations in the Rhine catchment, are in the range of 10–20 % for precipitation, 70–80 % for temperature, 10–20 % for humidity, and 40 % for radiation. Hence, especially local precipitation and humidity are governed by processes that are not completely represented by the large-scale distribution of pressure, temperature, and humidity. This result questions the widespread downscaling approaches that are based on weather pattern classification. The within-type variability dominates vs. the between-type variability, at least for local precipitation and humidity. Before applying the weather pattern based downscaling approach, one should therefore investigate whether the link between the large-scale synoptic situation and the local climate variable of interest is strong enough for the given purpose.

Although downscaling approaches based on weather patterns are widespread, there are not many studies that have assessed the skill of weather patterns for stratifying local climate variables. The available studies report skill values that are comparable to our results. For example, Osborn and Jones (2000) found large residuals between precipitation predicted from circulation indices and observed precipitation. Enke and Spekat (1997) obtained 20.5 % of explained variation for precipitation and 80.9 % for mean temperature. Huth et al. (2016) compared a large number of classifications from COST733 using different classification methods, numbers of patterns, spatial domains, classification variables, and sequence lengths of 1 or 4 days. For all domains and classification settings they obtained EV values of max. 0.33 for precipitation and max. 0.46 for mean temperature. The much higher values for temperature in our study can be explained by the use of 2 m temperature as an additional classification variable. Our classification using only sea level pressure obtains similarly low values. For those classifications that are best comparable to our study, i.e. method SANDRA, whole year, 1-day sequence, classification on sea level pressure, 9, 18, or 27 types, a comparable spatial domain, they obtain EV values of 0.07–0.28 for temperature and 0.08–0.27 for precipitation. These results are averages across all seasons, whereas the results for the winter are generally better. The study of Enke et al. (2005a) suggested that classifications that are highly optimized towards a certain local climate variable, such as precipitation, may have significantly better skill than classifications for several variables. However, highly optimized classifications have the disadvantage that their skill deteriorates when applied for other target variables.

Downscaling using the weather pattern approach is based on the assumption of a time-constant relationship between patterns and local climate variables. Instationarities in the relationship between weather types and local variables are a long-debated issue in downscaling (IPCC, 2007), and several studies indicated their presence (e.g. Beck et al., 2007; Haberlandt et al., 2015; Widmann and Schär, 1997). Those classifications were, however, based on sea level pressure only (Beck et al., 2007; Haberlandt et al., 2015) or additionally included geopotential height (Widmann and Schär, 1997). The addition of temperature and specific humidity might provide a better classification also in terms of capturing transient changes in local climate by changes in weather pattern sequencing. This suggestion is supported by the regional climate simulations of Schär et al., 1996. For the European Alps, they found that increased warming can lead to larger moisture fluxes and larger precipitation rates even when the synoptic situation remains unchanged. Thus, it should be further investigated whether classifications that are based on additional variables besides pressure fields show less instationarity in the link between synoptic situation and local climate.

3.5.2 On the skill of GCMs

Concerning the skill of the latest generation of GCMs in reproducing these weather patterns, we find that the main characteristics of weather patterns derived from ERA-20C reanalysis data are well represented in GCMs that are forced with observed GHG concentrations. Interestingly, the performance of GCMs is usually similar for a certain GCM for the analysed characteristics, i.e. frequency, seasonality, or persistence of patterns. This result suggests that some GCMs are much better suited for downscaling based on weather pattern classifications. Others should be excluded or their results should at least be interpreted with the greatest care. From the results obtained, it would be advisable not to consider the models BCC-CSM1.1, MIROC-ESM, and MIROC-ESM-CHEM. This would leave 12 GCMs with acceptable performance. However, it should be noted that the skill of GCMs may depend on the specific classification, i.e. the classification variables and the region. Other classifications might result in a different ranking of GCMs.

3.6 Conclusions

In the scope of an attribution study aimed at quantifying the role of climate change, in particular the contribution of anthropogenic climate change to changes in flood flows in the Rhine catchment, we developed a weather pattern classification. This classification is intended to be used for downscaling of general circulation model outputs with a multi-site, multi-variate weather generator. An optimal classification was selected by evaluating four different combinations of classification variables based on the ERA-20C reanalysis data, by testing six spatial domains and four numbers of classes. The best stratification of local variables (daily precipitation, humidity, radiation, and mean, minimum, and maximum temperature) was obtained when using 40 classes from the SANDRA classification, with sea level pressure, temperature, and specific humidity combined over a relatively small central European domain. The performance of different classifications was assessed with explained variation (EV) and Pseudo-F statistic. The optimal classification showed rather high EV (similar to the Pseudo-F statistic) for single variables except precipitation and humidity. A multi-variate evaluation demonstrates that the classification is reasonable, although single variables are not very well stratified. Different weather patterns can be similar in one variable (e.g. temperature), but exhibit very distinct behaviour in others (e.g. precipitation). Often, weather patterns are classified on pressure fields only. Our results suggest that adding humidity and temperature as classification variables improves the stratification considerably. This results in a very good stratification of weather patterns throughout the year. In this way a single classification can be used for the whole year, and there is no need to provide different classifications for each season. Adding further classification variables to pressure fields may also alleviate the often encountered problem that the link between the synoptic situation and the local climate is not constant in time.

GCMs should properly reproduce the climatology of weather patterns in order to be applicable for the attribution of flood changes. Hence, the performance of 15 GCMs from the CMIP5 project in matching the climatology of ERA-20C reanalysis in terms of frequency, seasonality (month of occurrence), and persistence (number of consecutive days) of weather patterns was evaluated. The frequency of weather patterns is matched well by the majority of GCMs, with a few GCMs showing systematic deviations. No season-specific deviations were found. Due to the use of temperature for pattern classification, the seasonality of weather patterns matched well in most of the GCMs. All GCMs were found to be able to better capture the seasonality of summer and winter patterns compared to spring and autumn ones. The mean duration of patterns was about 2 days, with most GCMs being able to reproduce this persistence. Overall, three GCMs, BCC-CSM1.1, MIROC-ESM, and MIROC-ESM-CHEM, were found to systematically deviate from the reanalysis weather pattern climatology. The variation between different realizations of one GCM was found to be small compared to the difference between various GCMs.

3.7 Data availability

CMIP5 data can be accessed via e.g. the esgf-data.dkrz.de node or any other node listed at `http://cmip-pcmdi.llnl.gov/cmip5/`. The following search criteria are needed to obtain our data set: project “CMIP5”, experiment family “Historical”, experiment “historical” and “historicalNat”, time frequency “day”, variable “huss”, “psl”, and “tas”. More information on the models used is given in Table 1. ERA-20C data are available from `http://apps.ecmwf.int/datasets/data/era20c-daily/`; level: surface; date: 1900-01-01 to 2010-12-31; time: all available; parameter: “2 metre temperature”, “Mean sea level pressure”; from Level 91: “Specific humidity”. The climate station data are owned by PIK and are not publicly accessible. A detailed description of the data processing method is given in Österle et al. (2006).

Author contribution

All authors contributed to the experiment design and the paper. A. Murawski performed the computations and created the figures.

Acknowledgements

We acknowledge the World Clim. Res. Programme’s Working Group on Coupled Modelling, which is responsible for CMIP, and we thank the climate modelling groups (listed in Table 3.1 of this paper) for producing and making available their model output. For CMIP the US Department of Energy’s Program for Climate Model Diagnosis and Intercomparison provides coordinating support and led development of software infrastructure in partnership with the Global Organization for Earth System Science Portals (from `http://cmip-pcmdi.llnl.gov/cmip5/citation.html`).

The ECMWF ERA-20C Reanalysis data used in this study were obtained from the ECMWF Data Server (`http://www.ecmwf.int`).

We gratefully appreciate the provision of data by the national meteorological services of Germany, Austria, and Switzerland, kindly provided and processed by the Potsdam Institute for Climate Impact Research (PIK).

Help and discussion on the COST733CLASS classification software by Dr. Tobias Pardowitz (FU Berlin) is greatly appreciated.

A. Murawski acknowledges funding by Climate KIC.

The article processing charges for this open-access publication were covered by a Research Centre of the Helmholtz Association.

Edited by: H. Cloke

Reviewed by: two anonymous referees

3.A Appendix

Maps of meteorological mean values for each pattern

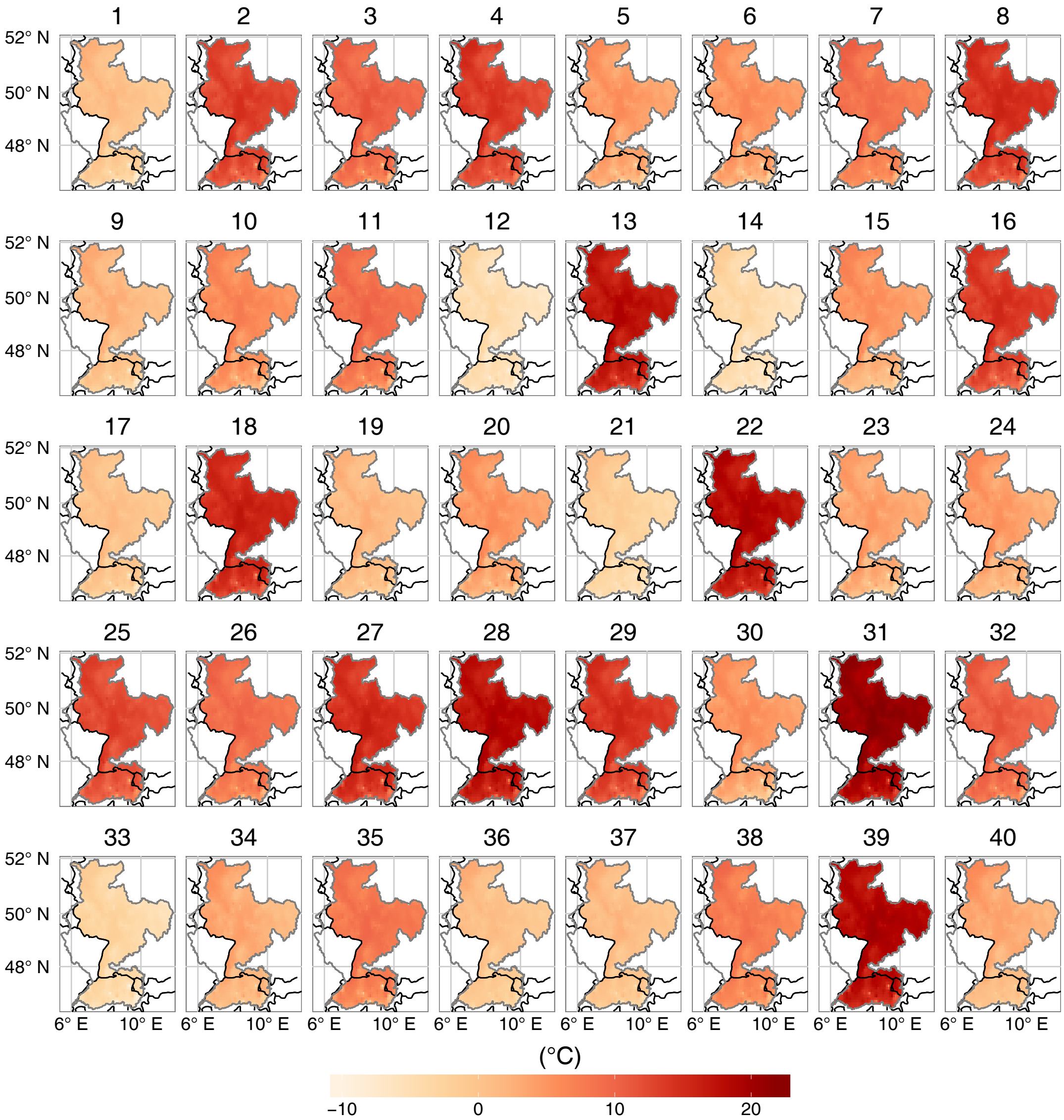

Figure 3.A1: Average (over all days with the respective pattern) mean temperature for all weather patterns. Black lines denote state borders, the grey line the Rhine catchment.

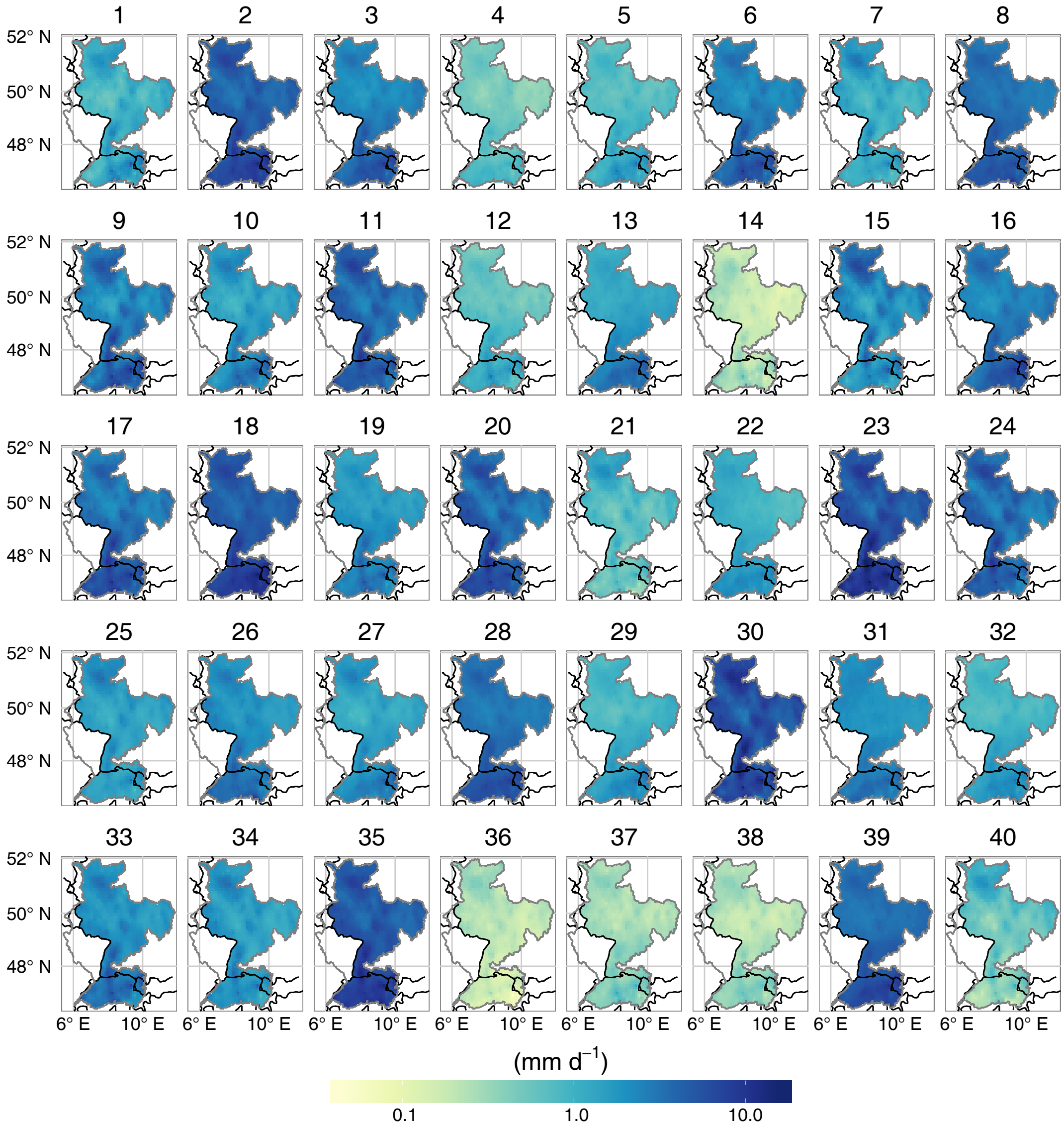

Figure 3.A2: As in Figure 3.A1 but for daily precipitation.

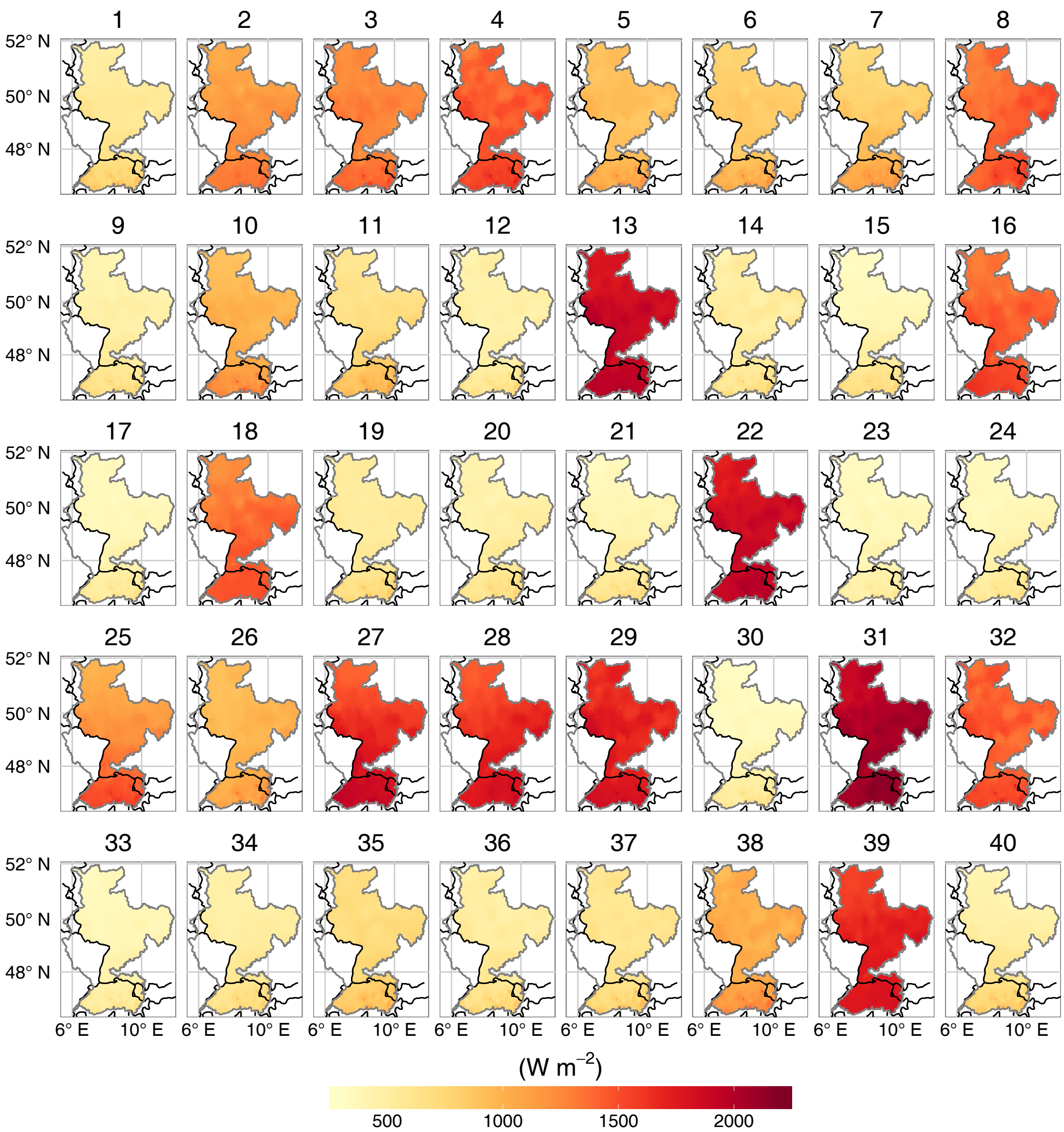

Figure 3.A3: As in Figure 3.A1 but for global radiation.

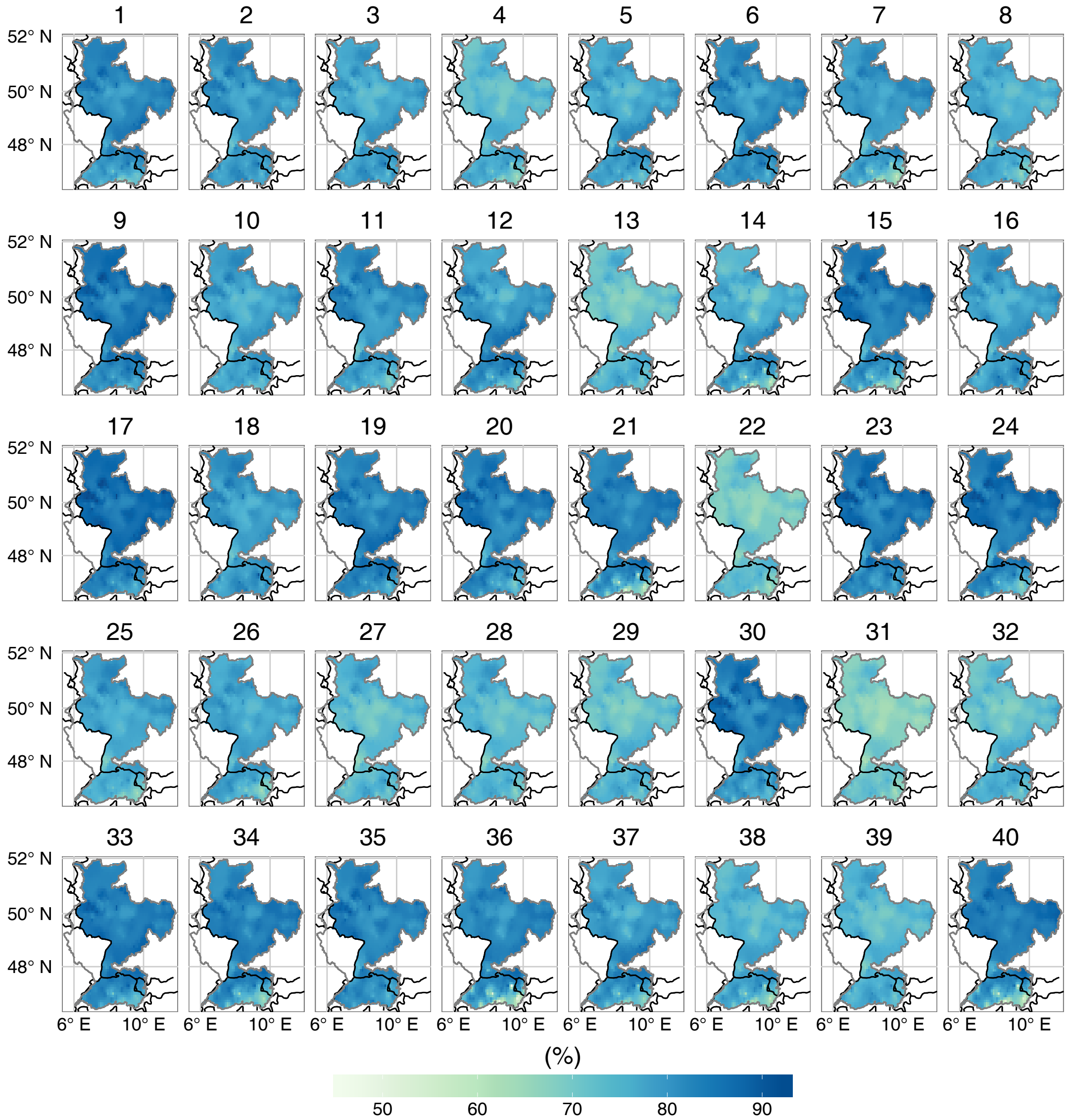

Figure 3.A4: As in Figure 3.A1 but for relative humidity.

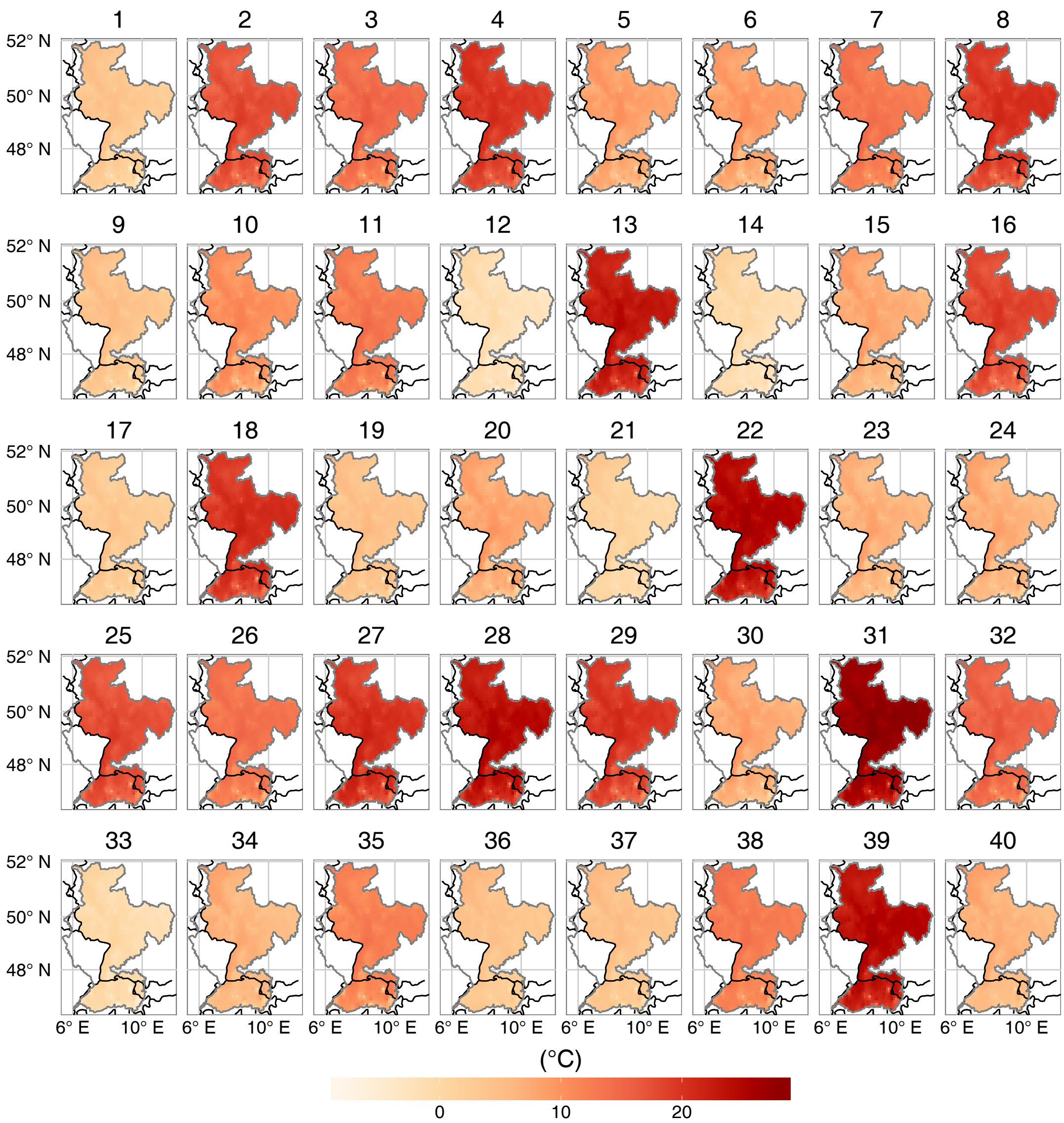

Figure 3.A5: As in Figure 3.A1 but for daily maximum temperature.

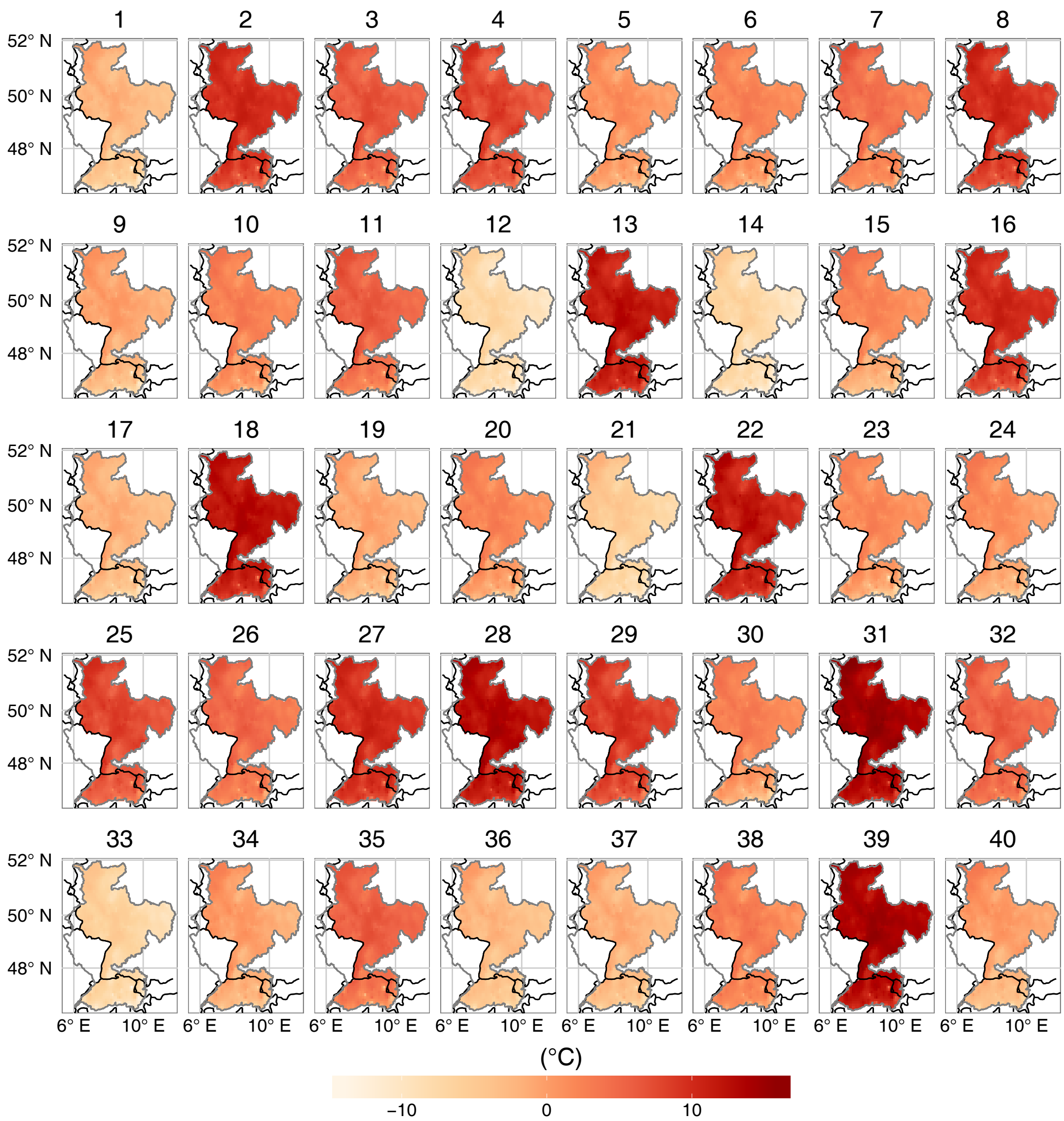

Figure 3.A6: As in Figure 3.A1 but for daily minimum temperature.

4. Do changing weather types explain observed climatic trends in the Rhine basin? An analysis of within and between-type changes

Abstract

For attributing hydrological changes to anthropogenic climate change, catchment models are driven by climate model output. A widespread approach to bridge the spatial gap between global climate and hydrological catchment models is to use a weather generator conditioned on weather patterns (WPs). This approach assumes that changes in local climate are characterized by between-type changes of patterns. In the presented study we test this assumption by analyzing a previously developed "optimal" WP classification for the Rhine basin. We quantify changes in pattern characteristics and associated climatic properties. The amount of between- and within-type changes is investigated by comparing observed trends to circulation-induced trends. To overcome uncertainties in trend detection resulting from the selected time period, all possible periods in 1901–2010 with a minimum length of 31 years are analyzed. Increasing frequency is found for some patterns associated with high precipitation, although the trend sign highly depends on the considered period. Trends and interannual variations of WP frequencies are related to the long-term variability of large-scale circulation modes, particularly the Scandinavian and the East-Atlantic/Western-Russia patterns. Long-term WP internal warming is evident for summer patterns and enhanced warming for spring/autumn patterns since the 1970s. Observed trends in temperature (and to a certain amount in precipitation) for recent decades are mainly attributed to frequency changes of specific WPs, but some amount of within-type changes remains. This restriction has to be kept in mind when using a weather-pattern/weather-generator approach for downscaling of climate fields for usage in hydrological attribution studies.

Keypoints

- large (490 stations) and long (111 years) data set for Rhine catchment
- testing fundamental assumption for weather pattern based downscaling using multiple periods
- changes in temperature and precipitation are mainly attributable to changes in the occurrence of patterns

Submitted as (current status "minor revision"):

Murawski, A., Vorogushyn, S., Bürger, G., Gerlitz, L., and Merz, B. (in review). "Do changing weather types explain observed climatic trends in the Rhine basin? An analysis of within and between-type changes". In: *Journal of Geophysical Research: Atmospheres*

4.1 Introduction

Understanding how hydrological change is linked to human-induced climate change is important for water resources management and climate adaptation. Various studies investigate the variability and change of hydrologically relevant climate variables for Central Europe. Specific regional scale weather patterns (WPs) or large-scale circulation modes have been found to be related with hydro-meteorological extremes, see e.g. Steirou et al. (2017) for a review. However, the length of observational time series (mostly below 100 years) is often insufficient to investigate the statistical relationships between climatic conditions and rare flood events. A widespread approach to link hydrological extremes to variations of the large-scale circulation is to force spatially distributed hydrological models at the catchment scale with the output from global climate models. To bridge the spatial gap between coarse global climate models and catchment models, numerous downscaling approaches have been developed, see e.g. Maraun et al. (2010) for a review. In particular, the approach of conditioning a weather generator (WGN) by means of climate model output data offers the possibility to generate very long ($\geq$ 10,000 years) synthetic time series at several locations considering the spatial correlation structure of meteorological variables (Elshamy et al., 2006; Fatichi et al., 2011; Fowler et al., 2000, 2005; Hewitson and Crane, 2006; Kilsby et al., 2007; Kim et al., 2016; te Linde et al., 2010; Lu et al., 2015; Steinschneider and Brown, 2013). This approach is particularly suitable for a robust estimation of changes in floods since their statistical moments can be better captured using very long time series of climate time series.

Weather generators produce sequences of stationary weather. Hence, to be useful for climate change impact investigation they need to be conditioned on large-scale climate fields as simulated e.g. by climate models. A natural way to do this is to decompose the large-scale variability into a discrete and finite set of dominant weather types, within which the weather is considered stationary. This can be done subjectively by inspecting synoptic weather charts (“Großwetterlagen”) (e.g. Brezowsky and Hess, 1952) or objectively by using automated statistical tools such as clustering.

Recently an optimal weather classification comprising 40 classes has been developed and validated for the Rhine catchment in Murawski et al. (2016a). This classification is based on the ERA-20C data for sea level pressure, near-surface temperature and specific humidity and utilizes the state-of-the-art SANDRA algorithm (Philipp et al., 2007; Philipp, 2009). In order to utilize a weather pattern classification for downscaling applications, a robust statistical relationship between WPs and local scale observations is required, i.e. the variance explained by the clustering (or rather the fraction of local between-type variance) should be substantial. If that fraction is large enough, local variability is believed to be sufficiently conditioned on the large-scale climate fields. To be applied to simulated climate fields, however, two more conditions are required to hold: i) the climate models reliably simulate the statistics of the weather types; and ii) the link between the weather types and the local weather remains valid.

The ability of the classification to stratify local climate variables (such as temperature and precipitation) has been proven in Murawski et al. (2016a). We found the majority of CMIP5 GCMs (Taylor et al., 2012) to be capable of reproducing the WP climatology of the ERA-20C reanalysis data. In this follow-up paper we tackle the last point, ii), about the stability of the link between weather types and local variables that is required to drive a hydrological model. Therefore we conduct a systematic analysis of trends in WP frequencies and WP internal characteristics and investigate whether observed trends in local climate variables can be attributed to changes in WP compositions. We explicitly emphasise that the classification of Murawski et al. (2016a) aims at optimising the amount of explained variance. It does not aim at separating between dynamical and thermodynamic fractions in past climate observations Shepherd (2014), as it includes both, dynamic and thermodynamic variables. The classification is tested for the assumption, that observed temporal changes can be fully explained by between-type changes. This is a prerequisite for using it for weather generator based downscaling.

The main goal of the ERA-20C reanalysis project was to create a century-long set of atmospheric fields that are as immune as possible to artificial trends induced by the growing data coverage, we assume that large-scale trends are well captured by the input data. This is further supported by Poli et al. (2013) who show that ERA-20C trends are particularly reliable near the surface of the Northern Hemispheric extra-tropics.

Climate change might manifest itself in WPs in two different manners. On the one hand, the occurrence of WPs might change, reflected in changes in the frequency of patterns (e.g. dry patterns occur more often), in the seasonality (e.g. a summer pattern being observed already in spring), or in the persistence of patterns (e.g. a dry and warm pattern occurs for longer periods). These changes are termed between-type changes. On the other hand, within-type changes can occur, i.e. the characteristics of local climate variables for a given WP can change (e.g. more precipitation). The assumption of a stationary link between WPs and local climate requires that climate change manifests only as between-type change. Although there are numerous studies that have relied on a stationary link between WPs and local climate, previous analyses indicated that this assumption might be violated (Widmann and Schär, 1997). Hewitson and Crane (2006) pointed out that land use and land cover changes could affect local climate and thus modify the link to WPs. Jacobeit et al. (2003) detected within-type changes in some circulation types over Europe. Beck et al. (2007) found that large parts of the climate variability between 1780 and 1995 in Central Europe could not be explained by variability in WPs. Cahynová and Huth (2010) applied decomposition of climatic differences and the hypothetical trend methodology to differentiate the role of frequency and within-type changes on trends in 6 climate variables over the Czech Republic. Both decomposition techniques, of which we only use the latter here, indicated that a relatively small share of changes could be explained by frequency changes in the period 1961–1998. Küttel et al. (2011) indicated a strong role of within-type changes for changes in winter temperature and precipitation in Eastern Europe and Scandinavia by comparing multiple 50-year periods back to 1750. Also Fleig et al. (2015) analyzed the role of frequency and within-type changes on monthly temperature and precipitation trends in Europe using the hypothetical trend technique. The relative share of frequency changes was found to vary strongly between 0 and 100 % depending on the month and particular area within the European domain. Haberlandt et al. (2015) investigated the stationarity of the weather pattern–precipitation link in a modeling study based on ECHAM/REMO climate model simulations and stochastic weather generator experiments. They concluded that the change in pattern frequency was not able to fully explain the change in future simulated total precipitation change.

This study extends the discussion on the stationarity of the weather pattern–local climate link in two ways. First, previous studies indicating non-stationarity used mainly circulation variables for classification. While such classifications are able to clearly separate between dynamic and thermodynamic changes, they might insufficiently stratify local climate variables like temperature and precipitation and thus lead to within-type variability, thus impeding the application of a weather generator based on WPs. To our knowledge only a few studies additionally consider other atmospheric variables to improve the discrimination of weather variables (Enke et al., 2005a; Fleig et al., 2015). We address the question if a classification based on mean sea level pressure, temperature and humidity is able to reduce within-type variability of WPs. Second, our analysis uses the idea of multiple trends, where all possible periods with a minimum length of 31 years are investigated. Since temporal changes are typically very sensitive to the selection of the start and end years of the time series, the multiple trend approach gives an indication of the robustness of the results.

In the following we introduce and interpret our WP classification with particular focus on classes associated with dry and moist conditions in the Rhine catchment. Typical characteristics i.e. the spatial distribution of sea level pressure, temperature and humidity are illustrated for each WP. Relationships with well known circulation indices (such as the North Atlantic Oscillation) are analyzed, which allows the interpretation of WPs, their frequencies and changes from a large-scale perspective. Subsequently, trends in frequency, seasonality and persistence of WPs are analyzed and compared with changes of large-scale circulation indices. Within-type changes in 4 meteorological variables based on homogenized daily observation series at 490 climate stations over the 110 year period 1901–2010 are quantified. Finally, the relative contribution of frequency-related changes in explaining trends in selected meteorological variables is estimated.

4.2 Data and weather pattern classification

A previously developed weather pattern classification (Murawski et al., 2016a) is tested for stationarity of the link between patterns and associated climate variables. The classification uses mean sea level pressure, 2 m temperature, and specific humidity from the ERA-20C reanalysis (Poli et al., 2013) in the period 1900–2010 (explained variation of the input fields: 0.82). It covers the spatial domain 3–26°E/43–58°N with 40 classes/patterns and was optimised in terms of variables used for classification, spatial domain, and number of classes, to provide the best stratification of local climate variables. The ensemble mean of ERA-20C was used here only, thus no conclusions regarding the uncertainty due to the reanalysis are possible. Due to the integration of dynamic (sea level pressure) and thermodynamic variables (temperature and specific humidity), the classification identifies weather patterns, characterized by anomalous pressure patters (and associated circulation modes) and specific thermal and hygric conditions. While major circulation patterns can be observed during the entire year, temperature and humidity feature a distinct seasonal cycle, enabling a continuous classification throughout the year and an assignment of weather patterns to individual seasons. The regional scale weather conditions for each WP are analysed in terms of daily mean precipitation, temperature, relative humidity and global shortwave radiation (hereafter referred to as PREC, T_{av}, RH, RAD). Each pattern shows a clear seasonality of occurrence, thus we can assign winter, summer and spring/autumn patterns.

The analysis is based on 490 stations in the Rhine catchment for the period 1901–2010 (432 stations for the German part, 9 stations for Austria, 49 stations for Switzerland and Liechtenstein; Figure 4.2). The station data were collected from the national meteorological services. Data processing and quality control was performed by the Potsdam Institute for Climate Impact Research (PIK) (Österle et al., 2006a; Österle et al., 2006b; Österle et al., 2016). This data set includes global shortwave radiation that was inferred from sunshine duration following Österle (2001) if not directly available. To date no station data for the French part of the Rhine catchment are available. A more detailed description of the data set and the homogenisation process is given in the Supplementary.

Figure 4.1 illustrates the spatial distribution of sea level pressure, temperature and humidity for WPs featuring exceptionally dry or moist conditions over the Rhine catchment (a complete overview of all WPs is provided in the Supplementary). Dry conditions include all days with mean precipitation sums (calculated as a spatial mean over all stations) below the 25 % quantile, moist conditions comprise days above the 75 % quantile of the empirical distribution. In general, moist conditions are characterized by significantly negative pressure anomalies over Central Europe, Scandinavia and/or the North Western Atlantic Ocean. The Rhine catchment is either located in the core region of the low pressure cell or at its southern/southeastern edge. The associated cyclonic circulation pattern is accompanied by enhanced westerly moisture fluxes resulting in positive moisture anomalies over vast parts of Central and Southern Europe. The temperature anomalies of moist WPs follow the seasonal cycle. In contrary, dry conditions (for all seasons) depict strong positive pressure anomalies over Scandinavia and/or Central Europe, triggering an anticyclonic circulation pattern. WPs featuring positive pressure anomalies over Central Europe (WP 21, 36, 40) are associated with a direct blocking of the prevailing westerly flow and precipitation suppressing subsidence over the Rhine catchment. WPs characterized by a high pressure centre over Scandinavia (WP 5, 12, 14, 32, 37, 38) provoke an anticyclonic circulation over Northern Europe. The Rhine is located at its southern edge and thus is under influence of north-easterly winds, advecting cold and dry air masses. Dry WPs are distinctly more often observed during winter than during all other seasons and are often accompanied with an intrusion of continental cold air, as represented by strongly negative temperature anomalies (e.g. in WP 12 and 14).

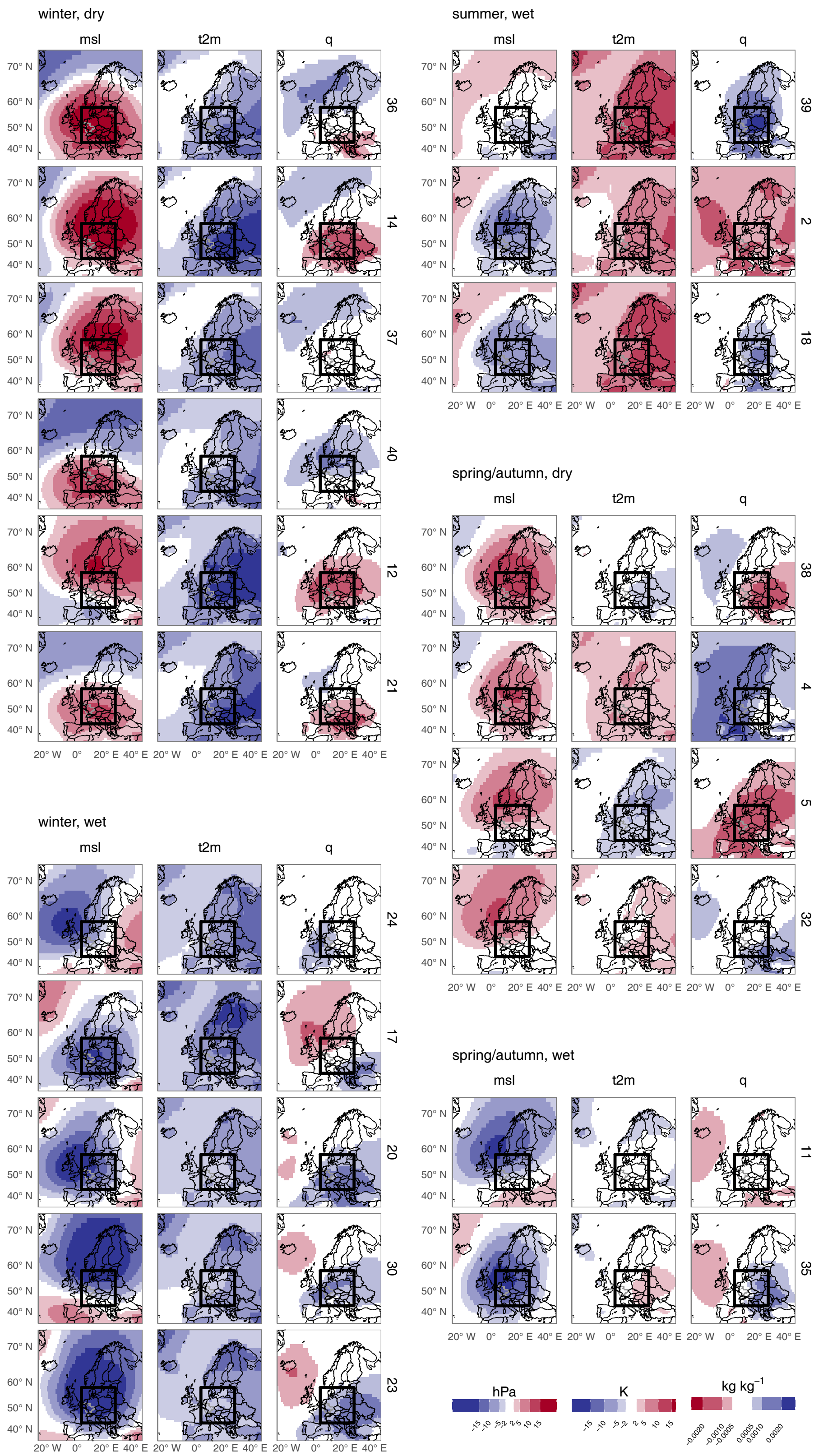

Figure 4.1: Centroids of patterns (wet and dry patterns only) expressed as anomalies (deviation from the overall mean (mean sea level pressure, msl; 2 m temperature, t2m), or the mean of the season's months only (specific humidity, q)). Black rectangle denotes the domain used for classification, grey outline indicates the Rhine catchment.

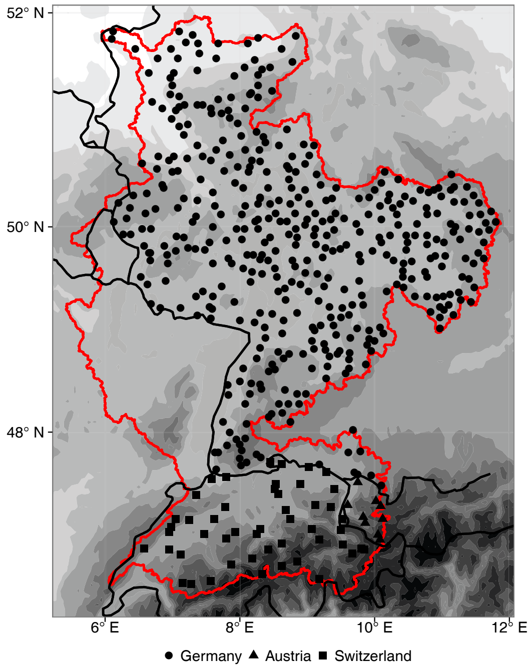

Figure 4.2: Locations of climate stations used. Red line shows Rhine catchment, black lines denote state borders. Background shading from light gray (low areas) to dark gray (high altitudes).

4.3 Methods

4.3.1 Relationship of WPs and large-scale circulation modes

In order to identify large-scale atmospheric mechanisms favouring the occurrence of particular WPs and to attribute trends of WP frequencies to changes of northern hemispheric circulation modes, we investigate the relationship between WP frequencies and well known teleconnection indices.

As potential large-scale drivers, we consider monthly time series of the North Atlantic Oscillation (NAO), Scandinavian pattern (SCA), East-Atlantic pattern (EA) and East-Atlantic/Western-Russia pattern (EAWR) for the period 1950–2010. These are based on a Rotated Principal Component Analysis of 500 hPa geopotential height (GPH) fields (Barnston and Livezey, 1987) and represent leading (statistically independent) circulation modes over a domain North of 20 °N. Positive and negative phases of each circulation mode are accompanied by specific large-scale pressure patterns and associated moisture fluxes. The NAO is characterized by two centres of action over the North Atlantic (Iceland Low) and the subtropical Atlantic (Azores High) and represents the strength of the meridional pressure gradient over the North Atlantic/European domain. Its positive phase features negative pressure anomalies over the North Atlantic and Scandinavia and positive anomalies over Southern Europe and is accompanied by a northward shift of westerly moisture fluxes. Positive (negative) precipitation anomalies during the positive NAO phase have been frequently reported for Northern Europe (the Mediterranean) (Steirou et al., 2017; Uvo, 2003). SCA is associated with strongly positive GPH anomalies over Scandinavia and is known to reflect blocking situations over Northern and Central Europe, accompanied by negative precipitation anomalies (Bueh and Nakamura, 2007; Comas-Bru and McDermott, 2014). EA is frequently referred to as a southward shifted NAO with its major center of action over the British Isles. Positive (negative) precipitation anomalies over Northern Europe (the Mediterranean) are characteristic during its positive phase. EAWR features a dipole like pattern of GPH anomalies between Central Europe and Russia. The positive phase is associated with strongly positive anomalies over Europe, which is accompanied by an anticyclonic circulation pattern and a southward deflection of westerly moisture fluxes (Krichak and Alpert, 2005).

We conduct a systematic spearman correlation analysis of WP frequencies with well-known teleconnection indices at a monthly scale, i.e. the time series of WP frequencies are correlated with the mean state of any index and correlations are tested for significance (t-test, $\alpha = 0.1$) for each month of the year, respectively. Positive (negative) correlations indicate an increased (decreased) WP frequency during the positive phase of the considered index. The circulation modes are obtained from NOAA (http://www.cpc.ncep.noaa.gov/ data/teledoc/telecontents.shtml).

With the aim of attributing potential changes of WP frequencies to changes (or multi-decadal variations) of large-scale circulation modes, a trend analysis for multiple periods is performed for the teleconnection indices and for each WP respectively (see subsection 4.3.2 for methodological details).

4.3.2 Trend detection methods

The fundamental assumption of weather pattern-based downscaling is a stationary link between patterns and local climate, i.e. no within-type change, and climate change manifests only as between-type change. In this way a constant parametrization of a weather generator conditioned on weather patterns can be used. To test this assumption, different trend analyses are performed.

For trend detection the non-parametric two-sided Mann-Kendall test (Kendall, 1938), which is based on a rank correlation coefficient, is applied ($p < 0.05$). The magnitude of change is derived from Sen's slope (Sen, 1968, Equation 4.1):

$$\beta = \text{median}\left(\frac{x_n - x_m}{n - m}\right) \quad ;\text{for all } n > m; x_n, x_m = \text{time series values in years n, m} \tag{4.1}$$

Trend magnitudes are known to be sensitive to the selection of start and end points of the investigation period. In particular in our analysis, it might be expected to have periods incorporated in the data that are mainly influenced by anthropogenic climate change, while this effect is not clearly evident in other periods (i.e. might be masked by internal variability or natural forcings). To eliminate any potential effect of a fixed time period, trend analyses for multiple periods are performed. Statistical tests are applied to every time period with a minimum length of 31 years resulting in trend matrices indicating the magnitude and (field) significance of multiple trends within the period 1900/01–2010. Each pixel/cell of the triangular matrix represents the trend results for a combination of a particular start year (x-axis) and end year (y-axis). In the case of variables derived at each climate station separately (e.g. pattern mean temperature), each pixel represents the spatial average across all stations.

To account for possible autocorrelation in the time series, which might distort the result of the Mann-Kendall trend test, a block bootstrap approach as proposed by Khaliq et al. (2009) is applied. This approach is based on resampling a correlated time series such that the correlation structure is preserved (i.e. taking blocks of data that are longer than the number of significantly autocorrelated time lags). The test statistic (here Kendall's tau) is derived from the resampled time series. Repeating this procedure a large number of times (1000) results in a simulated distribution of the test statistic. If the test statistic of the original series lies in the tails of this distribution it is unlikely to obtain that value from a time series with the same correlation structure but no temporal trend, thus the trend of the original time series is judged to be unaffected by autocorrelation.

When performing trend analyses on multiple stations within a region the question arises whether the observed number of trends is significantly larger than what might be found by chance only. Applying the block bootstrapping for all stations simultaneously, thus preserving the spatial correlation between neighbouring stations, field significance can be evaluated as well. The number of trends in the shuffled time series is counted and compared to the observed number. If the observed number lies in the tails of the distribution of simulated number of trends, this is judged to be field significant. Performing this analysis for each individual period and highlighting the field significant periods gives contours of field significance as presented e.g. in Figure 4.5.

For the detection of changes in pattern characteristics, trend analyses (i.e. Mann-Kendall test and Sen' slope) are performed on annual mean values of pattern frequency, seasonality, persistence (“between-type changes”) and on pattern-specific annual mean climatic values of all stations (“within-type changes”). Seasonality is expressed as the average date of pattern occurrence, taking into account the circular nature of dates when calculating trends (i.e. considering that the difference between day 365 and day 1 is +1 rather than −364) by using an approach of Bayliss and Jones (1993) that converts the date into an angular value. Patterns that occur mainly in spring and autumn show two distinct peaks of seasonal occurrence, which are analysed separately for shifts in seasonality. For aggregating trend results of climatic values across all stations, trend magnitudes were spatially averaged across all stations and field significance is calculated as described above.

4.3.3 Relative share of between- and within-type changes

For attributing the change in a certain meteorological variable to changes in pattern frequency, the “hypothetical trend” approach as proposed by e.g. Huth (2001) is applied, comparing the weather pattern-induced trend to the observed trend (Fleig et al., 2015). A hypothetical time series of daily (e.g. precipitation) values of a climate station is constructed by replacing each original daily value with the station-specific long-term monthly mean value of the respective weather pattern associated with that day (for a detailed description see Fleig et al., 2015). The ratio of the linear trend (i.e. Sen’s slope) in the weather pattern-induced (i.e. hypothetical) series to the linear trend in the observed time series is then computed. It can potentially take values from $-\infty$ to ∞. The meaning of some selected values is:

$$R > 0 : \text{Pattern-induced and original trend are of the same sign.} \tag{4.2}$$

$$R < 0 : \text{Pattern-induced and original trend are of opposite sign.} \tag{4.3}$$

$$R = 1 : \text{Original trend is completely attributed to trend in pattern frequency.} \tag{4.4}$$

$$0 < R < 1 : \text{Within-type trends are of the same sign as between-type trends.} \tag{4.5}$$

$$R > 1 : \text{Within-type trends are of the opposite sign to between-type trends.} \tag{4.6}$$

The hypothetical trend approach is able to identify opposing trends, e.g. in case a changed frequency of patterns would lead to an increase in precipitation, but a decreasing trend was observed due to drying of the corresponding patterns. The method is applied for multiple periods, calculating long-term monthly pattern mean values separately for each period. The trend ratio only gives meaningful results for significant trends (Cahynová and Huth, 2010). Although trend magnitudes of original and weather pattern-induced trends are presented for all stations, trend ratios are only calculated for stations with significant ($p < 0.05$) original trends.

4.4 Results

4.4.1 Attribution of WPs to large-scale circulation modes

Results of the correlation analysis (Figure 4.3) clearly reveal that WPs (particularly those triggering moist or dry conditions over the target region) result from the superposition and regional manifestation of large-scale pressure modes and thus represent major atmospheric processes, such as the formation of cyclonic and anticyclonic circulation patterns and the associated deflection of large-scale heat and moisture fluxes. Moisture conditions during winter are strongly related with the state of the East-Atlantic/Western-Russia and the Scandinavian patterns. WPs showing a strong positive correlation with EAWR and SCA are associated with blocking over Central Europe and Scandinavia, respectively. Monthly frequencies of dry WPs 36, 14, 40, and 21 show positive (and partially statistically significant) correlations with EAWR, which indicates an increased occurrence of dry WPs during its positive state. The same applies for SCA (positive correlations for WP 14, 37 and 12). Moist WPs (characterized by negative pressure anomalies over Northern and/or Central Europe and a consequential cyclonic circulation) show an inverse relationship. A clear influence of the North Atlantic Oscillation on the frequency of dry and moist WPs during winter is not detectable, slight positive correlations with NAO are found for the dry WPs 36 and 40, negative correlations are detected for the moist WP 17. During spring, summer, and autumn the relationship between WP frequencies and

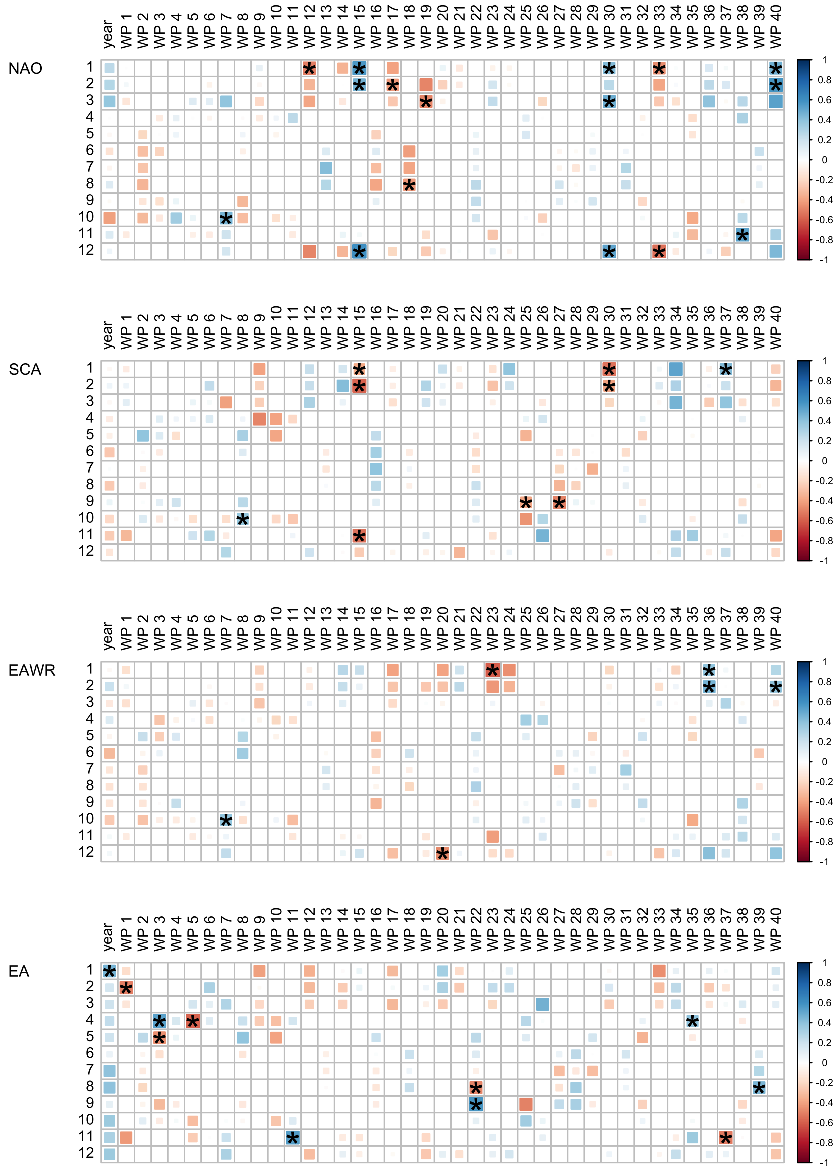

Figure 4.3: Correlation of pattern frequency and averaged index of selected large-scale atmospheric circulation modes. Correlations are only shown if the pattern has a maximal occurrence of at least 20 % in the respective months. Asterisks indicate significant correlations.

large-scale atmospheric conditions is less pronounced. For the moist WPs 2, 18 and 35 a negative relationship with NAO is detected.

The trend analysis of teleconnection indices for multiple periods (Appendix, Figure 4.A1) indicates significant positive trends of EA and NAO for the period after 1948, particularly for the winter season. Likewise for EAWR trends are positive (although not statistically significant) during most periods. For wintertime SCA a slight negative trend is detected. These trends might be interpreted as a consequence of an intrinsic multi-decadal variability of wintertime circulation modes (Hurrell et al., 1995; Krichak and Alpert, 2005; Selten et al., 1999; Wang et al., 2012), which however might explain observed trends of WP frequencies (and local scale observations) to a certain extent.

4.4.2 Between-Type Changes

Changes in pattern frequency are detected for many patterns in distinct periods and with varying trend direction and magnitude (Figure 4.4, for full set of WPs see Supplementary). For wet winter patterns 24 and 17 slightly decreasing frequencies of up to 0.05 % per year (season and precipitation intensity are depicted by icons in the sub-plots) are detected in most periods since the 1950s and increasing trends in periods ending around 1970 and 1980. Both patterns are negatively correlated with EAWR and recent changes of WP frequencies are clearly related to positive trends of the winter EAWR index after 1950. Wet winter WPs 30 and 23, featuring a strong negative relationship with SCA, show increasing frequencies (only statistically significant for WP 30) since the 1950s, which is also in agreement with observed trends of the SCA index. For both WPs long-term increases in frequency of up to 0.05 % are detected. Both feature very similar temperature and humidity patterns, with a low pressure anomaly over Scandinavia (see Figure 4.1), which is slightly shifted southwards in WP 23. This similarity results in rather similar mean local climate (see Appendix in Murawski et al., 2016a). Dry winter WPs, which are positively correlated with the EAWR pattern (36, 14, 40), show slightly positive frequency trends in recent periods (increasing frequency in WP 40 is detected for many periods ending between 1990 and 2010 with magnitudes of up to 0.1 % per year) and decreasing frequency ending in the 1970/1980s. Although WP 36 and 14 feature rather similar msl and humidity patterns, they clearly differ in temperature. Thus, this pair of WPs would be prone for capturing temperature changes by a mere exchange of these two, but their trends in frequency are in the same direction for most periods. Dry winter WPs 40 and 12 show almost opposite frequency trends: decreasing (increasing) trends for periods ending between 1990 and 2010 with particularly higher magnitudes around 1960, and increasing (decreasing) trends until the 1970s. While WP 40 might be interpreted as a superposition of a positive NAO and a positive EAWR pattern, which favours blocking over Central Europe, WP 12 rather occurs under negative NAO conditions in combination with a positive state of SCA (see Figure 4.3). Again the observed frequency trends of both WPs follow those of relevant large-scale circulation modes after 1950. For WP 37, being strongly positively correlated with SCA, slightly decreasing frequency is detected for several periods starting around 1910 and 1920 or ending in 1970 or 1980.

Wet summer patterns 39 and 18 became more frequent in recent decades (more than 0.1 % per year for WP 39), but show alternating trend direction in earlier periods (negative in the middle of the century, positive again between 1900 and 1930), but no trends persisting over the whole century. Although trends in the frequency of these WPs are quite similar throughout the century, they have notably different pressure anomalies (see Figure 4.1). While WP 18 is dominated by a low pressure anomaly over central Europe, the pressure anomaly is less pronounced and rather located in the south-east of Europe in WP 39, which is furthermore associated with higher temperature and humidity than WP 18. Both WPs are positively correlated with EA, which features a strong inter-decadal variability with mainly positive trends during recent decades. WP 18 is also strongly negatively correlated with NAO.

While most spring/autumn patterns do not show significant trends in recent decades, for wet WP 35 increasing frequency is detected for periods beginning after 1930 and ending after 2000, which is in agreement with positive trends of the positively correlated EA pattern in spring and autumn. In contrary the negatively correlated WP 5 (dry) shows slightly (but mostly not significant) decreasing frequency after 1930. For wet WP 11 (also positively correlated with EA)

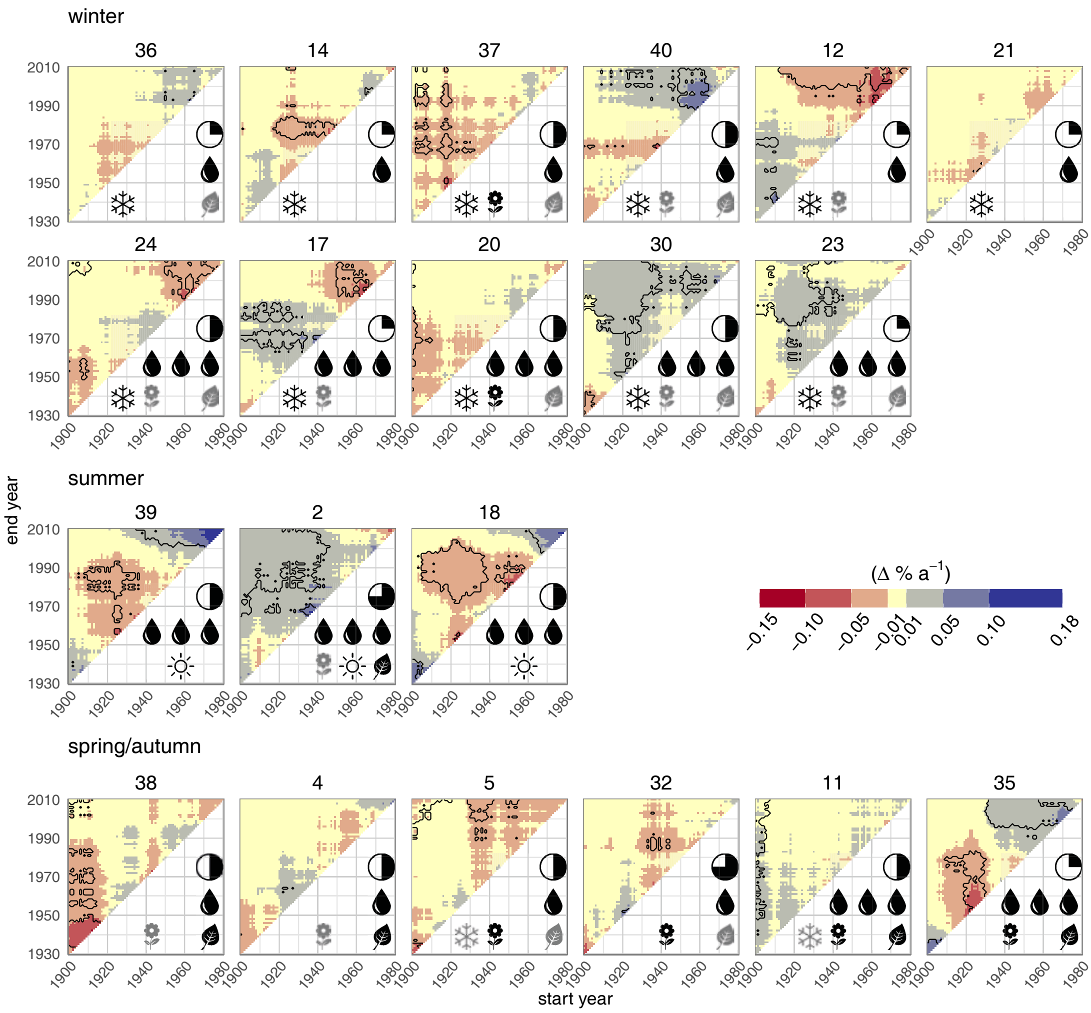

Figure 4.4: Multiple trends of pattern frequency (dry and wet patterns only). Each value of the upper triangle denotes the trend magnitude of a specific period, given by its start year (horizontal axis) and end year (vertical axis). Black contours enclose time periods with statistically significant trends (Mann-Kendall test, $p < 0.05$). Icons in lower right corner of panels denote season(s) of pattern occurrence (snowflake – DJF, flower – MAM, sun – JJA, leaf – SON; black – main season, grey – few occurrences), mean daily precipitation (1 drop: [0, 1.25] $\mathrm{mm\,d^{-1}}$, 2 drops: (1.25, 4] $\mathrm{mm\,d^{-1}}$, 3 drops: (4, 7.4] $\mathrm{mm\,d^{-1}}$), and frequency of pattern (one quarter of circle filled black: pattern occurs in [0, 2] % of days, two quarters filled: (2, 3] %, three quarters filled: (3, 3.5] %, all filled: (3.5, 3.8] %). (Icons (drop and seasons) made by Freepik and Icon Works from www.flaticon.com)

only few increasing trends of low magnitude are detected, mostly for periods starting around 1900. For dry WP 38, which is positively correlated with NAO and EAWR, decreasing trends in frequency are only detected for periods starting between 1900 and 1920.

Summarizing, the trend patterns of WP frequencies are found to follow the trends (or more likely the long-term variability) of Northern Hemispheric circulation modes. This is most pronounced during winter season where dry (wet) conditions are related with the positive (negative) manifestation of EAWR and/or SCA. Those dry patterns related with a positive EAWR state show significant positive trends during recent decades, for patterns related to a positive SCA a frequency decrease is detected. Reversal relationships are found for wet WPs.

The seasonality of patterns (Appendix, Figure 4.A2, for full set of WPs see Supplementary) changes only little with usually less than one day change per year. For dry and wet winter patterns many weak short-term trends are found, usually of alternating direction and being close to zero for century-long periods. Some general trend patterns are evident in association with large-scale pressure modes, e.g. WP 40 (and 12) are positively (negatively) correlated with NAO and show tendencies towards later (earlier) occurrence of up to 1 day per year for the most recent decades and earlier (later) occurrence of the same magnitude for periods roughly ending before 1990. For the wet winter pattern 20 earlier occurrence of up to 2 days per year is detected for periods ending before 1970 and starting after 1950, and later occurrence of the same magnitude is detected for periods in between. The seasonality of wet summer patterns exhibits hardly any significant trends and is of low magnitude only. For spring/autumn a clear tendency of earlier occurrence in spring of up to 1 day per year (translating to a shift of one month for a 30-year period) is evident for recent periods. Simultaneously, the autumn peak of many patterns shifted to later occurrence in recent periods. However, the latter is less pronounced than the shift in spring.

The majority of patterns does not exhibit a change in persistence and only very few show long-term but weak changes (Appendix, Figure 4.A3, for full set of WPs see Supplementary). Increasing persistence in long-term periods is found for wet summer pattern 2, although the trend weakened and is not significant in recent decades. This is in general consistent with the observed increases in frequency of this pattern. Dry winter WP 14 shows a significant increase in persistence for periods starting in the 1960s and lower persistence for periods ending around 1980. This suggests a local minimum in persistence of this relatively dry winter pattern in this decade. The magnitude of these trends average around 0.05 and -0.03 days per year, respectively, which sums up to a change of 1.5 (-0.9) days for 30 years. Considering an average persistence of this pattern of almost 3 days, this change translates to a relatively significant proportion (average persistence of patterns varies between 1.4 and 3 days). In general, most signals detected in pattern frequency are found in persistence as well. This synchronization indicates that changes in pattern frequency are mostly caused by changes in persistence, which are likewise related to the inter-decadal variability of the Northern Hemispheric circulation, as represented by the NAO-, SCA-, EA- and EAWR-teleconnection indices.

4.4.3 Within-Type Changes

Multiple trend analyses on pattern-specific mean climatic values are presented in Figure 4.5 and 4.6 and Appendix, Figure 4.A4 and Figure 4.A5 (for panels with full set of patterns see Supplementary). For T_{av} (Figure 4.5) many dry winter patterns show a warming trend until the 1980s and a cooling trend for recent periods (WP 36, 14, 37, 12). The cooling is not pronounced for wet winter patterns (except WP 20), but warming trends are detected for some short periods in the middle of the century (WP 20, 23). All wet summer patterns exhibit long-term significant warming, however of low magnitudes of max. 0.05 K. Spring/autumn patterns reveal warming trends in the beginning of the century which do not persistent in recent decades.

Trends in precipitation (Figure 4.6) are most pronounced (i.e. highest absolute magnitudes) in wet patterns, while for dry patterns almost no significant trends were detected and if so, their magnitudes are close to zero. Wet winter patterns show long-term wetting trends of up to 0.05 mm per year, however, all of them (except WP 30) indicate non-significant drying trends in very recent periods. Wet summer pattern 39 shows significant long-term decreasing precipitation, while wet summer WP 18 indicates opposite trends. In spring/autumn only for WP 35 significant wetting is detected for periods starting between the 1920s and 1950.

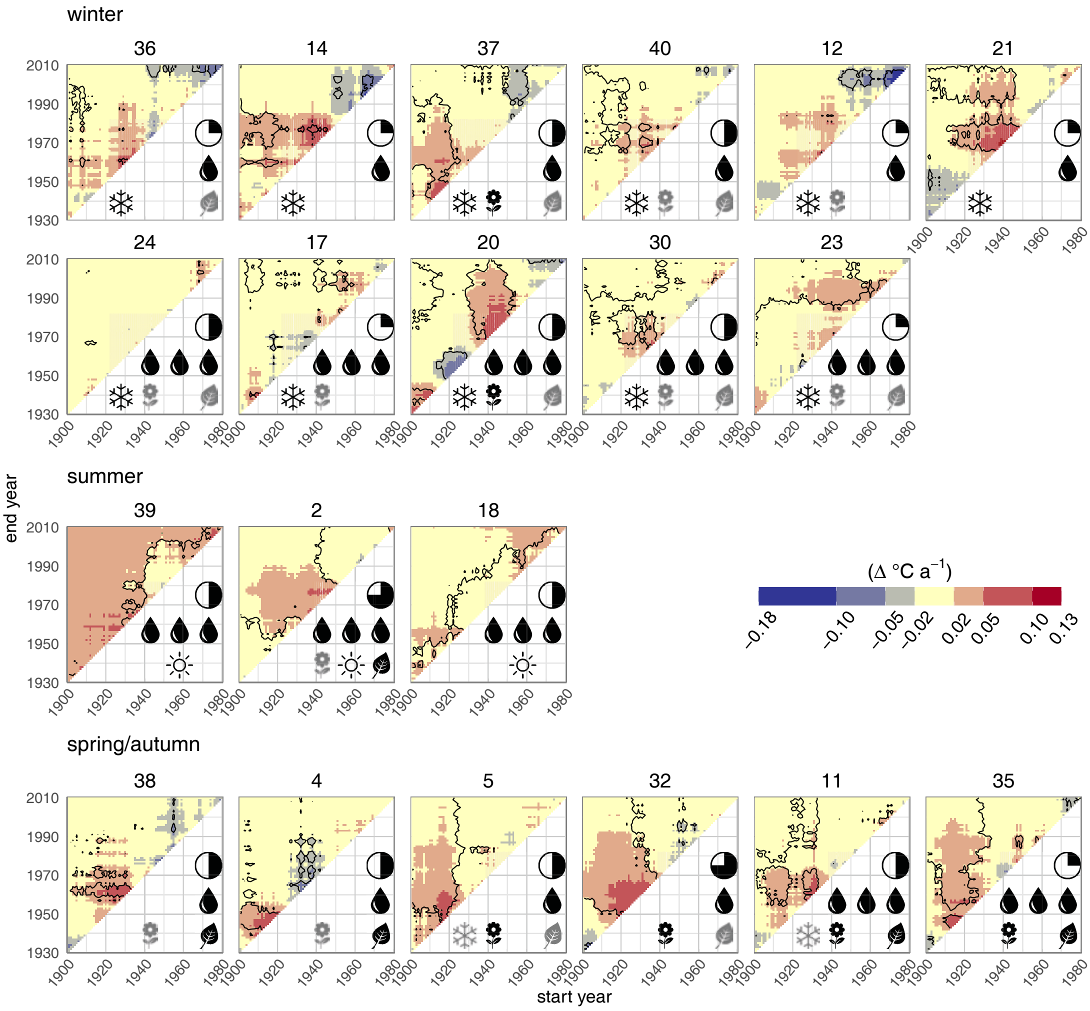

Figure 4.5: Multiple trends of pattern mean daily temperature (dry and wet patterns only). Plot as in Figure 4.4, except that black contours enclose time periods with field significant trends ($p < 0.05$).

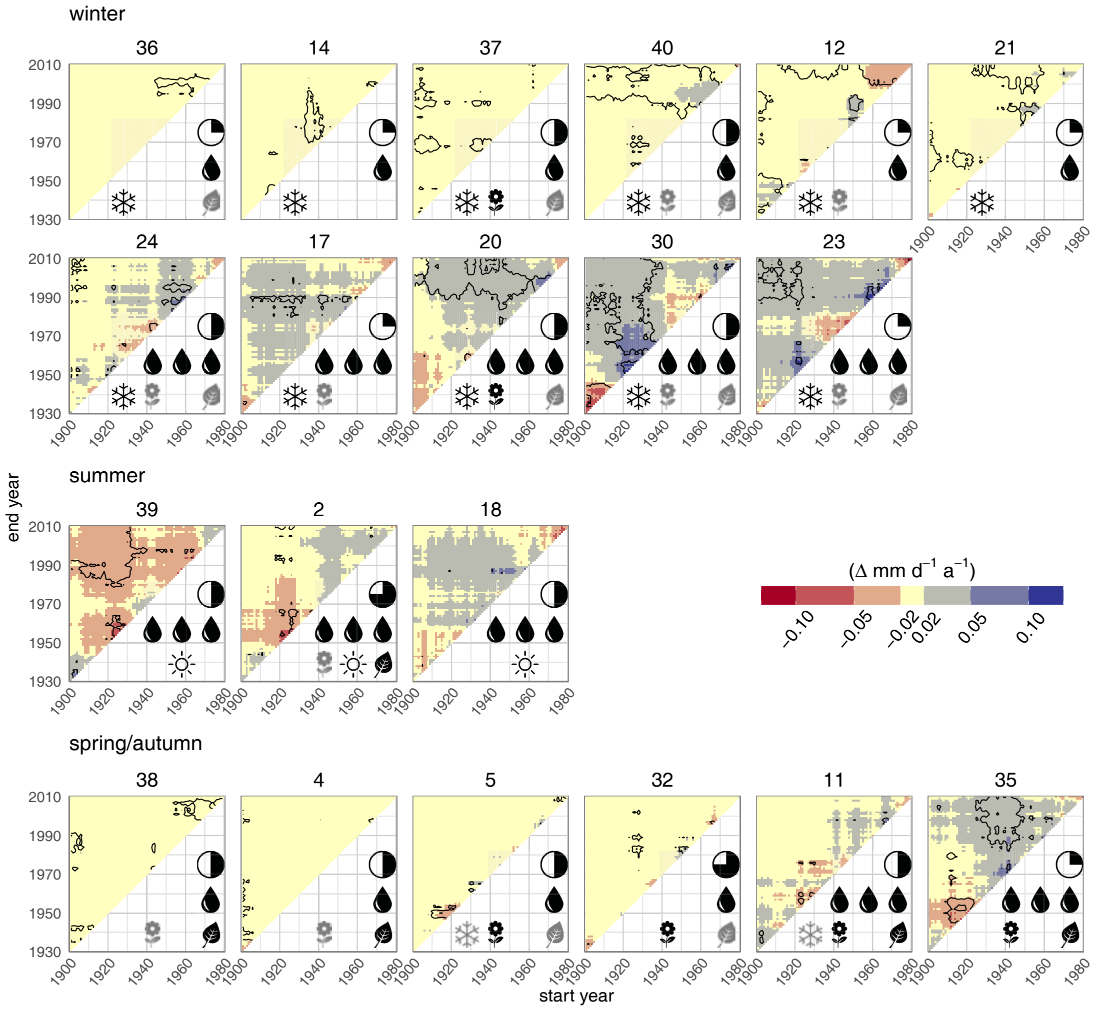

Figure 4.6: Multiple trends of pattern mean daily precipitation (dry and wet patterns only). As in Figure 4.5.

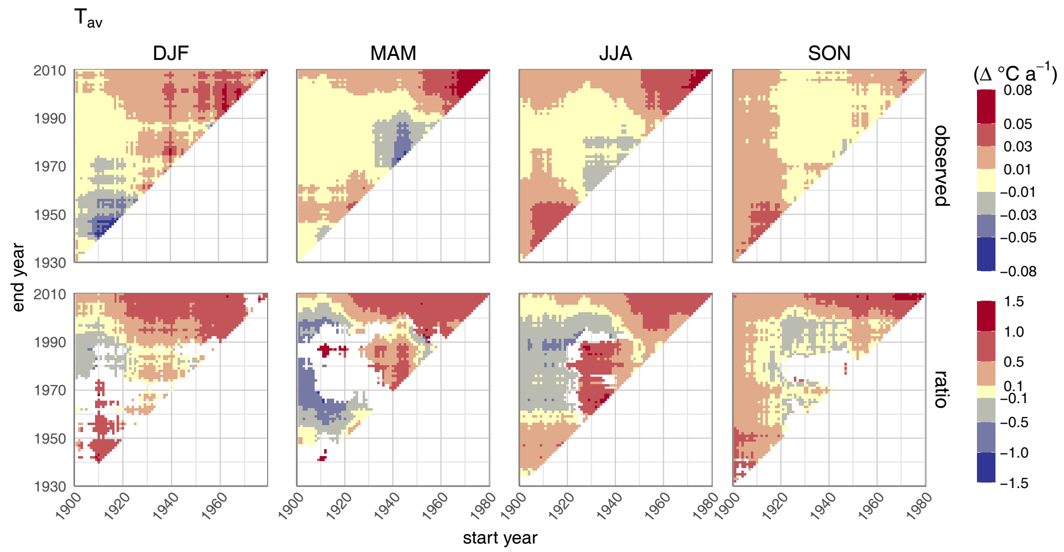

Figure 4.7: Trends in catchment average mean daily temperature for all seasons (upper panel) and associated ratio of weather pattern-induced and original trend slopes (see subsection 4.3.3). Ratios are only calculated for stations with significant original trends and presented as averages across stations. Gaps appear for periods with no significant trends.

Most trends in shortwave radiation (Appendix, Figure 4.A4) are rather short-term and only few sustain during the whole century. This suggests the presence of decadal fluctuations in shortwave radiation associated with various weather patterns. Especially for winter, trends, if present at all, prevail only in very few periods. In spring/autumn many wet or dry pattern show increasing trends for periods ending around 1960 and decreasing trends for periods starting around 1940. For summer WPs 39 and 2 long-term increasing trends in shortwave radiation are detected, which weakened or switched sign in more recent decades.

For relative humidity (Appendix, Figure 4.A5) very heterogeneous trends are found with periods of positive and negative trends in most patterns. Especially for wet summer and dry spring/autumn patterns trends in relative humidity are parallel to those in shortwave radiation. This also suggests strongly pronounced fluctuations in weather pattern related humidity.

4.4.4 Relative share of between- and within-type changes

Trends in annual climatic variables averaged over the catchment are analysed for multiple periods (Figure 4.7 and 4.8, upper panel). Trends in temperature variables are positive over nearly all periods starting after 1950 or ending after 2000 in all seasons (less pronounced in autumn). Increased warming of more than 0.03 °C a^{-1} since the 1960s is detected. A pronounced cooling is found for winter for periods ending before 1950 and for spring for periods starting around 1940. Weather pattern-induced trends (lower panel) follow the observed trends to a large degree and explain 50 % to almost 100 %, especially for recent periods with high magnitudes of change. Periods with negative slope ratios (i.e. weather pattern-induced trends are of opposite sign to the original trends) occur only for periods with almost no trends.

Trends in precipitation are detected for winter in almost all periods (magnitude of change usually less than 1 mm per year and up to more than 2 mm per year only for very few periods). For spring and autumn increasing precipitation was mainly found for periods starting after 1940, whereas changes in summer precipitation are close to zero and only pronounced negative for few periods starting in the 1950s. Up to 50 % of the changes in precipitation, although only weak, can be explained by weather pattern-induced changes. For periods with more pronounced precipitation changes (e.g. winter, periods around 1930–1960, and spring, periods starting around 1940) more than half of the change is attributable to between-type changes.

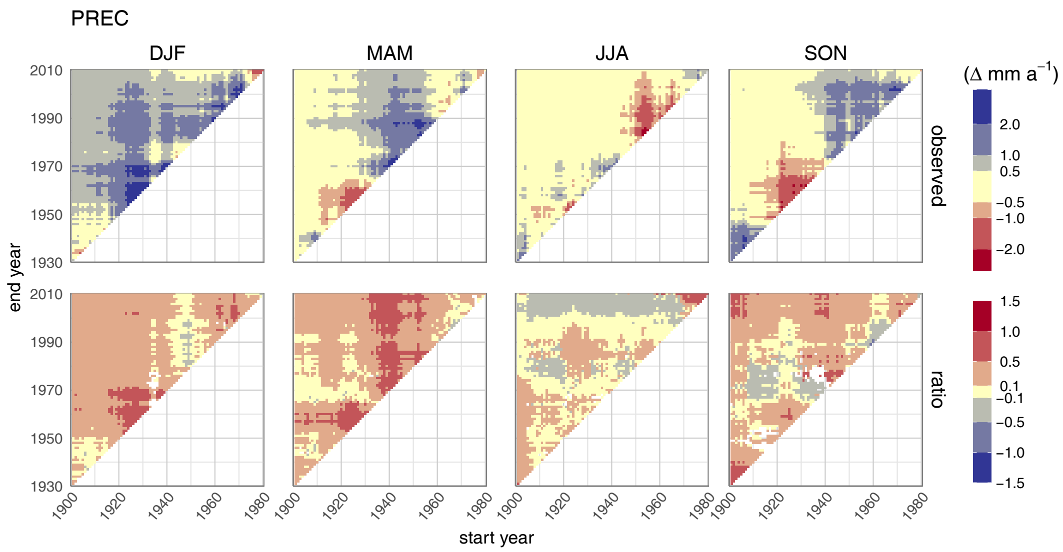

Figure 4.8: Trends in catchment average daily precipitation for all seasons. As in Figure 4.7.

Changes in shortwave radiation and relative humidity (Appendix, Figure 4.A6 and 4.A7) show decadal variations in trend direction, which is most pronounced in spring and summer. Weather pattern-induced changes are usually of not more than half the magnitude of original trends, indicating some substantial proportion of within-type changes.

4.5 Discussion and conclusions

In this paper we analysed the "optimal" weather pattern classification presented in Murawski et al. (2016a) for trends within and between patterns. The climatic properties of the patterns will be used to parametrise a weather generator to serve as a downscaling tool in a climate change attribution study. The assumption for this weather generator-based approach is that changes in local climate variables can be explained by changes in the pattern frequency, seasonality, and persistence. This assumption was examined here by applying trend analyses to pattern characteristics and the mean climatic properties of patterns over multiple periods. Between-type and within-type changes analysed here cannot be interpreted as dynamic and thermodynamic changes, because temperature and specific humidity are included in the classification. The classification of Murawski et al. (2016a) aims at optimising the amount of explained variance rather than to purely separate between dynamic and thermodynamic predictors. However, the analysis shows that such kind of classification is superiour in terms of the envisaged application. WP classifications are common in the literature (e.g. Hewitson and Crane, 2006; Kalkstein et al., 1987) and are different from the circulation pattern classifications that use only pressure variables (Huth et al., 2008).

Trends in the frequency of patterns were found in most patterns, although they were usually not uniform across all periods, but might change direction between decades and smooth out for longer periods. Some increases in frequency were detected particularly in winter patterns that are associated with high precipitation. It was shown that trends of Central European WPs in recent decades follow the variability of large-scale teleconnection indices, such as the North Atlantic Oscillation and the Scandinavian, East-Atlantic and East-Atlantic/Western Russia patterns. Thus the WP classification is capable to depict major Northern Hemispheric circulation modes and associated anomalies of moisture and heat fluxes.

Changes in persistence were usually less pronounced, but are in agreement with observed changes of WP frequencies. For pattern seasonality a tendency, albeit small, in recent decades towards earlier occurrence of wet spring patterns was found, representing increased precipitation during snow melt and thus potentially increase flood severity.

The hypothetical trend analysis shows, that a substantial portion of changes in precipitation and particularly temperature at 490 stations within the Rhine catchment can be attributed to changes of the WP composition. These periods coincide with the highest observed warming, thus clearly emphasizing the importance of between-type changes for overall temperature trends. This relation is already indicated in Corti et al. (1999), but seems to not hold true anymore after 1995 (Yiou et al., 2007) – however, conclusions on the periods after 1995 are not possible from our analyses (using at least 30-year periods until 2010 latest). Explained trend ratios were especially high during winter season, where moist and dry conditions are strongly related to variations of the East-Atlantic/Western-Russia and the Scandinavian pattern. The significant link between large scale circulation modes and weather pattern frequencies as well as the high potential of the WP classification to explain observed trends of surface variables support the utilization of a modelling chain, including WP classification, a stochastic weather generator and a distributed catchment model, to investigate the variability and change of flood probabilities in the Rhine catchment.

However, some weather patterns are characterised by heterogeneous local weather conditions and high ratios of within-type trends. A long-term warming trend was found for all summer patterns. Such a clear signal was not evident for winter patterns where trends were weaker and not persistent on long periods. Winter patterns rather showed a cooling in the last decades and slight warming before. Many spring/autumn patterns showed a strong warming trend until about 1970. Trends for pattern-specific shortwave radiation and relative humidity were dominated by decadal fluctuations. These results hint towards the high variability of trend detection results depending on the selected time period and emphasise the usefulness of assessing multiple periods.

We found that within-type changes dominated in periods with overall small changes in temperature. In the literature different percentages for within-type temperature changes were reported depending on the selected period and methodology. Küttel et al. (2011) found 70 % within-type change of winter temperature for central Europe when comparing the first and second half of the 20th century. Cahynová and Huth (2016) and Huth (2001) summarized that trends in summer temperature (1949–1980) at two Czech Republic stations were unrelated to frequency changes, while a warming trend in winter could be assigned to changes in pattern frequency. Also Philipp et al. (2007) found higher amounts of between-type temperature changes since 1850 for winter (59 %) than for summer (33.9 %) and again evidence for high within-type variability. Cahynová and Huth (2010) concluded that internal changes were “responsible for a major part of the observed climatic trends in spring, summer, and autumn; but also in winter for variables other than temperature”. In contrast to the previous studies, our results suggest a much stronger role of between-type trends (75–100 %) for periods with notable temperature changes revealed by multiple period analyses. This advantage can clearly be assigned to the optimised weather pattern classification (Murawski et al., 2016a), which included temperature as a characteristic variable additionally to the pressure fields. We show indeed that observed changes in temperature and precipitation can be attributed to weather patterns (if thermodynamic variables are included), which finally allows a weather generator based analysis of flood changes during recent decades. This is only possible, because the classification accounts for both, dynamical and thermodynamical changes.

Although considering the specific humidity for weather pattern classification, we were not able to significantly improve the amount of changes in relative humidity that is attributable to changes in pattern frequency. Cahynová and Huth (2010) found near zero (summer) to only 20 % of between-type changes in humidity, which is clearly supported by our results. Changes in shortwave radiation were attributable to changes in pattern frequency by a slightly higher proportion than humidity (around 50 % for periods with decreasing trends), but were nevertheless highly influenced by within-type changes. Decreasing shortwave radiation in periods starting around 1940 and ending around 1990 might be attributed to high aerosol loading in the atmosphere: Andronova and Schlesinger (2000) found a cooling of near-surface temperature between 1940 and 1970 being explained by volcanic activities and partly by solar irradiance, while Walter and Schönwiese (2003) found a particularly strong cooling-effect of sulphur dioxide at a global scale in this period. The same cooling effect was reported in an updated study by Schönwiese et al. (2010), who found almost zero trends in temperature for

1945–1975 along with a strong increase in forcing by sulphate aerosols. The cooling found in our data is only weak, possibly being masked by other effects. The high aerosol loading, however, is clearly visible in decreasing trends of shortwave radiation in these periods.

Observed precipitation changes were represented by weather pattern-induced trends in nearly all periods, i.e. observed and weather pattern-induced trends were of the same direction and slope ratios were positive. However, weather pattern-induced trends accounted for somewhat more than half of the observed changes only in periods ending in the 2000s, earlier periods were dominated by within-type changes. Comparable amounts of within-type changes were also found by Küttel et al. (2011) (60 % of winter precipitation), however, for other periods. A general trend direction for a specific season was not evident – the two wettest summer patterns (18 and 39) showed rather opposite within-type trend directions.

In the presented paper, being a follow-up from Murawski et al. (2016a) where an “optimal” classification of weather patterns was developed, we thoroughly analysed the underlying assumptions for a WP–WGN based downscaling approach. Contrary to previous studies, we found a higher portion of observed trends in temperature and precipitation being explained by pattern frequency. This would justify an application of a pattern-conditioned weather generator, although a certain portion of uncertainty (i.e. non-attributable amount of changes) is inherent to the method. Low explained share of humidity and shortwave radiation trends is a clear limitation. However, for the purpose of flood change attribution to anthropogenic climate change, the role of the latter two variables for higher floods is believed to be minor and can be investigated in a sensitivity study. Hence, the use of WP–WGN based downscaling can be acceptable for flood attribution if properly interpreted.

Acknowledgements

We thank three anonymous reviewers for their suggestions and comments on this manuscript.

We gratefully appreciate the provision of data by the national meteorological services of Germany, Austria, and Switzerland, kindly provided and processed by the Potsdam-Institute for Climate Impact Research (PIK).

A. Murawski acknowledges funding by Climate KIC.

The climate station data are owned by PIK and are not publicly accessible. The weather pattern classification catalogue used here is provided in the supporting information along with netcdf files of the centroids of the patterns.

4.A Appendix

Circulation modes

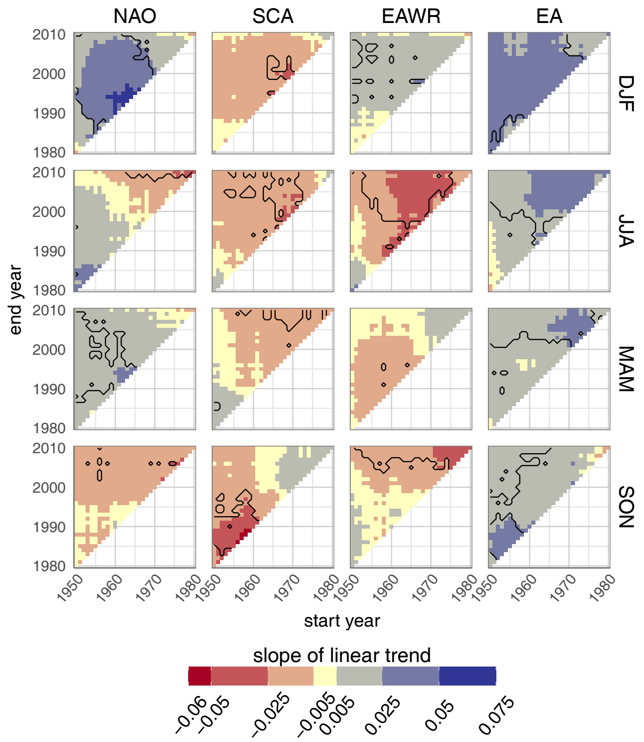

Figure 4.A1: Multiple trends of large-scale atmospheric circulation modes. Note: start of axes differs from other trend plots.

Trend results

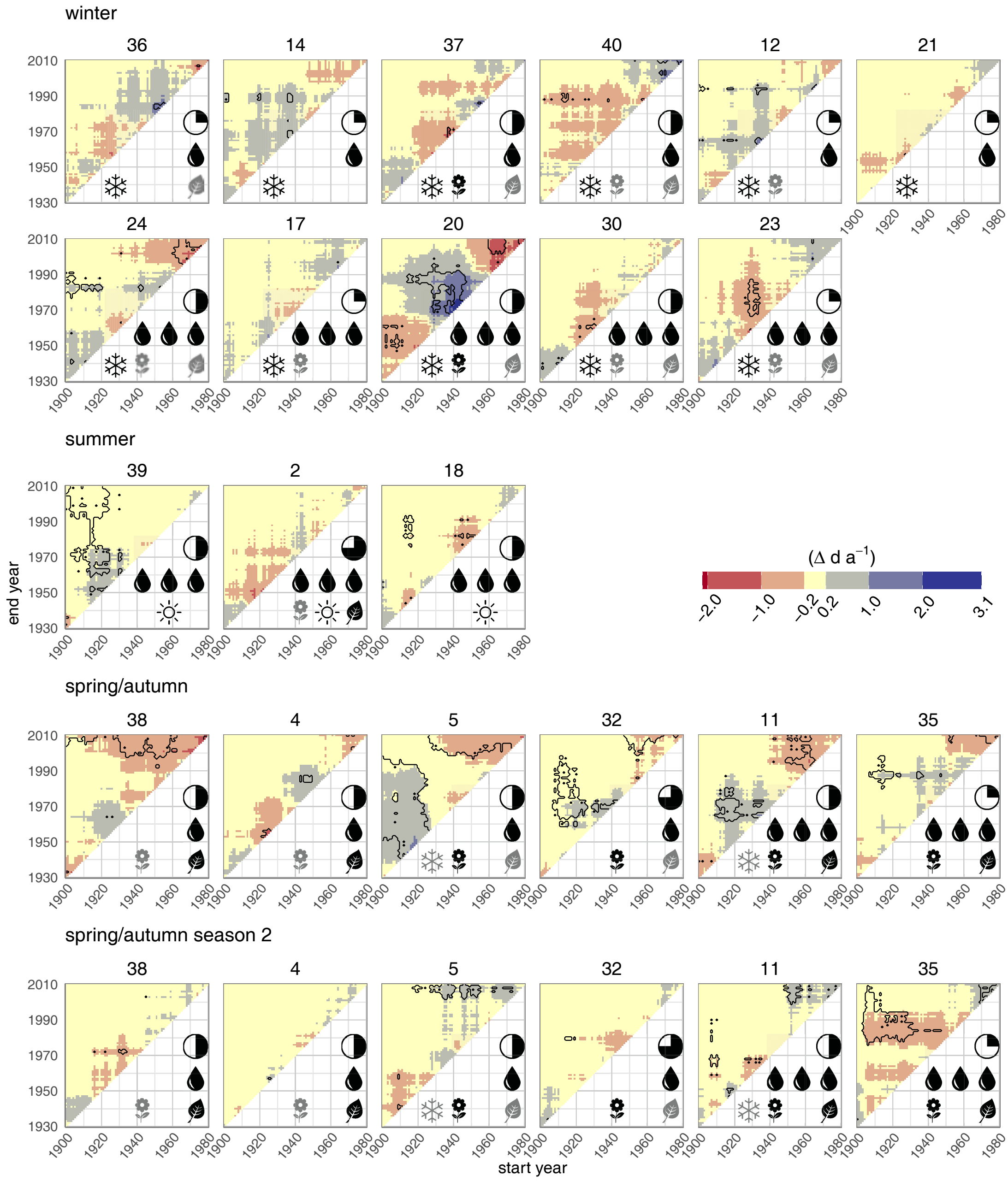

Figure 4.A2: Multiple trends of pattern seasonality (dry and wet patterns only). As in Fig. 4.4

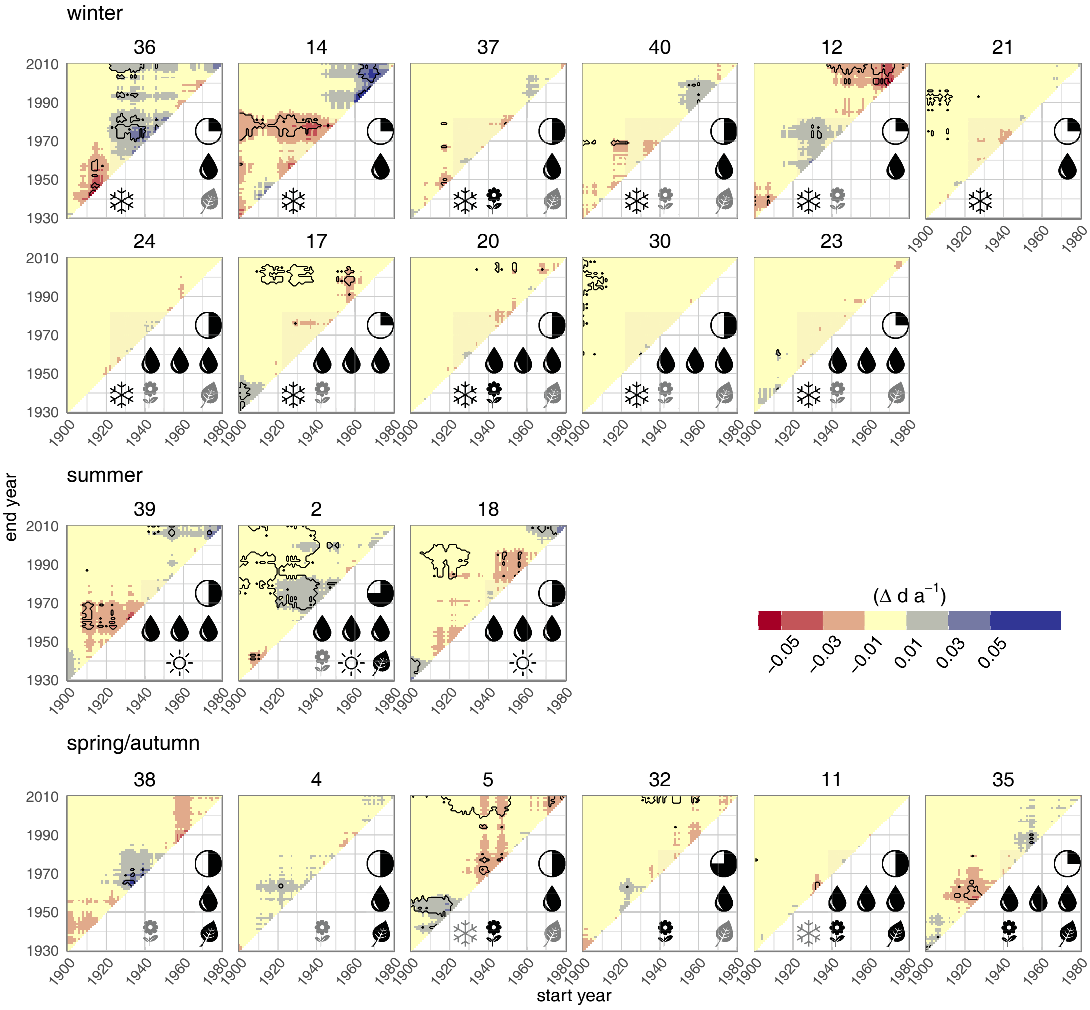

Figure 4.A3: Multiple trends of pattern persistence (dry and wet patterns only). As in Fig. 4.4

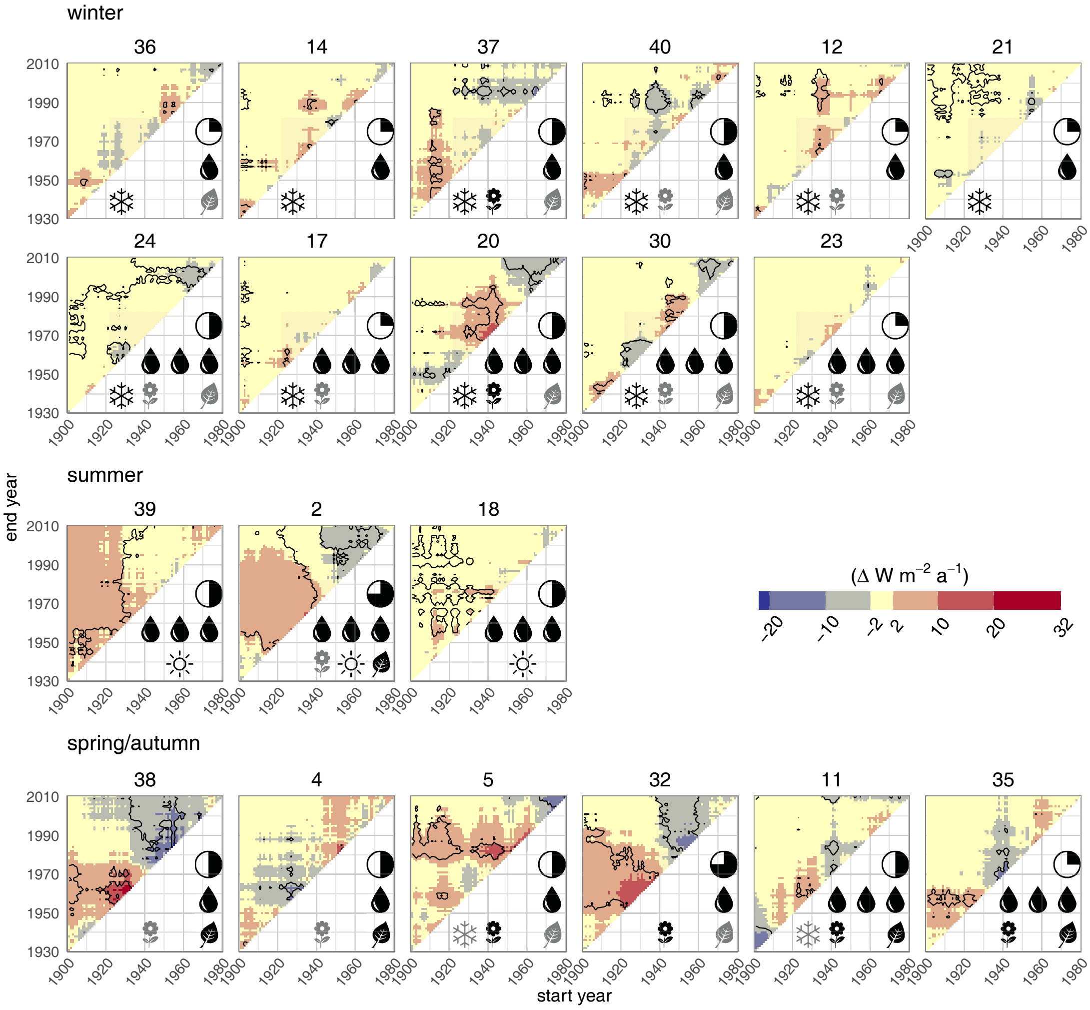

Figure 4.A4: Multiple trends of pattern mean daily shortwave radiation (dry and wet patterns only). As in Fig. 4.5.

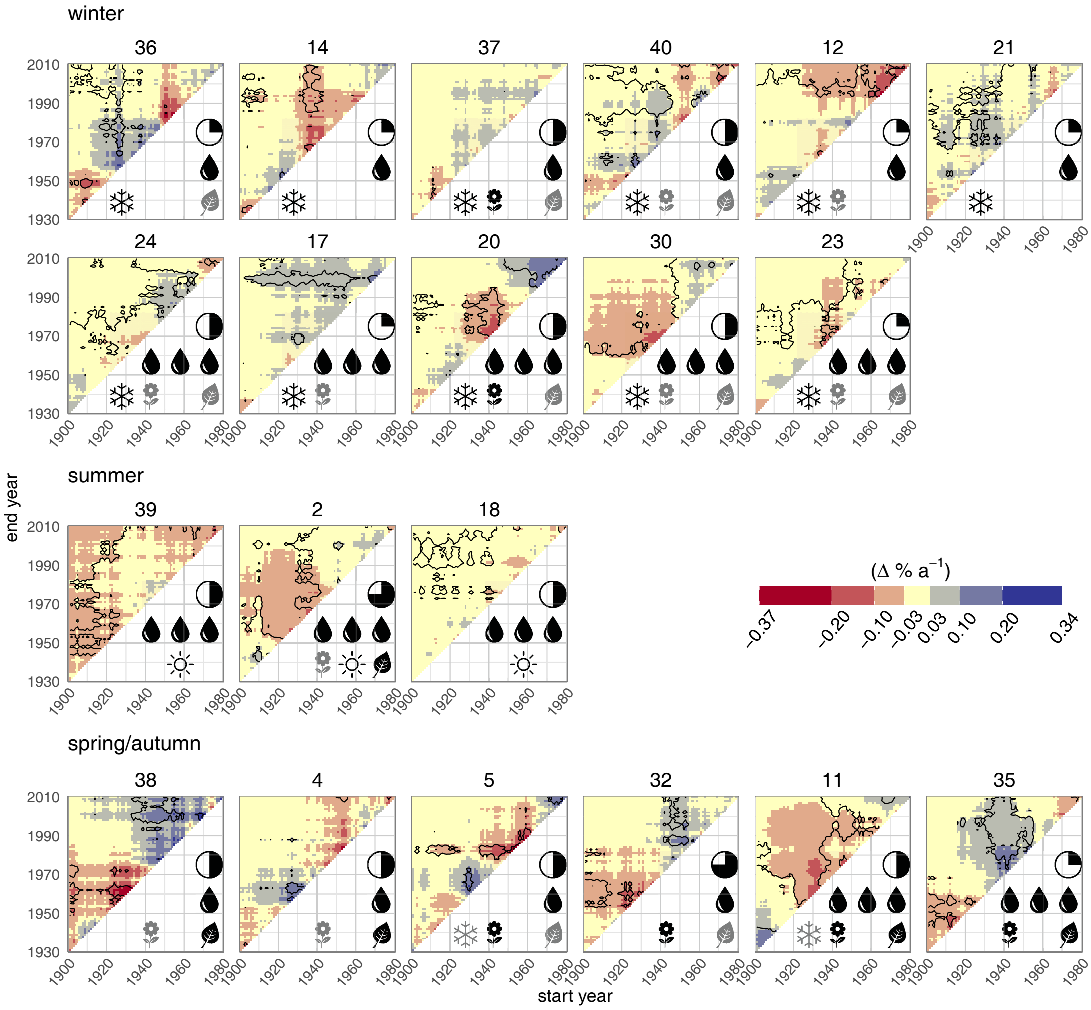

Figure 4.A5: Multiple trends of pattern mean daily relative humidity (dry and wet patterns only). As in Fig. 4.5.

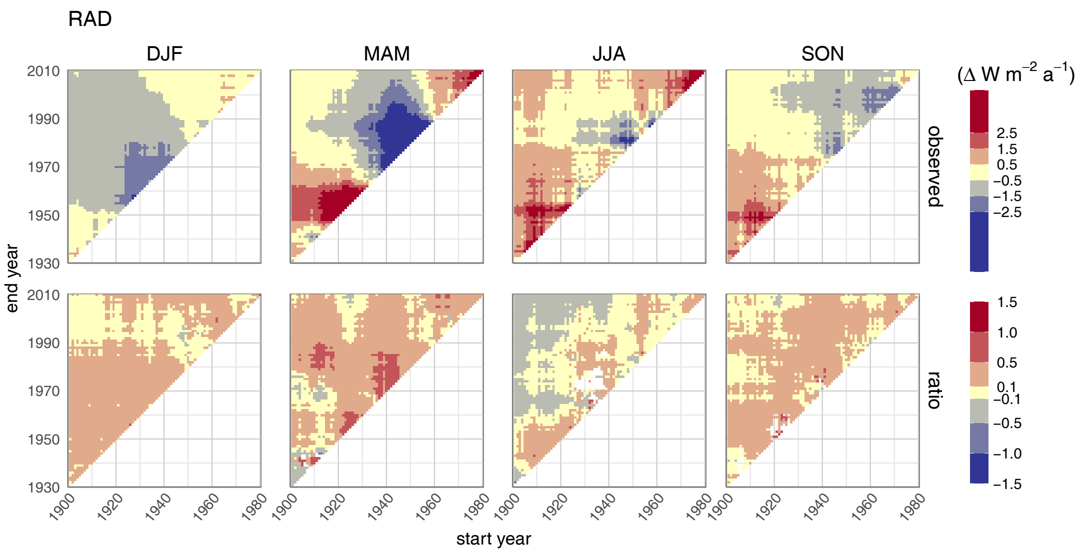

Figure 4.A6: Trends in catchment average mean daily shortwave radiation for all seasons (upper panel) and associated ratio of weather pattern-induced and original trend slopes (see section 4.3.3). Ratios are only calculated for stations with significant original trends and presented as averages across stations. Gaps appear for periods with no significant trends.

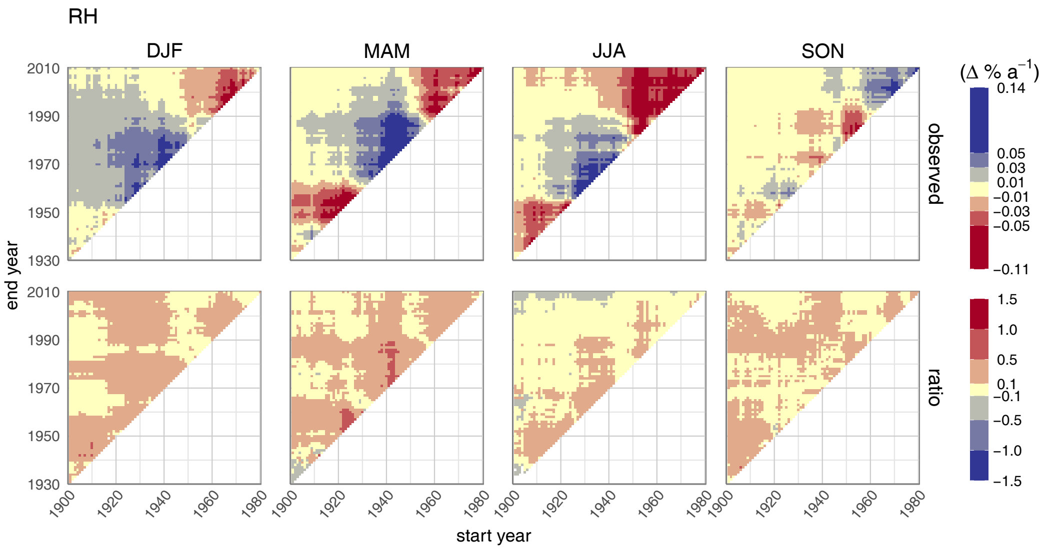

Figure 4.A7: Trends in catchment average daily relative humidity for all seasons. As in Fig. 4.A6.

4.S Supplementary

Contents

Additional supporting information (files available electronically)

1. Archive containing:
    - weather pattern catalogue,
    - mean sea level pressure fields of pattern centroids,
    - 2 m temperature fields of pattern centroids,
    - specific humidity fields of pattern centroids

Introduction

Here we provide additional information on the climate station data used.

The weather pattern classification used in the manuscript was derived using the COST733-CLASS software (http://cost733.geo.uni-augsburg.de/cost733class-1.2/). Details regarding the classification are given in "Can local climate variability be explained by weather patterns? A multi-station evaluation for the Rhine basin".

The classification uses mean sea level pressure, 2 m temperature, and specific humidity from the ERA20C reanalysis in the period 1900–2010. It covers the spatial domain 3–26 °E/43–58 °N with 40 classes/patterns. The classification catalogue (i.e. time series of patterns) and the centroids of the 40 classes are provided here as original data files, along with a plot of the centroids.

Text S1. Description of the climate station data processing and quality control

Climate station data used in this paper were provided by the Potsdam Institute for Climate Impact Research (PIK), obtained from the national meteorological services. The data set used here covers the period 1901–2010. Descriptions of the data processing and quality control for a previous version of the data set (covering the period 1951–2003) are given in Österle et al. (2006a), Österle et al. (2006b), and Österle et al. (2016). The data set was extended to the current period of 1901–2010 as new data became available, using the same procedures. Since the data availability in the beginning of the century is considerably lower, the data set starting in 1901 contains only 1440 stations (of which 432 are located in the Rhine catchment) for Germany compared to 2342 stations for the period starting in 1951.

The data processing done by PIK included filling of missing values and correction of non-natural inhomogeneities such as changes in the station location, measurement methods or devices. The procedure is shortly summarised here, for more detailed information please refer to the given references. Checking for missing values in the data included checking a) for values exceeding the physically possible range of the respective parameter, b) the consistency between average, minimum, and maximum daily temperature and between sun shine duration and cloudiness, and c) the plausibility of occurrence of sequences with the same value. Filling the gaps of a station time series was done by finding the neighbouring station with the highest correlation and adding the difference between the long-term monthly mean values of both stations to the neighbouring station's value. For parameters with a fixed range of values (e.g. relative humidity), the gaps were filled using relative differences. Global shortwave radiation, if not available at the station, was obtained from sunshine duration as described in Österle (2001). Inhomogenities due to the relocation of stations were identified by removing the annual cycle from the data and comparing the time series before and after the relocation using the t-test. If the t-test indicated a significant difference between the two sub-series, the same test was applied to a neighbouring station without relocations. If this station showed the same inhomogeneity, it was judged to be natural. Otherwise the homogeneity was corrected by adapting the sub-series previous to the relocation using a similar procedure as for filling gaps.

In a last step the homogeneity in relation to neighbouring stations was tested, considering 10 neighbouring stations.

Data Set S1. Weather pattern classification files

Archive with classification data files: classification catalogue with columns: year, month, day, weather pattern; netcdf files of pattern centroids.

Figure 4.S1. Plots of pattern centroids

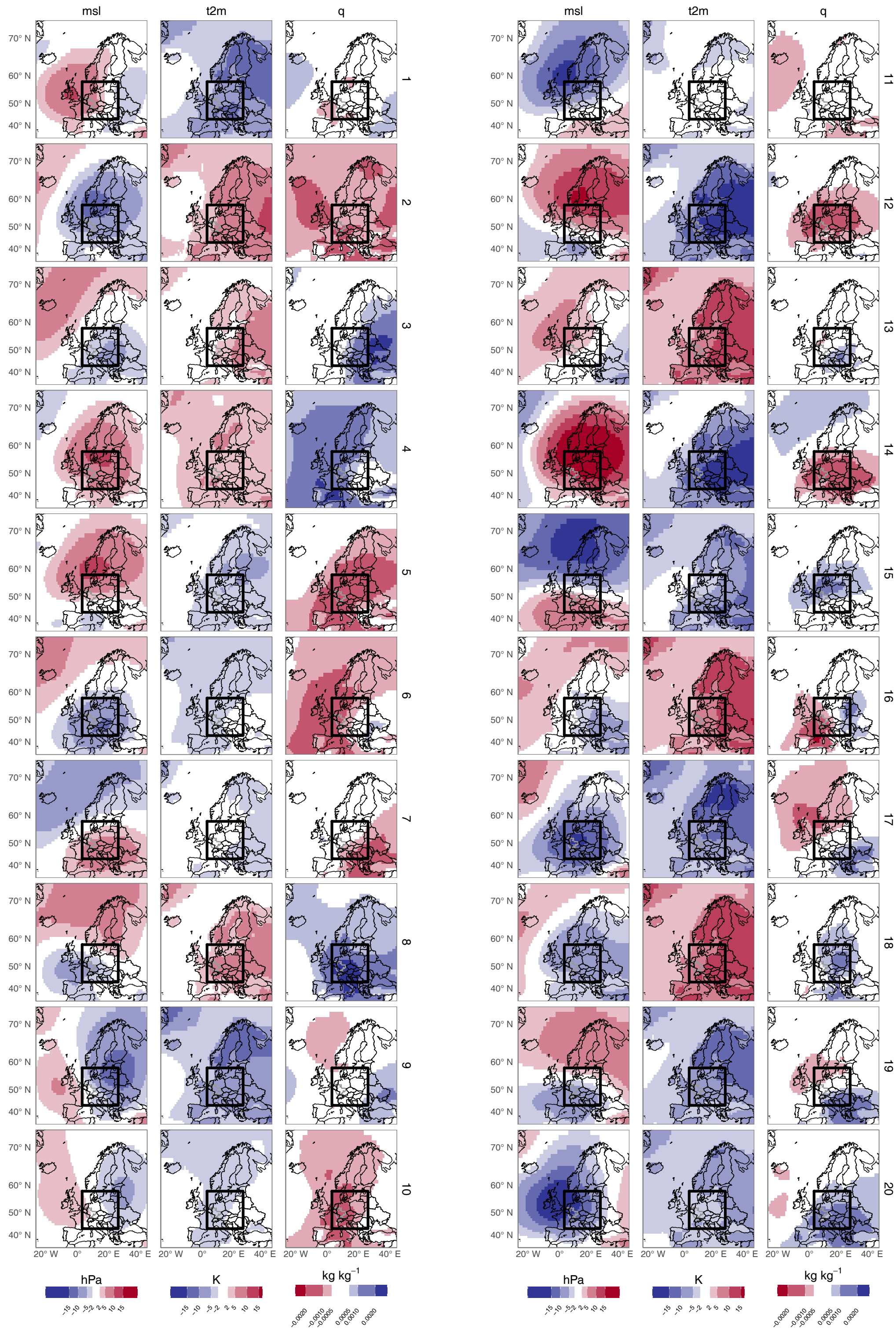

Figure 4.S1: Centroids of msl, t2m, and q anomalies for the 40 patterns. Note that the input fields have been rescaled to [-1,1] for classification (not as shown here) and that for classification only the area enclosed by the rectangle has been considered.

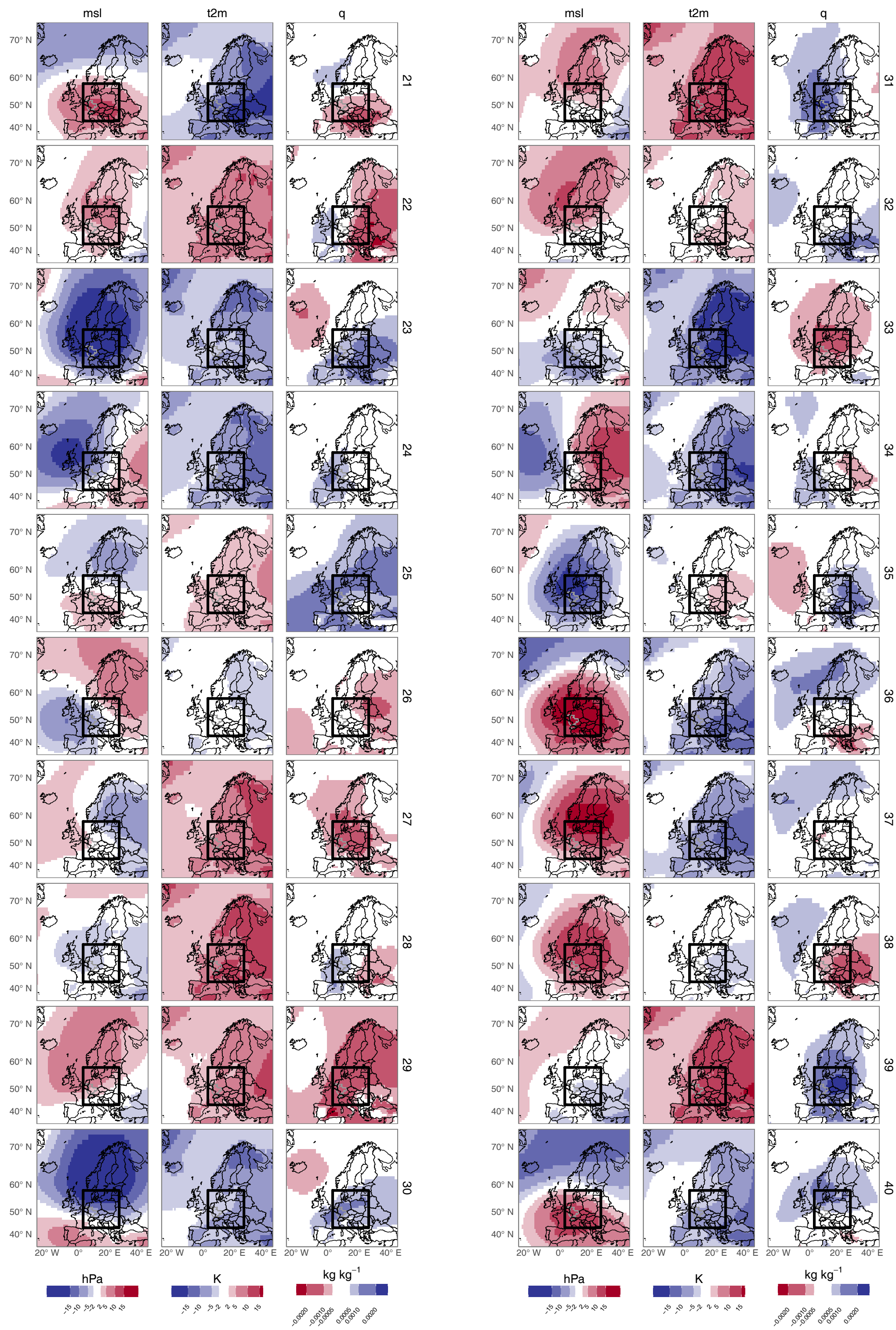

Figure 4.S1: Continued.

Figures 4.S2–4.S4. Plots of multiple between-type trends for all WPs

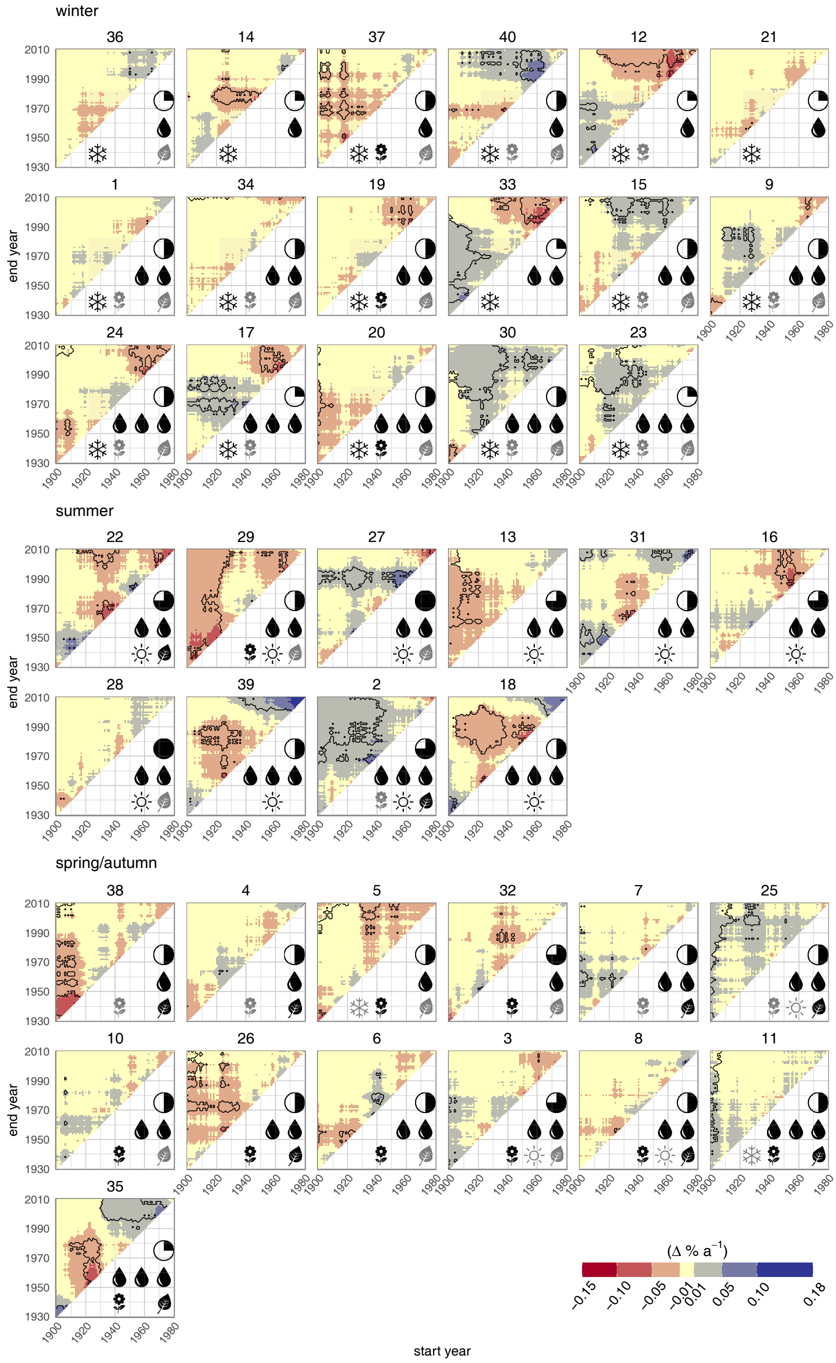

Figure 4.S2: Multiple trends of pattern frequency. Each value of the upper triangle denotes the trend magnitude of a specific period, given by its start year (horizontal axis) and end year (vertical axis). Black contours enclose time periods with statistically significant trends (Mann-Kendall test, $p < 0.05$). Icons as in Figure 4.4, page 73.

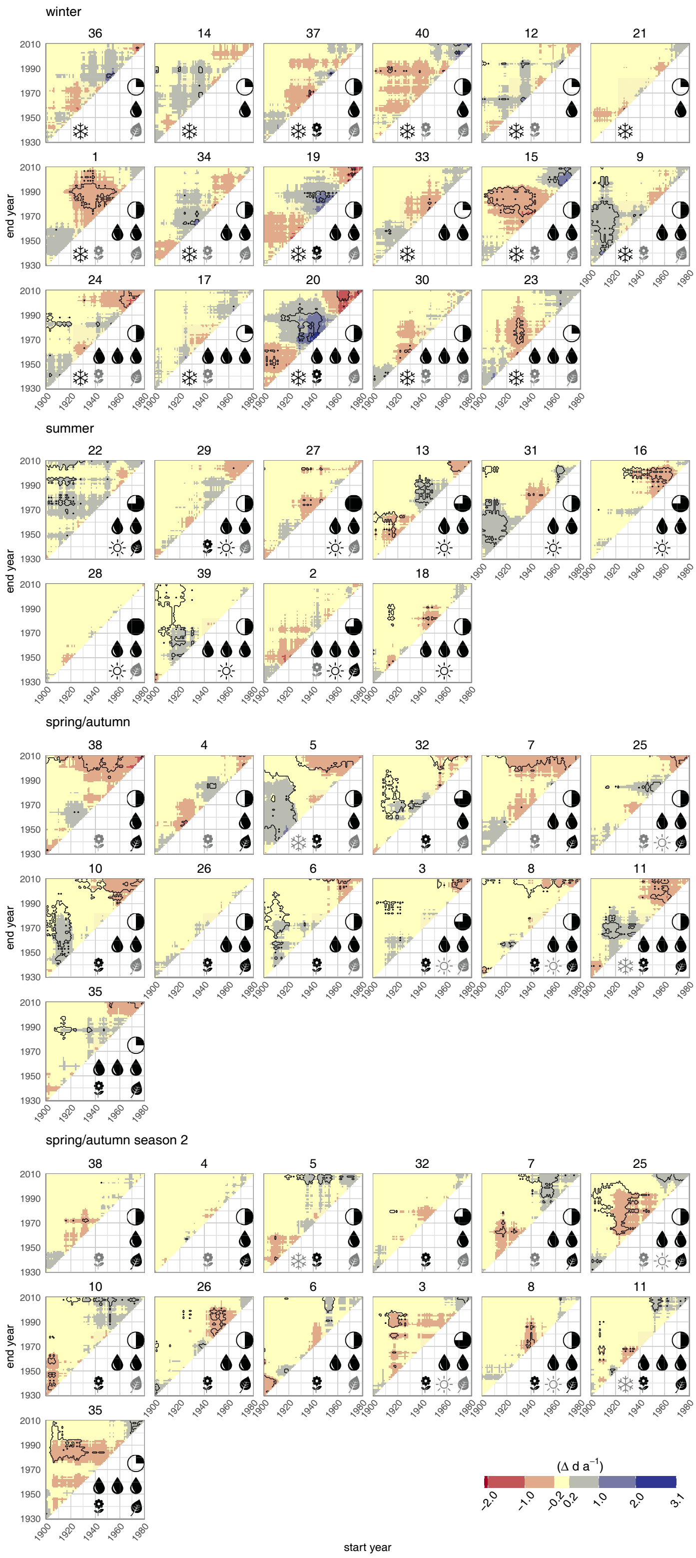

Figure 4.S3: Multiple trends of pattern seasonality. As in Fig. 4.S2

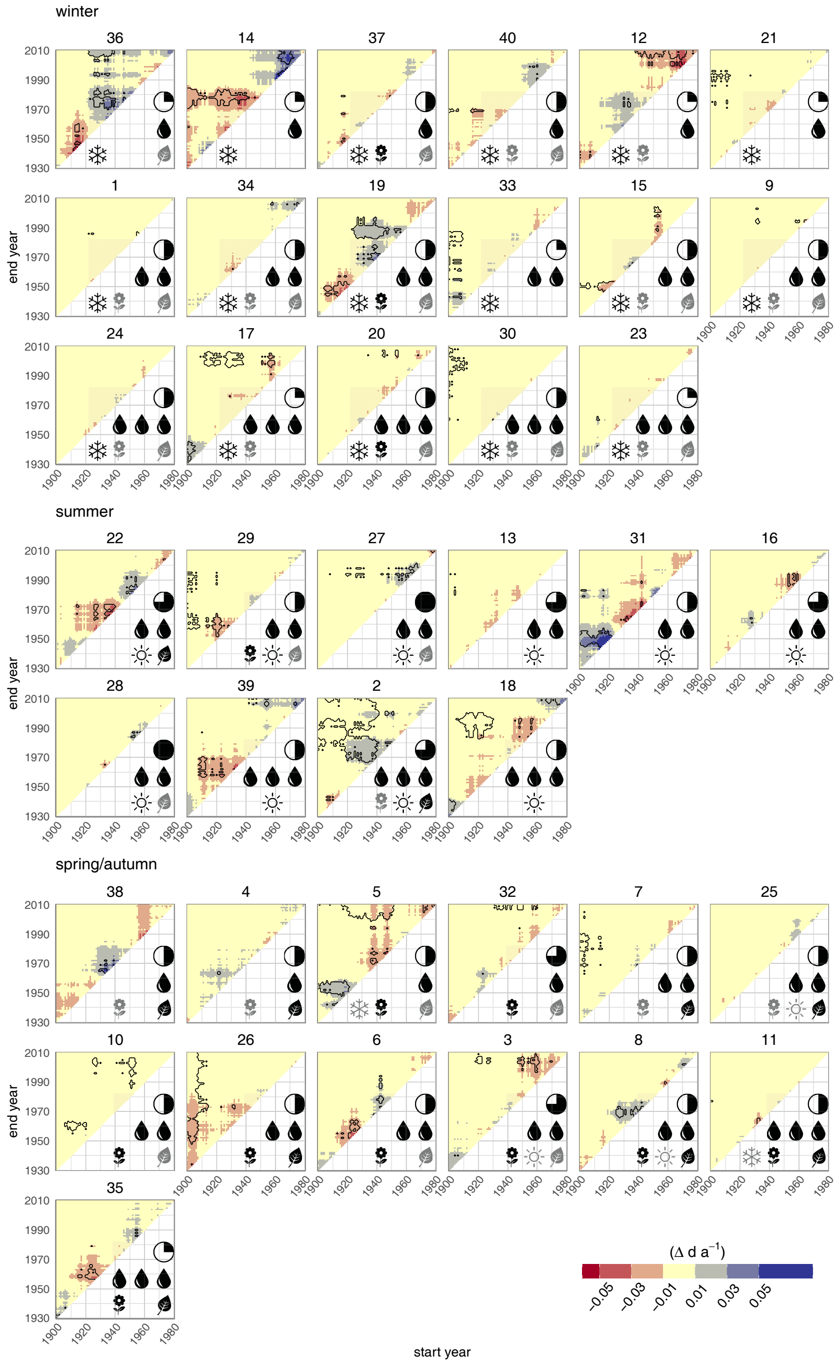

Figure 4.S4: Multiple trends of pattern persistence. As in Fig. 4.S2

Figures 4.S5–4.S8. Plots of multiple within-type trends for all WPs

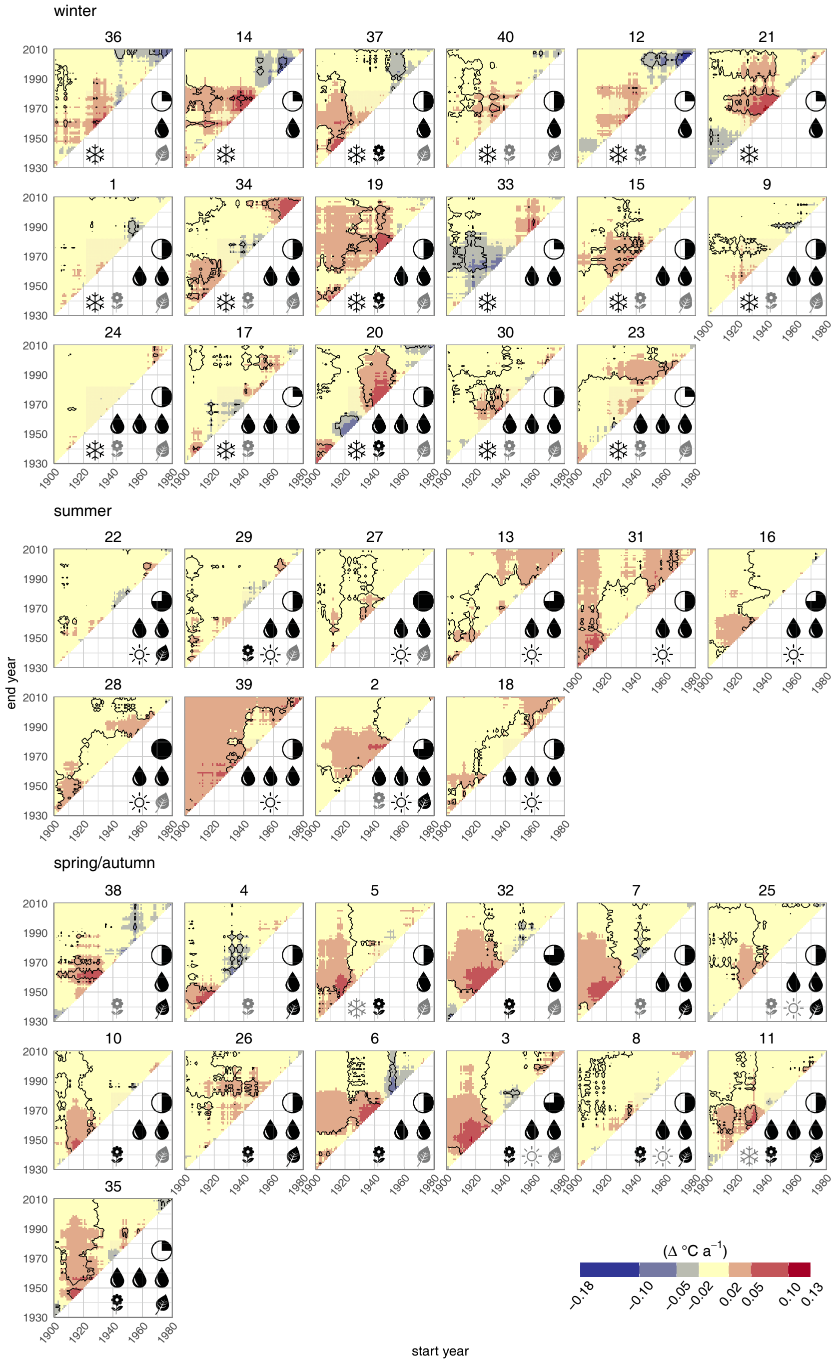

Figure 4.S5: Multiple trends of pattern mean daily temperature. Plot as in Fig. 4.S2, except that black contours enclose time periods with field significant trends ($p < 0.05$).

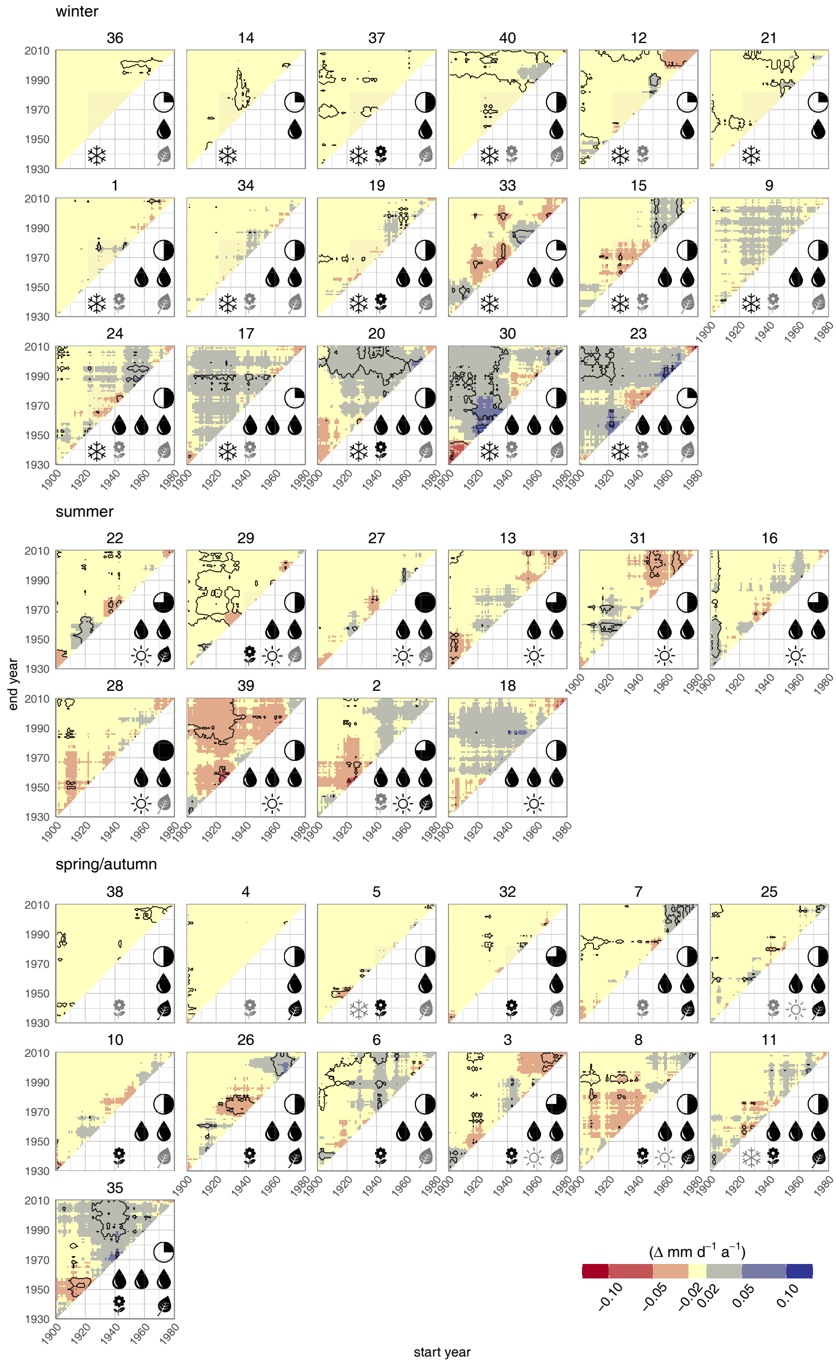

Figure 4.S6: Multiple trends of pattern mean daily precipitation. As in Fig. 4.S5.

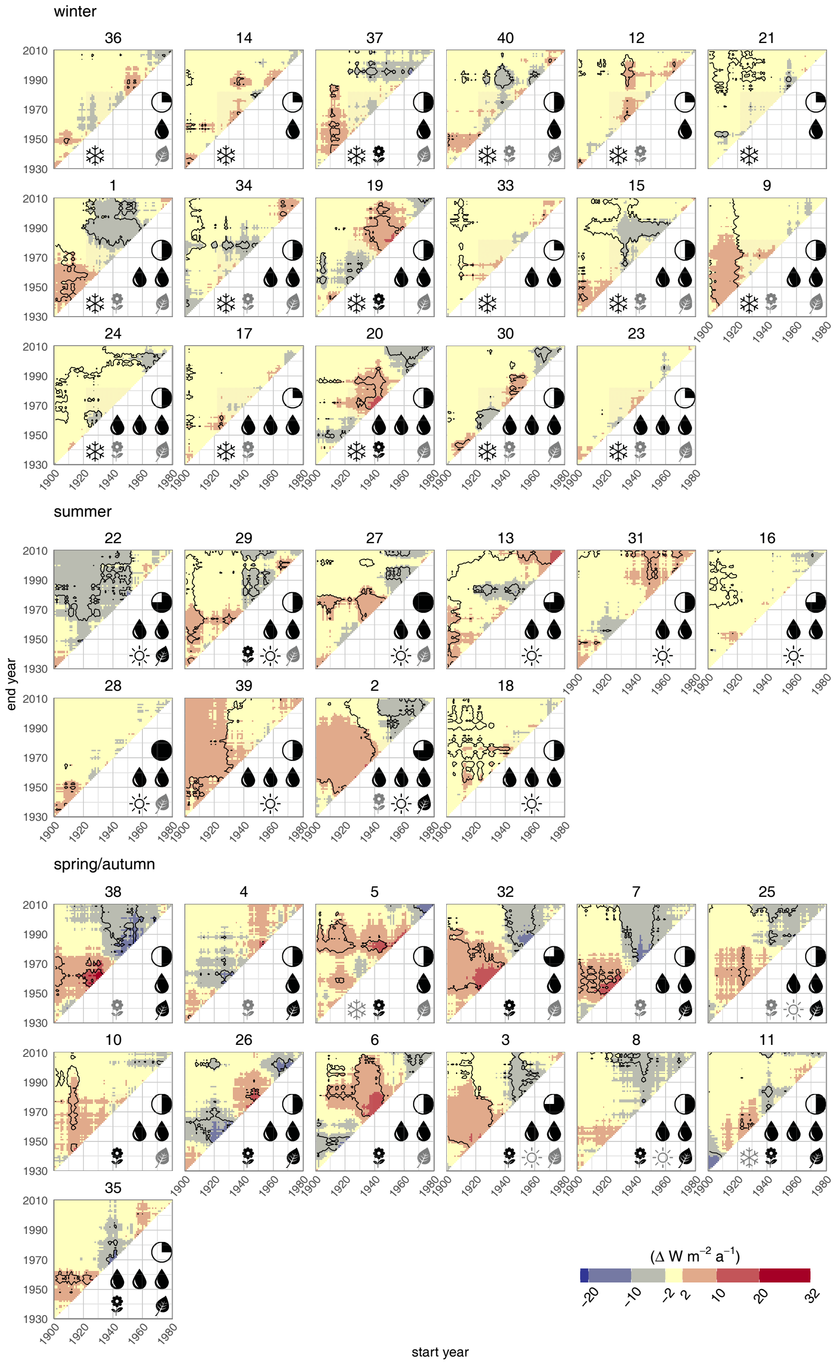

Figure 4.S7: Multiple trends of pattern mean daily shortwave radiation. As in Fig. 4.S5.

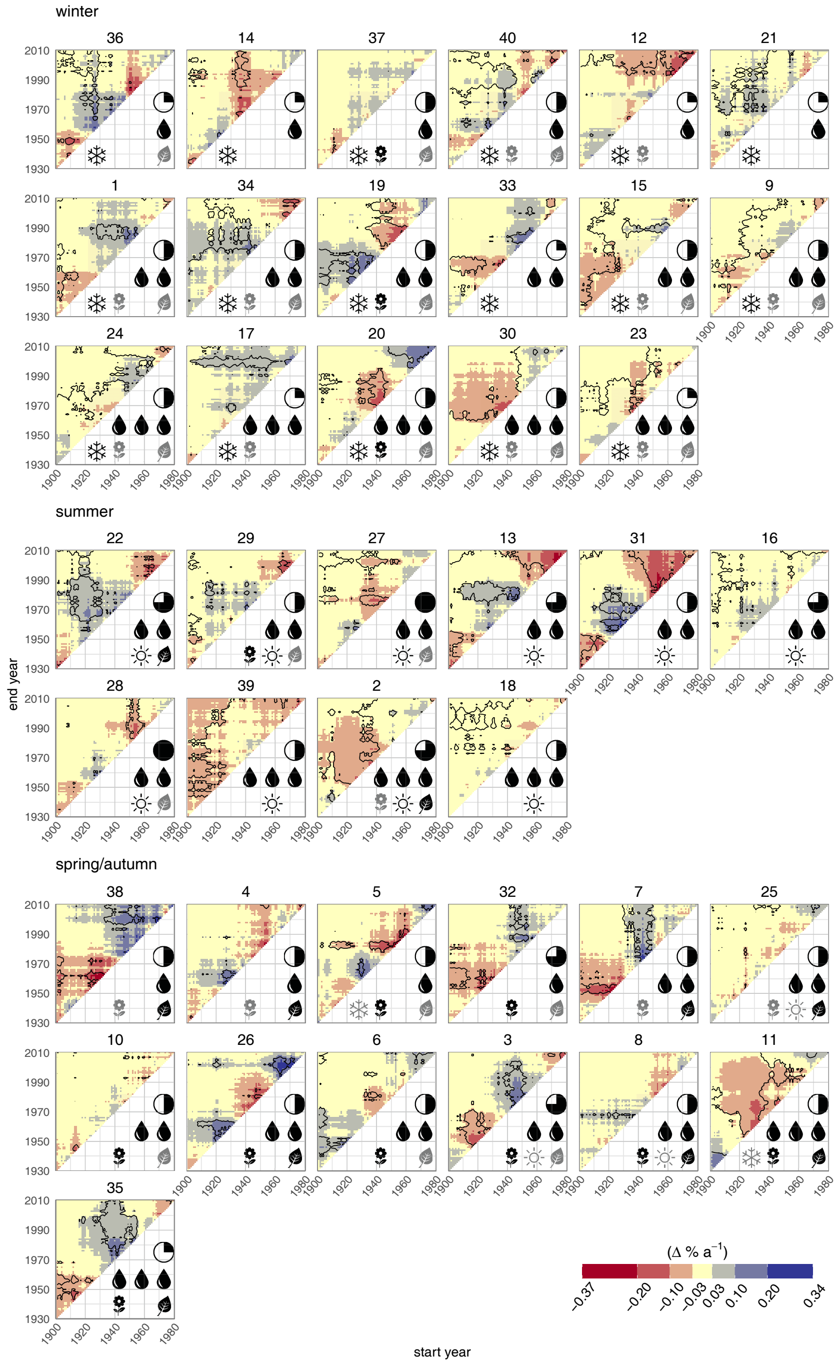

Figure 4.S8: Multiple trends of pattern mean daily relative humidity. As in Fig. 4.S5.

5. Discussion and conclusions

5.1 Main results

The objective of this thesis was to analyse past precipitation changes in Germany and the Rhine basin, and to relate these to changes in weather patterns. Being able to explain precipitation changes by pattern changes allows for using a weather pattern-based approach for downscaling of GCM output to use in climate change attribution studies and helps to understand whether observed precipitation changes are likely to persist or will fluctuate along with decadal oscillations of large-scale atmospheric circulations. This chapter summarises the main achievements with respect to the research questions framed in the beginning.

What changes in precipitation can be detected in the past century?
Are these changes rather decadal fluctuations or long-term trends (persistent in time)?

Changes in precipitation in Germany and the Rhine basin are highly dissimilar, depending on the investigated region, period, season, and even month. A general trend towards more precipitation was found for winter. This trend is persistent basically over the whole century, although the magnitude of the trend is variable (see Figure 4.8, page 78 for spatially aggregated results of the Rhine basin). In chapter 2, a parallel shift in most winter precipitation characteristics was found – total precipitation increases along with daily mean and extreme precipitation as well as persistence of precipitation (i.e. transition probabilities). Although multiple periods were investigated only for mean daily totals, it is to be expected to observe the same parallel behaviour also for other precipitation characteristics throughout the century. Trends towards wetter spring/autumn and dryer summer that were observed for the 1951–2006 period are not persistent during the whole century (see Figure 4.8, page 78). No long-term trend was observed and detected short-term trends are of varying direction, but generally point rather towards increasing spring and autumn precipitation in the second half of the 20th century. Thus, only for winter a clear and long-term persistent trend signal was detected, meaning higher precipitation amounts, longer wet periods, and increased extreme events. In combination with the expected warming, which is also clearly observed in winter temperatures for the Rhine basin (see Figure 4.7, page 77), the increased precipitation is likely to occur in the form of rain rather than snow. Only for the most recent decades (since the 70s), decreasing winter precipitation was observed in the Rhine basin. Whether this trend is going to continue in future, has yet to be validated. The opposite signal was detected for summer precipitation, although the century-long time series shows no signal.

Detected trends do not only differ depending on the time period under consideration, but also show high spatial variability. Thus, it is hardly possible to find a general conclusion that is valid for the entire region. This heterogeneity is also reflected in the large amount of published work on detection of trends in precipitation (see Table 2.1, page 22). Each of these studies represents only one small pixel of the overall image of which this thesis sheds light on, first, a great variety of precipitation characteristics, and, second, a comprehensive range of time periods. Considering the results found here, it is strongly recommended to authors of future trend analysis studies to not only consider the full period of available data, but also investigate sub-periods, as apparent trends may actually consist of different, opposing short-term trends.

Can variability of daily precipitation be explained by weather patterns?
Daily precipitation follows a positively skewed distribution with many observations close to zero and (luckily) only few high and extremely high values. Nearly the full range of these values can be observed under nearly all weather patterns. It was not possible to obtain a classification that associates only a narrow range of precipitation values with each pattern. Nevertheless, the distribution of precipitation differs strongly among patterns and predominantly dry patterns exist as well as patterns with raised likelihood for high and extreme precipitation. In section 3.4.1, page 49 the issue of small explained variance for precipitation was elaborated on in greater detail, showing that the low skill is inherent to the skewed distribution of daily precipitation.

Can precipitation trends be related to changes in large-scale atmospheric patterns?
Large-scale atmospheric circulation is the main driver of local weather. Under the effect of climate change, it is commonly assumed to observe changes in circulation (i.e. changes in the frequency of patterns, termed between-type changes), thus affecting local weather (Beck et al., 2007; Cahynová and Huth, 2010; Hewitson and Crane, 2006). However, circulation may as well remain constant, but simply cause different local weather (termed within-type changes) (Beck et al., 2007; Brinkmann, 1999; Fleig et al., 2015). Within this thesis, a weather pattern classification was developed, optimising the amount of explained variability in local weather for the Rhine basin. Although deriving the optimal classification for the target region, only part of the trends and variability of local precipitation can be attributed to between-type changes. Usually more than half of the magnitude of changes is related to changing internal characteristics of weather patterns. However, within-type changes are highest for periods with low overall trends (see Figure 4.8, page 78), especially in winter and spring. The long-term increasing trend for winter precipitation is related to accordingly increasing frequency of high-intensity winter patterns. Particularly these patterns are highly correlated with the state of large-scale teleconnection indices such as the North Atlantic Oscillation (NAO), the Scandinavian pattern (SCA), the East-Atlantic pattern (EA), and the East-Atlantic/Western-Russia pattern (EAWR). Trends in precipitation can partly be explained by the frequency of weather patterns and these are in turn associated with large-scale circulation. However, a considerable amount of change within the patterns remains, possing a considerable source of uncertainty to any application in downscaling.

5.2 Discussion and directions for further research

5.2.1 Weather pattern classification for downscaling

The skill of an optimised weather pattern classification to explain changes in local precipitation and other variables can be exploited for downscaling of large-scale circulation model output. GCMs are widely known to have deficiencies in correctly representing particularly precipitation (Hewitson and Crane, 2006; Sunyer et al., 2015), but are believed to capture large-scale circulation comparatively well. Thus, it is a promising approach to infer local precipitation and other meteorological variables of interest only from circulation information of the GCMs. These data may then be used, e.g. for running a hydrological model, thus investigating the influence of different climate realisations on streamflow characteristics, such as floods.

A possible further research goal could be to attribute observed changes in floods to climate change, as outlined in Figure 1.3, page 15. The prerequisites to make a weather pattern-based downscaling approach applicable are completed and validated within this thesis. Using a stochastic weather generator that generates fields of local weather conditioned on weather patterns, allows for employing runs of GCMs using different greenhouse gas forcings. The ability of recent GCMs to reproduce the main characteristics of weather patterns has been tested and proven for most of the individual GCMs (see subsection 3.4.2, page 50).

The general skill of weather pattern classification compared to other downscaling methods was recently evaluated for the prediction of droughts in north-eastern Brazil (Delgado et al., 2017). Although the classification used there was, of course, optimised for the specific purpose and region, the classification method and optimisation workflow was the same as used within this thesis. Three different downscaling methods (empirical quantile mapping (Wetterhall et al., 2012), expanded downscaling (Bürger, 1996), weather patterns) in combination with two GCMs were compared by their skill in predicting meteorological drought conditions. While the former two methods work with daily precipitation (and temperature) values from the GCMs as input and allow to directly calculate the desired drought indices, the classification method relates monthly (or even longer) average conditions of different variables at surface and tropospheric levels, such as sea surface temperature, near-surface wind, 850 hPa geopotential height and temperature, to discrete drought index values. The classification approach showed competitive skill in predicting the correct drought index value when considering the full range, but has deficiencies particularly in capturing the extremes (i.e. droughts). Due to the nature of the method to assign only one fixed (averaged) value per pattern, a limited range of values can be predicted only.

However, the downscaling approach outlined in this thesis would combine weather patterns and a stochastic weather generator, thus having the potential to generate different values for the same pattern (the values following the pattern's specific distribution of the respective variable). A good classification would consist of patterns whose distributions are as different from each other as possible. This goal was not completely achieved by the "optimised" classification used here, as indicated in section 3.A. When investigating the empirical distribution of precipitation for each pattern (not shown here), some patterns share a rather similar distribution. In the ideal case, each pattern would be associated with a narrow and very confined range of values for each meteorological variable under consideration. Given this, a changed frequency of patterns would have a clear effect on local climate which would be beneficial in the attribution study. Since this clear stratification of local climate (and especially precipitation) is only partly achieved by the presented classification, it is to be expected to find only small differences in local climate simulated by the stochastic weather generator under the two different "climates". Thus, it has to be summarised that some limitations exist in the outlined attribution approach. These are discussed further in the following section.

5.2.2 Limitations for downscaling

For any application of the weather pattern classification, e.g. as a downscaling tool as described above, one has to keep in mind that a considerable amount of precipitation changes could not be assigned to changing frequency of weather patterns. This amount certainly holds part of the climate change signal and would be missing in the climate data resulting from the downscaling. Thus, two possible errors are to be expected: either the within-type change that is neglected is in the same direction as the between-type change – this would lead to an underestimation of the climate change impact. Or the within-type changes are actually opposing to the between-type changes, which would result in an overestimation. The uncertainties imposed by within-type changes have to be kept in mind when applying a weather pattern-based downscaling approach and attempts should be made to quantify them.

Another drawback in the attribution approach is the low skill of the weather pattern classification to stratify especially precipitation. While for local temperature, due to including temperature as a classification variable, a good stratification (meaning narrow distribution per pattern) was achieved, the possible range of precipitation values per pattern is much wider. This problem was intensively discussed in section 3.4.1, page 49.

Apart from these uncertainties, it should be clearly noted, that the downscaling approach was only validated for the past, i.e. the period on which the patterns have been established. For conditioning a stochastic weather generator on the weather patterns, a distribution per pattern and variable has to be implemented based on observed data. Whether this distribution would hold under future climate change conditions cannot be proved here. However, the same would occur for the hydrological model – is the parametrisation fitted on observed periods still valid in the future? Nevertheless, the first goal when attributing changes in floods to climate change would be to focus on past periods.

5.3 Concluding remarks

Two general conclusions on precipitation changes can be drawn: due to the spatial and temporal heterogeneity of trends, the validity of trend analyses is clearly restricted to the respective time period and region. Changes in precipitation are partly attributable to large-scale circulation changes.

The workflow used here for obtaining an optimal weather pattern classification, can be applied to any other region, as demonstrated by Delgado et al. (2017) for north-eastern Brazil. The very classification used here is limited to the Rhine basin, for which it has been optimised. However, some general advice can be given for further applications: a small spatial domain, combined with a reasonably high number of classes allows for a good stratification of local variables. Although the weather pattern classification mixes information on the atmospheric circulation with thermo-dynamic variables, which hampers the physical interpretability (see related discussion in subsection 1.1.2, page 12), the correlation to large-scale circulation modes (chapter 4, page 63) demonstrates that the patterns derived are able to capture the general circulation. The addition of temperature as a classification variable aids in adding seasonal information which is valuable when conditioning a weather generator for generating continuous time series of local climate data.

This thesis validates the necessary assumptions for a downscaling approach based on weather patterns and a weather generator. Any further work in this direction may directly build upon the results obtained here.

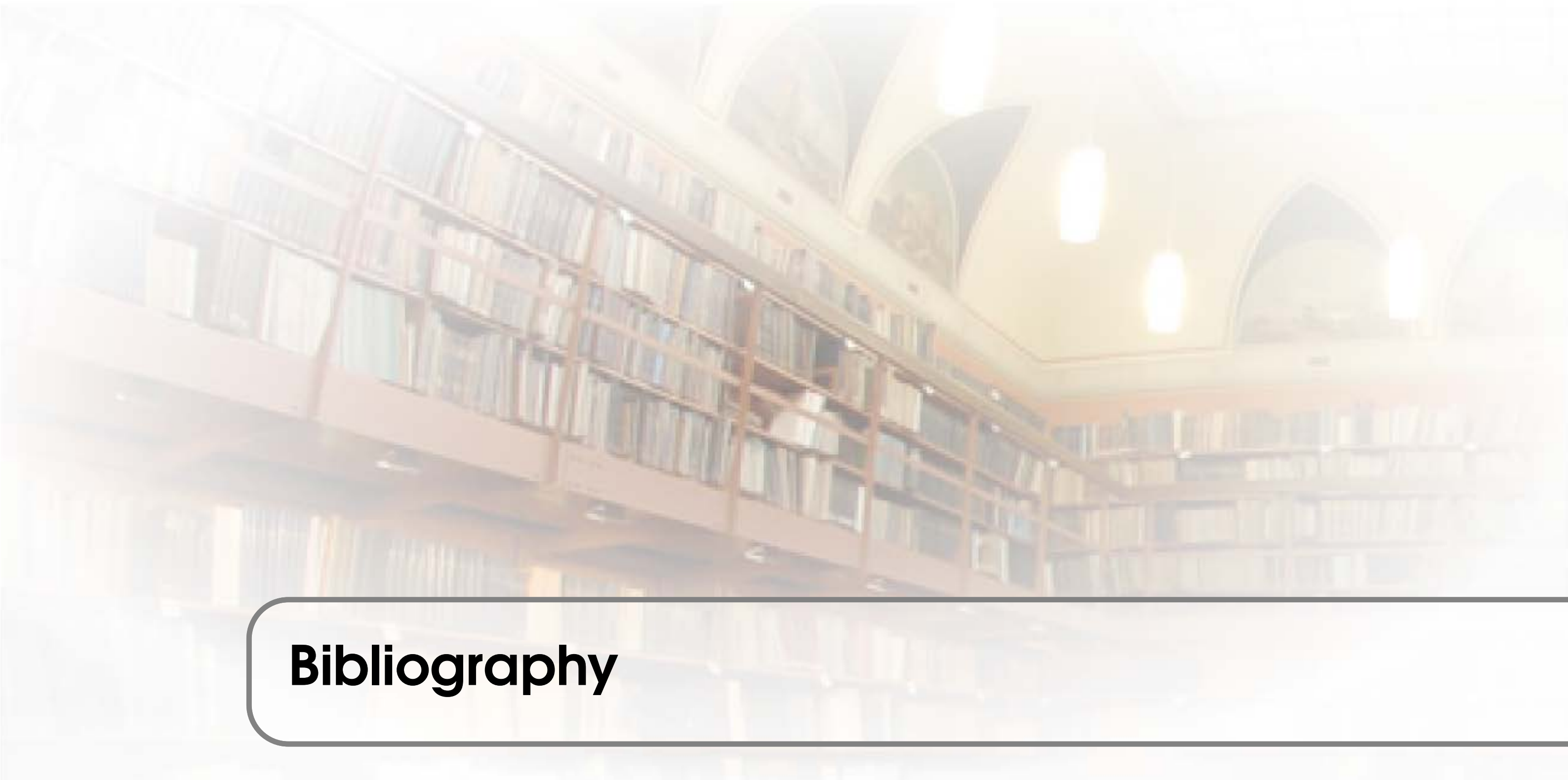

Bibliography

Alexander, L. V., Zhang, X., Peterson, T. C., Caesar, J., Gleason, B., Klein Tank, A. M. G., Haylock, M., Collins, D., Trewin, B., Rahimzadeh, F., et al. (2006). "Global observed changes in daily climate extremes of temperature and precipitation". In: *Journal of Geophysical Research: Atmospheres* 111.D5. DOI: 10.1029/2005jd006290.

Anagnostopoulou, C., Tolika, K., Maheras, P., Kutiel, H., and Flocas, H. A. (2008). "Performance of the general circulation HadAM3P model in simulating circulation types over the Mediterranean region". In: *International Journal of Climatology* 28.2, pp. 185–203. DOI: 10.1002/joc.1521.

Andronova, N. G. and Schlesinger, M. E. (2000). "Causes of global temperature changes during the 19th and 20th centuries". In: *Geophysical Research Letters* 27.14, pp. 2137–2140.

Bárdossy, A. and Plate, E. J. (1991). "Modeling daily rainfall using a semi-Markov representation of circulation pattern occurrence". In: *Journal of Hydrology* 122.1, pp. 33–47. DOI: 10.1016/0022-1694(91)90170-M.

Bárdossy, A. and Plate, E. J. (1992). "Space-time model for daily rainfall using atmospheric circulation patterns". In: *Water Resources Research* 28.5, pp. 1247–1259. DOI: 10.1029/91WR02589.

Bárdossy, A., Stehlík, J., and Caspary, H.-J. (2002). "Automated objective classification of daily circulation patterns for precipitation and temperature downscaling based on optimized fuzzy rules". In: *Climate Research* 23.1, pp. 11–22. DOI: 10.3354/cr023011.

Barnston, A. G. and Livezey, R. E. (1987). "Classification, seasonality and persistence of low-frequency atmospheric circulation patterns". In: *Monthly weather review* 115.6, pp. 1083–1126.

Bayliss, A. C. and Jones, R. C. (1993). *Peaks-over-threshold flood database: Summary statistics and seasonality*. Institute of Hydrology.

van Bebber, W. J. (1892). *Das Wetter in den barometrischen Maxima*. Hammerich & Lesser.

Beck, C., Jacobeit, J., and Jones, P. D. (2007). "Frequency and within-type variations of large-scale circulation types and their effects on low-frequency climate variability in central europe since 1780". In: *International Journal of Climatology* 27.4, pp. 473–491. DOI: 10.1002/joc.1410.

Beck, C. and Philipp, A. (2010). "Evaluation and comparison of circulation type classifications for the European domain". In: *Physics and Chemistry of the Earth* 35.9-12, pp. 374–387. DOI: 10.1016/j.pce.2010.01.001.

Belleflamme, A., Fettweis, X., and Erpicum, M. (2014). “Do global warming-induced circulation pattern changes affect temperature and precipitation over Europe during summer?” In: *International Journal of Climatology* 35.7, pp. 1484–1499. DOI: 10.1002/joc.4070.

Belleflamme, A., Fettweis, X., Lang, C., and Erpicum, M. (2013). “Current and future atmospheric circulation at 500 hPa over Greenland simulated by the CMIP3 and CMIP5 global models”. In: *Climate Dynamics* 41.7-8, pp. 2061–2080. DOI: 10.1007/s00382-012-1538-2.

van den Besselaar, E. J. M., Klein Tank, A. M. G., and Buishand, T. A. (2013). “Trends in European precipitation extremes over 1951–2010”. In: *International Journal of Climatology* 33.12, pp. 2682–2689. DOI: 10.1002/joc.3619.

Bettolli, M. L. and Penalba, O. C. (2012). “Synoptic sea level pressure patterns-daily rainfall relationship over the Argentine Pampas in a multi-model simulation”. In: *Meteorological Applications* 21.2, pp. 376–383. DOI: 10.1002/met.1349.

Bissolli, P. and Dittmann, E. (2001). “The objective weather type classification of the German Weather Service and its possibilities of application to environmental and meteorological investigations”. In: *Meteorologische Zeitschrift* 10.4, pp. 253–260. DOI: 10.1127/0941-2948/2001/0010-0253.

Bosshard, T., Kotlarski, S., Zappa, M., and Schär, C. (2014). “Hydrological Climate-Impact Projections for the Rhine River: GCM–RCM Uncertainty and Separate Temperature and Precipitation Effects”. In: *Journal of Hydrometeorology* 15.2, pp. 697–713. DOI: 10.1175/jhm-d-12-098.1.

Brands, S., Herrera, S., Fernández, J., and Gutiérrez, J. M. (2013). “How well do CMIP5 Earth System Models simulate present climate conditions in Europe and Africa?” In: *Climate Dynamics* 41.3, pp. 803–817. DOI: 10.1007/s00382-013-1742-8.

Brezowsky, H. and Hess, P. (1952). “Katalog der Großwetterlagen Europas”. In: *Berichte der Deutscher Wetterdenst in der US-Zone* 33.

Brienen, S., Kapala, A., Mächel, H., and Simmer, C. (2013). “Regional centennial precipitation variability over Germany from extended observation records”. In: *International Journal of Climatology* 33.9, pp. 2167–2184. DOI: 10.1002/joc.3581.

Brinkmann, W. A. R. (1999). “Within-type variability of 700 hPa winter circulation patterns over the Lake Superior basin”. In: *International Journal of Climatology* 19.1, pp. 41–58.

Brinkmann, W. A. R. (2000). “Modification of a correlation-based circulation pattern classification to reduce within-type variability of temperature and precipitation”. In: *International Journal of Climatology* 20.8, pp. 839–852. DOI: 10.1002/1097-0088(20000630)20:8<839::aid-joc500>3.0.co;2-x.

Brisson, E., Demuzere, M., Kwakernaak, B., and Van Lipzig, N. P. M. (2010). “Relations between atmospheric circulation and precipitation in Belgium”. In: *Meteorology and Atmospheric Physics* 111.1-2, pp. 27–39. DOI: 10.1007/s00703-010-0103-y.

Bronstert, A., Agarwal, A., Boessenkool, B., Fischer, M., Heistermann, M., Köhn-Reich, L., Moran, T., and Wendi, D. (2017). “Die Sturzflut von Braunsbach am 29. Mai 2016 – Entstehung, Ablauf und Schäden eines "‘Jahrhundertereignisses"’. Teil 1: Meteorologische und hydrologische Analyse”. In: *Hydrologie & Wasserbewirtschaftung* 61.3, pp. 150–162. DOI: 10.5675/HyWa_2017,3_1.

Bueh, C. and Nakamura, H. (2007). “Scandinavian pattern and its climatic impact”. In: *Quarterly Journal of the Royal Meteorological Society* 133.629, pp. 2117–2131.

Bürger, G., Heistermann, M., and Bronstert, A. (2014). “Towards Subdaily Rainfall Disaggregation via Clausius–Clapeyron”. In: *Journal of Hydrometeorology* 15.3, pp. 1303–1311. DOI: 10.1175/jhm-d-13-0161.1.

Bürger, G. (1996). “Expanded downscaling for generating local weather scenarios”. In: *Climate Research* 7.2, pp. 111–128.

Cahynová, M. and Huth, R. (2010). “Circulation vs. climatic changes over the Czech Republic: A comprehensive study based on the COST733 database of atmospheric circulation classifications”. In: *Physics and Chemistry of the Earth* 35.9-12, pp. 422–428. DOI: 10.1016/j.pce.2009.11.002.

Cahynová, M. and Huth, R. (2016). “Atmospheric circulation influence on climatic trends in Europe: an analysis of circulation type classifications from the COST733 catalogue”. In: *International Journal of Climatology* 36.7, pp. 2743–2760. DOI: 10.1002/joc.4003.

Caliński, T. and Harabasz, J. (1974). “A dendrite method for cluster analysis”. In: *Communications in Statistics – Theory and Methods* 3.1, pp. 1–27. DOI: 10.1080/03610927408827101.
Comas-Bru, L. and McDermott, F. (2014). “Impacts of the EA and SCA patterns on the European twentieth century NAO–winter climate relationship”. In: *Quarterly Journal of the Royal Meteorological Society* 140.679, pp. 354–363.
Corte-Real, J., Hu, H., and Qian, B. (1999). “A weather generator for obtaining daily precipitation scenarios based on circulation patterns”. In: *Climate Research* 13.1, pp. 61–75.
Corti, S., Molteni, F., and Palmer, T. N. (1999). “Signature of recent climate change in frequencies of natural atmospheric circulation regimes”. In: *Nature* 398.6730, pp. 799–802.
Dankers, R. and Feyen, L. (2009). “Flood hazard in Europe in an ensemble of regional climate scenarios”. In: *Journal of Geophysical Research* 114.D16, p. D16108. DOI: 10.1029/2008JD011523.
Delgado, J. M., Voss, S., Bürger, G., Vormoor, K., Murawski, A., Rodrigues, M., Martins, E., Vasconcelos Júnior, F., and Francke, T. (2017). “Seasonal Drought Prediction for Semiarid Northeast Brazil: Verification of Six Hydro-Meteorological Forecast Products”. In: *Hydrology and Earth System Sciences Discussions*, pp. 1–18. DOI: 10.5194/hess-2017-572.
Douglas, E. M., Vogel, R. M., and Kroll, C. N. (2000). “Trends in floods and low flows in the United States: impact of spatial correlation”. In: *Journal of hydrology* 240.1, pp. 90–105. DOI: 10.1016/s0022-1694(00)00336-x.
Duethmann, D., Bolch, T., Farinotti, D., Kriegel, D., Vorogushyn, S., Merz, B., Pieczonka, T., Jiang, T., Su, B., and Güntner, A. (2015). “Attribution of streamflow trends in snow and glacier melt-dominated catchments of the Tarim River, Central Asia”. In: *Water Resources Research* 51.6, pp. 4727–4750. DOI: 10.1002/2014WR016716.
Elshamy, M. E., Wheater, H. S., Gedney, N., and Huntingford, C. (2006). “Evaluation of the rainfall component of a weather generator for climate impact studies”. In: *Journal of Hydrology* 326.1-4, pp. 1–24. DOI: 10.1016/j.jhydrol.2005.09.017.
Enke, W., Schneider, F., and Deutschländer, T. (2005a). “A novel scheme to derive optimized circulation pattern classifications for downscaling and forecast purposes”. In: *Theoretical and Applied Climatology* 82.1-2, pp. 51–63. DOI: 10.1007/s00704-004-0116-x.
Enke, W. and Spekat, A. (1997). “Downscaling climate model outputs into local and regional weather elements by classification and regression”. In: *Climate Research* 8.3, pp. 195–207.
Enke, W., Deutschländer, T., Schneider, F., and Küchler, W. (2005b). “Results of five regional climate studies applying a weather pattern based downscaling method to ECHAM4 climate simulation”. In: *Meteorologische Zeitschrift* 14.2, pp. 247–257. DOI: 10.1127/0941-2948/2005/0028.
Falter, D., Schröter, K., Dung, N. V., Vorogushyn, S., Kreibich, H., Hundecha, Y., Apel, H., and Merz, B. (2015). “Spatially coherent flood risk assessment based on long-term continuous simulation with a coupled model chain”. In: *Journal of Hydrology* 524, pp. 182–193. DOI: 10.1016/j.jhydrol.2015.02.021.
Fatichi, S., Ivanov, V. Y., and Caporali, E. (2011). “Simulation of future climate scenarios with a weather generator”. In: *Advances in Water Resources* 34.4, pp. 448–467. DOI: 10.1016/j.advwatres.2010.12.013.
Fleig, A. K., Tallaksen, L. M., James, P., Hisdal, H., and Stahl, K. (2015). “Attribution of European precipitation and temperature trends to changes in synoptic circulation”. In: *Hydrology and Earth System Sciences* 19.7, pp. 3093–3107. DOI: 10.5194/hess-19-3093-2015.
Førland, E. J. and Hanssen-Bauer, I. (2000). “Increased precipitation in the Norwegian Arctic: true or false?” In: *Climatic Change* 46.4, pp. 485–509.
Fowler, H. J., Blenkinsop, S., and Tebaldi, C. (2007). “Linking climate change modelling to impacts studies: recent advances in downscaling techniques for hydrological modelling”. In: *International Journal of Climatology* 27.12, pp. 1547–1578. DOI: 10.1002/joc.1556.
Fowler, H. J., Kilsby, C. G., and O’Connell, P. E. (2000). “A stochastic rainfall model for the assessment of regional water resource systems under changed climatic condition”. In: *Hydrology and Earth System Sciences* 4.2, pp. 263–281. DOI: 10.5194/hess-4-263-2000.
Fowler, H. J., Kilsby, C. G., O’Connell, P. E., and Burton, A. (2005). “A weather-type conditioned multi-site stochastic rainfall model for the generation of scenarios of climatic variability and

change". In: *Journal of Hydrology* 308.1-4, pp. 50–66. DOI: 10.1016/j.jhydrol.2004.10.021.

Francis, J. A. and Vavrus, S. J. (2012). "Evidence linking Arctic amplification to extreme weather in mid-latitudes". In: *Geophysical Research Letters* 39.6. DOI: 10.1029/2012gl051000.

Furrer, E. M. and Katz, R. W. (2008). "Improving the simulation of extreme precipitation events by stochastic weather generators". In: *Water Resources Research* 44.12. DOI: 10.1029/2008wr007316.

Goodess, C. M. and Jones, P. D. (2002). "Links between circulation and changes in the characteristics of Iberian rainfall". In: *International Journal of Climatology* 22.13, pp. 1593–1615. DOI: 10.1002/joc.810.

Groisman, P. Y., Karl, T. R., Easterling, D. R., Knight, R. W., Jamason, P. F., Hennessy, K. J., Suppiah, R., Page, C. M., Wibig, J., Fortuniak, K., Razuvaev, V. N., Douglas, A., Førland, E., and Zhai, P.-M. (1999). "Changes in the probability of heavy precipitation: important indicators of climatic change". In: *Weather and Climate Extremes*. Springer, pp. 243–283. DOI: 10.1007/978-94-015-9265-9_15.

Groisman, P. Y., Knight, R. W., Easterling, D. R., Karl, T. R., Hegerl, G. C., and Razuvaev, V. N. (2005). "Trends in intense precipitation in the climate record". In: *Journal of climate* 18.9, pp. 1326–1350. DOI: 10.1175/jcli3339.1.

Haberlandt, U., Belli, A., and Bárdossy, A. (2015). "Statistical downscaling of precipitation using a stochastic rainfall model conditioned on circulation patterns – an evaluation of assumptions". In: *International Journal of Climatology* 35.3, pp. 417–432. DOI: 10.1002/joc.3989.

Hamlet, A. F. and Lettenmaier, D. P. (2007). "Effects of 20th century warming and climate variability on flood risk in the western U.S." In: *Water Resources Research* 43.6, W06427. DOI: 10.1029/2006WR005099.

Hamlet, A. F., Mote, P. W., Clark, M. P., and Lettenmaier, D. P. (2007). "Twentieth-century trends in runoff, evapotranspiration, and soil moisture in the western United States". In: *Journal of Climate* 20, pp. 1468–1486. DOI: doi:10.1175/JCLI4051.1.

Hänsel, S., Petzold, S., and Matschullat, J. (2009). "Precipitation trend analysis for central eastern Germany 1851–2006". In: *Bioclimatology and natural hazards*. Springer, pp. 29–38. DOI: 10.1007/978-1-4020-8876-6_3.

Hewitson, B. C. and Crane, R. G. (2006). "Consensus between GCM climate change projections with empirical downscaling: precipitation downscaling over South Africa". In: *International Journal of Climatology* 26.10, pp. 1315–1337. DOI: 10.1002/joc.1314.

Hundecha, Y. and Bárdossy, A. (2005). "Trends in daily precipitation and temperature extremes across western Germany in the second half of the 20th century". In: *International Journal of Climatology* 25.9, pp. 1189–1202. DOI: 10.1002/joc.1182.

Hundecha, Y. and Merz, B. (2012). "Exploring the relationship between changes in climate and floods using a model-based analysis". In: *Water Resources Research* 48.4, W04512. DOI: 10.1029/2011wr010527.

Hundecha, Y., Pahlow, M., and Schumann, A. (2009). "Modeling of daily precipitation at multiple locations using a mixture of distributions to characterize the extremes". In: *Water Resources Research* 45.12, W12412. DOI: 10.1029/2008wr007453.

Hurrell, J. W. et al. (1995). "Decadal trends in the North Atlantic Oscillation: regional temperatures and precipitation". In: *Science* 269.5224, pp. 676–678.

Huth, R. (2001). "Disaggregating climatic trends by classification of circulation patterns". In: *International Journal of Climatology* 21.2, pp. 135–153.

Huth, R. (2010). "Synoptic-climatological applicability of circulation classifications from the COST733 collection: First results". In: *Physics and Chemistry of the Earth* 35.9-12, pp. 388–394. DOI: 10.1016/j.pce.2009.11.013.

Huth, R., Beck, C., and Kučerová, M. (2016). "Synoptic-climatological evaluation of the classifications of atmospheric circulation patterns over Europe". In: *International Journal of Climatology* 36.7, pp. 2710–2726. DOI: 10.1002/joc.4546.

Huth, R., Beck, C., Philipp, A., Demuzere, M., Ustrnul, Z., Cahynová, M., Kyselý, J., and Tveito, O. E. (2008). "Classifications of Atmospheric Circulation Patterns". In: *Annals of the New York Academy of Sciences* 1146.1, pp. 105–152. DOI: 10.1196/annals.1446.019.

IPCC (2007). *Climate change 2007: The physical science basis, Contribution of Working Group I to the Fourth Assessment Report of the Intergovernmental Panel on Climate Change*. Ed. by Solomon, S., Qin, D., Manning, M., Chen, Z., Marquis, M., Averyt, K. B., Tignor, M., and Miller, H. L. Cambridge, United Kingdom and New York, NY, USA: Cambridge University Press.

Jacobeit, J., Wanner, H., Luterbacher, J., Beck, C., Philipp, A., and Sturm, K. (2003). “Atmospheric circulation variability in the North-Atlantic-European area since the mid-seventeenth century”. In: *Climate Dynamics* 20.4, pp. 341–352. DOI: 10.1007/s00382-002-0278-0.

Jones, P. D. and Lister, D. H. (2009). “The influence of the circulation on surface temperature and precipitation patterns over Europe”. In: *Climate of the Past* 5.2, pp. 259–267. DOI: 10.5194/cp-5-259-2009.

Kalkstein, L. S., Tan, G., and Skindlov, J. A. (1987). “An evaluation of three clustering procedures for use in synoptic climatological classification”. In: *Journal of Climate and Applied Meteorology* 26.6, pp. 717–730. DOI: 10.1175/1520-0450(1987)026<0717:AEOTCP>2.0.CO;2.

Karl, T. R., Wang, W.-C., Schlesinger, M. E., Knight, R. W., and Portman, D. (1990). “A method of relating general circulation model simulated climate to the observed local climate. Part I: Seasonal statistics”. In: *Journal of Climate* 3.10, pp. 1053–1079.

Katz, R. W. (1996). “Use of conditional stochastic models to generate climate change scenarios”. In: *Climatic Change* 32.3, pp. 237–255. DOI: 10.1007/BF00142464.

Keil, C., Volkert, H., and Majewski, D. (1999). “The Oder flood in July 1997: Transport routes of precipitable water diagnosed with an operational forecast model”. In: *Geophysical research letters* 26.2, pp. 235–238.

Kendall, M. G. (1938). “A new measure of rank correlation”. In: *Biometrika* 30.1/2, pp. 81–93.

Khaliq, M. N., Ouarda, T. B. M. J., Gachon, P., Sushama, L., and St-Hilaire, A. (2009). “Identification of hydrological trends in the presence of serial and cross correlations: A review of selected methods and their application to annual flow regimes of Canadian rivers”. In: *Journal of Hydrology* 368.1-4, pp. 117–130. DOI: 10.1016/j.jhydrol.2009.01.035.

Kidson, J. W. (1994). “Relationship of New Zealand daily and monthly weather patterns to synoptic weather types”. In: *International Journal of Climatology* 14.7, pp. 723–737. DOI: 10.1002/joc.3370140703.

Kilsby, C. G., Cowpertwait, P. S. P., O’connell, P. E., and Jones, P. D. (1998). “Predicting rainfall statistics in England and Wales using atmospheric circulation variables”. In: *International Journal of Climatology* 18.5, pp. 523–539.

Kilsby, C., Jones, P., Burton, A., Ford, A., Fowler, H., Harpham, C., James, P., Smith, A., and Wilby, R. (2007). “A daily weather generator for use in climate change studies”. In: *Environmental Modelling & Software* 22.12, pp. 1705–1719. DOI: 10.1016/j.envsoft.2007.02.005.

Kim, J., Ivanov, V. Y., and Fatichi, S. (2015). “Climate change and uncertainty assessment over a hydroclimatic transect of Michigan”. In: *Stochastic Environmental Research and Risk Assessment* 30.3, pp. 923–944. DOI: 10.1007/s00477-015-1097-2.

Kim, J., Ivanov, V. Y., and Fatichi, S. (2016). “Climate change and uncertainty assessment over a hydroclimatic transect of Michigan”. In: *Stochastic Environmental Research and Risk Assessment* 30.3, pp. 923–944. DOI: 10.1007/s00477-015-1097-2.

Klein Tank, A. M. G. and Können, G. P. (2003). “Trends in indices of daily temperature and precipitation extremes in Europe, 1946–99”. In: *Journal of climate* 16.22, pp. 3665–3680. DOI: 10.1175/1520-0442(2003)016<3665:tiiodt>2.0.co;2.

Köppen, W. and Geiger, R. (1930). *Handbuch der klimatologie*. Vol. 3. 1. Gebrüder Borntraeger Berlin, Germany.

Krichak, S. O. and Alpert, P. (2005). “Decadal trends in the east Atlantic–west Russia pattern and Mediterranean precipitation”. In: *International Journal of Climatology* 25.2, pp. 183–192.

Kundzewicz, Z. W., Radziejewski, M., and Pińskwar, I. (2006). “Precipitation extremes in the changing climate of Europe”. In: *Climate Research* 31.1, pp. 51–58. DOI: 10.3354/cr031051.

Küttel, M., Luterbacher, J., and Wanner, H. (2011). “Multidecadal changes in winter circulation-climate relationship in Europe: frequency variations, within-type modifications, and long-term trends”. In: *Climate Dynamics* 36.5-6, pp. 957–972. DOI: 10.1007/s00382-009-0737-y.

Kyselý, J. (2007). “Implications of enhanced persistence of atmospheric circulation for the occurrence and severity of temperature extremes”. In: *International Journal of Climatology* 27.5, pp. 689–695. DOI: 10.1002/joc.1478.

Lammersen, R., Engel, H., van de Langemheen, W., and Buiteveld, H. (2002). “Impact of river training and retention measures on flood peaks along the Rhine”. In: *Journal of Hydrology* 267.1â€“2, pp. 115–124. DOI: 10.1016/S0022-1694(02)00144-0.

te Linde, A. H., Aerts, J. C. J. H., Bakker, A. M. R., and Kwadijk, J. C. J. (2010). “Simulating low-probability peak discharges for the Rhine basin using resampled climate modeling data”. In: *Water Resources Research* 46.3, W03512. DOI: 10.1029/2009wr007707.

Lu, Y., Qin, X. S., and Mandapaka, P. V. (2015). “A combined weather generator and K-nearest-neighbour approach for assessing climate change impact on regional rainfall extremes”. In: *International Journal of Climatology* 35.15, pp. 4493–4508. DOI: 10.1002/joc.4301.

Łupikasza, E. (2010). “Relationships between occurrence of high precipitation and atmospheric circulation in Poland using different classifications of circulation types”. In: *Physics and Chemistry of the Earth* 35.9-12, pp. 448–455. DOI: 10.1016/j.pce.2009.11.012.

Łupikasza, E. B., Hänsel, S., and Matschullat, J. (2011). “Regional and seasonal variability of extreme precipitation trends in southern Poland and central-eastern Germany 1951–2006”. In: *International Journal of Climatology* 31.15, pp. 2249–2271. DOI: 10.1002/joc.2229.

Maraun, D., Wetterhall, F., Ireson, A. M., Chandler, R. E., Kendon, E. J., Widmann, M., Brienen, S., Rust, H. W., Sauter, T., Themeßl, M., Venema, V. K. C., Chun, K. P., Goodess, C. M., Jones, R. G., Onof, C., Vrac, M., and Thiele-Eich, I. (2010). “Precipitation downscaling under climate change: Recent developments to bridge the gap between dynamical models and the end user”. In: *Reviews of Geophysics* 48.3, RG3003. DOI: 10.1029/2009rg000314.

Masson, D. and Frei, C. (2014). “Spatial analysis of precipitation in a high-mountain region: exploring methods with multi-scale topographic predictors and circulation types”. In: *Hydrology and Earth System Sciences* 18.11, pp. 4543–4563. DOI: 10.5194/hess-18-4543-2014.

Merz, B., Aerts, J., Arnbjerg-Nielsen, K., Baldi, M., Becker, A., Bichet, A., Blöschl, G., Bouwer, L. M., Brauer, A., Cioffi, F., Delgado, J. M., Gocht, M., Guzzetti, F., Harrigan, S., Hirschboeck, K., Kilsby, C., Kron, W., Kwon, H.-H., Lall, U., Merz, R., Nissen, K., Salvatti, P., Swierczynski, T., Ulbrich, U., Viglione, A., Ward, P. J., Weiler, M., Wilhelm, B., and Nied, M. (2014). “Floods and climate: emerging perspectives for flood risk assessment and management”. In: *Natural Hazards and Earth System Sciences* 14.7, pp. 1921–1942. DOI: 10.5194/nhess-14-1921-2014.

Merz, B., Vorogushyn, S., Uhlemann, S., Delgado, J., and Hundecha, Y. (2012). “HESS Opinions “More efforts and scientific rigour are needed to attribute trends in flood time series””. In: *Hydrology and Earth System Sciences* 16.5, pp. 1379–1387. DOI: 10.5194/hess-16-1379-2012.

Min, S.-K., Zhang, X., Zwiers, F. W., and Hegerl, G. C. (2011). “Human contribution to more-intense precipitation extremes”. In: *Nature* 470.7334, pp. 378–381. DOI: 10.1038/nature09763.

Moberg, A., Jones, P. D., Lister, D., Walther, A., Brunet, M., Jacobeit, J., Alexander, L. V., Della-Marta, P. M., Luterbacher, J., Yiou, P., et al. (2006). “Indices for daily temperature and precipitation extremes in Europe analyzed for the period 1901–2000”. In: *Journal of Geophysical Research: Atmospheres* 111.D22.

Murawski, A., Bürger, G., Vorogushyn, S., and Merz, B. (2016a). “Can local climate variability be explained by weather patterns? A multi-station evaluation for the Rhine basin”. In: *Hydrology and Earth System Sciences* 20.10, pp. 4283–4306. DOI: 10.5194/hess-20-4283-2016.

Murawski, A., Vorogushyn, S., Bürger, G., Gerlitz, L., and Merz, B. (in review). “Do changing weather types explain observed climatic trends in the Rhine basin? An analysis of within and between-type changes”. In: *Journal of Geophysical Research: Atmospheres*.

Murawski, A., Zimmer, J., and Merz, B. (2016b). “High spatial and temporal organization of changes in precipitation over Germany for 1951–2006”. In: *International Journal of Climatology* 36.6, pp. 2582–2597. DOI: 10.1002/joc.4514.

Nied, M., Pardowitz, T., Nissen, K., Ulbrich, U., Hundecha, Y., and Merz, B. (2014). “On the relationship between hydro-meteorological patterns and flood types”. In: *Journal of Hydrology* 519, pp. 3249–3262. DOI: 10.1016/j.jhydrol.2014.09.089.

Osborn, T. J. and Jones, P. D. (2000). “Air flow influences on local climate: observed United Kingdom climate variations”. In: *Atmospheric Science Letters* 1.1, pp. 62–74.

Österle, H. (2001). “Reconstruction of daily global radiation for past years for use in agricultural models”. In: *Physics and Chemistry of the Earth, Part B: Hydrology, Oceans and Atmosphere* 26.3, pp. 253–256. DOI: http://dx.doi.org/10.1016/S1464-1909(00)00248-3.

Österle, H., F.-W., G., and P.C., W. (2006a). “Qualitätsprüfung, Ergänzung und Homogenisierung der täglichen Datenreihen in Deutschland, 1951–2003: ein neuer Datensatz.” In: *Deutsche Klimatagung, 9.-11. Oktober 2006, Klimatrends: Vergangenheit und Zukunft, Meteorologisches Institut der Ludwig- Maximilians-Universität, München*.

Österle, H., Gerstengarbe, F. W., and Werner, P. C. (2006b). *Ein neuer meteorologischer Datensatz für Deutschland, 1951–2003*.

Österle, H., Gerstengarbe, F.-W., and Werner, P. C. (2016). “Die Elbe im globalen Wandel”. In: ed. by Gräfe, F. W. V. H. S. K. M. V. B. H. P. Stuttgart, Germany: Schweizerbart Science Publishers. Chap. 2.2 Ein meteorologischer Datensatz für Deutschland, 1951–2003, pp. 81–84.

Panorska, A. K., Gershunov, A., and Kozubowski, T. J. (2007). “From diversity to volatility: Probability of daily precipitation extremes”. In: *Nonlinear Dynamics in Geosciences*, pp. 465–484. DOI: 10.1007/978-0-387-34918-3_26.

Pauling, A. and Paeth, H. (2007). “On the variability of return periods of European winter precipitation extremes over the last three centuries”. In: *Climate of the Past* 3.1, pp. 65–76. DOI: 10.5194/cp-3-65-2007.

Perez, J., Menendez, M., Mendez, F. J., and Losada, I. J. (2014). “Evaluating the performance of CMIP3 and CMIP5 global climate models over the north-east Atlantic region”. In: *Climate Dynamics* 43.9-10, pp. 2663–2680. DOI: 10.1007/s00382-014-2078-8.

Petrow, T., Zimmer, J., and Merz, B. (2009). “Changes in the flood hazard in Germany through changing frequency and persistence of circulation patterns”. In: *Natural Hazards and Earth System Sciences* 9.4, pp. 1409–1423. DOI: 10.5194/nhess-9-1409-2009.

Petrow, T. and Merz, B. (2009). “Trends in flood magnitude, frequency and seasonality in Germany in the period 1951-2002”. In: *Journal of Hydrology* 371.1-4, pp. 129–141. DOI: 10.1016/j.jhydrol.2009.03.024.

Philipp, A., Della-Marta, P. M., Jacobeit, J., Fereday, D. R., Jones, P. D., Moberg, A., and Wanner, H. (2007). “Long-Term Variability of Daily North Atlantic-European Pressure Patterns since 1850 Classified by Simulated Annealing Clustering”. In: *Journal of Climate* 20.16, pp. 4065–4095. DOI: 10.1175/jcli4175.1.

Philipp, A. (2009). “Comparison of principal component and cluster analysis for classifying circulation pattern sequences for the European domain”. In: *Theoretical and Applied Climatology* 96.1-2, pp. 31–41. DOI: 10.1007/s00704-008-0037-1.

Philipp, A., Bartholy, J., Beck, C., Erpicum, M., Esteban, P., Fettweis, X., Huth, R., James, P., Jourdain, S., Kreienkamp, F., Krennert, T., Lykoudis, S., Michalides, S. C., Pianko-Kluczynska, K., Post, P., Álvarez, D. R., Schiemann, R., Spekat, A., and Tymvios, F. S. (2010). “Cost733cat – A database of weather and circulation type classifications”. In: *Physics and Chemistry of the Earth* 35.9-12, pp. 360–373. DOI: 10.1016/j.pce.2009.12.010.

Philipp, A., Beck, C., Huth, R., and Jacobeit, J. (2016). “Development and comparison of circulation type classifications using the COST 733 dataset and software”. In: *International Journal of Climatology* 36.7, pp. 2673–2691. DOI: 10.1002/joc.3920.

Pinter, N., van der Ploeg, R. R., Schweigert, P., and Hoefer, G. (2006). “Flood magnification on the River Rhine”. In: *Hydrological Processes* 20.1, pp. 147–164. DOI: 10.1002/hyp.5908.

Poli, P., Hersbach, H., Tan, D., Dee, D., Thepaut, J.-N., Simmons, A., Peubey, C., Laloyaux, P., Komori, T., Berrisford, P., Dragani, R., Trémolet, Y., Hólm, E., Bonavita, M., Isaksen, L., and Fisher, M. (2013). *The data assimilation system and initial performance evaluation of the ECMWF pilot reanalysis of the 20th-century assimilating surface observations only (ERA-20C)*. ERA Report Series 14. European Centre for Medium-Range Weather Forecasts (ECMWF).

Robine, J.-M., Cheung, S. L. K., Roy, S. L., Oyen, H. V., Griffiths, C., Michel, J.-P., and Herrmann, F. R. (2008). “Death toll exceeded 70,000 in Europe during the summer of 2003”. In: *Comptes*

Rendus Biologies 331.2. Dossier : Nouveautés en cancérogenèse / New developments in carcinogenesis, pp. 171–178. DOI: https://doi.org/10.1016/j.crvi.2007.12.001.

Schär, C., Frei, C., Lüthi, D., and Davies, H. C. (1996). "Surrogate climate-change scenarios for regional climate models". In: *Geophysical Research Letters* 23.6, pp. 669–672. DOI: 10.1029/96GL00265.

Schönwiese, C.-D., Walter, A., and Brinckmann, S. (2010). "Statistical assessments of anthropogenic and natural global climate forcing. An update". In: *Meteorologische Zeitschrift* 19.1, pp. 3–10. DOI: 10.1127/0941-2948/2010/0421.

Schröter, K., Kunz, M., Elmer, F., Mähr, B., and Merz, B. (2015). "What made the June 2013 flood in Germany an exceptional event? A hydro-meteorological evaluation". In: *Hydrology and Earth System Sciences* 19.1, pp. 309–327. DOI: 10.5194/hess-19-309-2015.

Selten, F. M., Haarsma, R. J., and Opsteegh, J. D. (1999). "On the mechanism of North Atlantic decadal variability". In: *Journal of Climate* 12.7, pp. 1956–1973.

Semenov, M. A. and Barrow, E. M. (1997). "Use of a stochastic weather generator in the development of climate change scenarios". In: *Climatic Change* 35.4, pp. 397–414. DOI: 10.1023/a:1005342632279.

Sen, P. K. (1968). "Estimates of the Regression Coefficient Based on Kendall's Tau". In: *Journal of the American Statistical Association* 63.324, pp. 1379–1389. DOI: 10.1080/01621459.1968.10480934.

Shepherd, T. G. (2014). "Atmospheric circulation as a source of uncertainty in climate change projections". In: *Nature Geoscience* 7.10, pp. 703–708. DOI: 10.1038/ngeo2253.

Spekat, A., Kreienkamp, F., and Enke, W. (2010). "An impact-oriented classification method for atmospheric patterns". In: *Physics and Chemistry of the Earth* 35.9-12, pp. 352–359. DOI: 10.1016/j.pce.2010.03.042.

Steinschneider, S. and Brown, C. (2013). "A semiparametric multivariate, multisite weather generator with low-frequency variability for use in climate risk assessments". In: *Water Resources Research* 49.11, pp. 7205–7220. DOI: 10.1002/wrcr.20528.

Steirou, E., Gerlitz, L., Apel, H., and Merz, B. (2017). "Links between large-scale circulation patterns and streamflow in Central Europe: A review". In: *Journal of Hydrology* 549, pp. 484–500. DOI: 10.1016/j.jhydrol.2017.04.003.

Sunyer, M. A., Hundecha, Y., Lawrence, D., Madsen, H., Willems, P., Martinkova, M., Vormoor, K., Bürger, G., Hanel, M., Kriaučiūnienė, J., Loukas, A., Osuch, M., and Yücel, I. (2015). "Inter-comparison of statistical downscaling methods for projection of extreme precipitation in Europe". In: *Hydrology and Earth System Sciences* 19.4, pp. 1827–1847. DOI: 10.5194/hess-19-1827-2015.

Taylor, K. E., Stouffer, R. J., and Meehl, G. A. (2012). "An Overview of CMIP5 and the Experiment Design". In: *Bulletin of the American Meteorological Society* 93.4, pp. 485–498. DOI: 10.1175/bams-d-11-00094.1.

Thieken, A. H., Apel, H., and Merz, B. (2015). "Assessing the probability of large-scale flood loss events: a case study for the river Rhine, Germany". In: *Journal of Flood Risk Management* 8.3, pp. 247–262. DOI: 10.1111/jfr3.12091.

Trenberth, K. E., Jones, P. D., Ambenje, P., Bojariu, R., Easterling, D., Tank, A. K., Parker, D., Rahimzadeh, F., Renwick, J. A., Rusticucci, M., Soden, B., and Zhai, P. (2007). "Climate Change 2007: The Physical Science Basis. Contribution of Working Group I to the Fourth Assessment Report of the Intergovernmental Panel on Climate Change." In: ed. by Solomon, S., Qin, D., Manning, M., Marquis, M., Averyt, K. B., Tignor, M., Miller, H. L., and Chen, Z. Cambridge University Press, Cambridge, UK and New York, NY, USA. Chap. Observations: Surface and Atmospheric Climate Change, pp. 235–336.

Trenberth, K. E., Dai, A., Rasmussen, R. M., and Parsons, D. B. (2003). "The Changing Character of Precipitation". In: *Bulletin of the American Meteorological Society* 84.9, pp. 1205–1217. DOI: 10.1175/BAMS-84-9-1205.

Trömel, S. and Schönwiese, C.-D. (2007). "Probability change of extreme precipitation observed from 1901 to 2000 in Germany". In: *Theoretical and Applied Climatology* 87.1, pp. 29–39.

Tveito, O. E. (2010). "An assessment of circulation type classifications for precipitation distribution in Norway". In: *Physics and Chemistry of the Earth* 35.9-12, pp. 395–402. DOI: 10.1016/j.pce.2010.03.044.

Ulbrich, U., Brücher, T., Fink, A. H., Leckebusch, G. C., Krüger, A., and Pinto, J. G. (2003). "The central European floods of August 2002: Part 1 – Rainfall periods and flood development". In: *Weather* 58.10, pp. 371–377. DOI: 10.1256/wea.61.03A.

Uvo, C. B. (2003). "Analysis and regionalization of northern European winter precipitation based on its relationship with the North Atlantic Oscillation". In: *International Journal of Climatology* 23.10, pp. 1185–1194.

Villarini, G., Smith, J. A., Serinaldi, F., and Ntelekos, A. A. (2011). "Analyses of seasonal and annual maximum daily discharge records for central Europe". In: *Journal of Hydrology* 399.3-4, pp. 299–312. DOI: 10.1016/j.jhydrol.2011.01.007.

Vorogushyn, S. and Merz, B. (2013). "Flood trends along the Rhine: the role of river training". In: *Hydrology and Earth System Sciences* 17.10, pp. 3871–3884. DOI: 10.5194/hess-17-3871-2013.

Walter, A. and Schönwiese, C.-D. (2003). "Nonlinear statistical attribution and detection of anthropogenic climate change using a simulated annealing algorithm". In: *Theoretical and applied Climatology* 76.1-2, pp. 1–12.

Wang, J., Tsang, W. W., and Marsaglia, G. (2003). "Evaluating Kolmogorov's distribution". In: *Journal of Statistical Software* 8.18. DOI: 10.18637/jss.v008.i18.

Wang, Y.-H., Magnusdottir, G., Stern, H., Tian, X., and Yu, Y. (2012). "Decadal variability of the NAO: introducing an augmented NAO index". In: *Geophysical Research Letters* 39.21.

Wetterhall, F., Pappenberger, F., He, Y., Freer, J., and Cloke, H. (2012). "Conditioning model output statistics of regional climate model precipitation on circulation patterns". In: *Nonlinear Processes in Geophysics* 19.6, pp. 623–633.

Widmann, M. and Schär, C. (1997). "A principal component and long-term trend analysis of daily precipitation in Switzerland". In: *International Journal of Climatology* 17.12, pp. 1333–1356. DOI: 10.1002/(SICI)1097-0088(199710)17:12<1333::AID-JOC108>3.0.CO;2-Q.

Wilby, R. L. and Quinn, N. W. (2013). "Reconstructing multi-decadal variations in fluvial flood risk using atmospheric circulation patterns". In: *Journal of Hydrology* 487, pp. 109–121. DOI: 10.1016/j.jhydrol.2013.02.038.

Wilks, D. S. (1992). "Adapting stochastic weather generation algorithms for climate change studies". In: *Climatic Change* 22.1, pp. 67–84. DOI: 10.1007/bf00143344.

Wilks, D. S. and Wilby, R. L. (1999). "The weather generation game: a review of stochastic weather models". In: *Progress in physical geography* 23.3, pp. 329–357. DOI: 10.1191/030913399666525256.

Wójcik, R. (2015). "Reliability of CMIP5 GCM simulations in reproducing atmospheric circulation over Europe and the North Atlantic: a statistical downscaling perspective". In: *International Journal of Climatology* 35.5, pp. 714–732. DOI: 10.1002/joc.4015.

Yang, D., Ishida, S., Goodison, B. E., and Gunther, T. (1999). "Bias correction of daily precipitation measurements for Greenland". In: *Journal of Geophysical Research: Atmospheres* 104.D6, pp. 6171–6181. DOI: 10.1029/1998jd200110.

Yiou, P., Vautard, R., Naveau, P., and Cassou, C. (2007). "Inconsistency between atmospheric dynamics and temperatures during the exceptional 2006/2007 fall/winter and recent warming in Europe". In: *Geophysical Research Letters* 34.21. DOI: 10.1029/2007gl031981.

Yue, S., Pilon, P., and Phinney, B. (2003). "Canadian streamflow trend detection: impacts of serial and cross-correlation". In: *Hydrological Sciences Journal* 48.1, pp. 51–63. DOI: 10.1623/hysj.48.1.51.43478.

Zolina, O. (2014). "Multidecadal trends in the duration of wet spells and associated intensity of precipitation as revealed by a very dense observational German network". In: *Environmental Research Letters* 9.2, p. 025003. DOI: 10.1088/1748-9326/9/2/025003.

Zolina, O., Simmer, C., Belyaev, K., Gulev, S. K., and Koltermann, P. (2013). "Changes in the duration of European wet and dry spells during the last 60 years". In: *Journal of Climate* 26.6, pp. 2022–2047. DOI: 10.1175/jcli-d-11-00498.1.

Zolina, O., Simmer, C., Belyaev, K., Kapala, A., and Gulev, S. (2009). "Improving estimates of heavy and extreme precipitation using daily records from European rain gauges". In: *Journal of Hydrometeorology* 10.3, pp. 701–716. DOI: 10.1175/2008jhm1055.1.

Zolina, O., Simmer, C., Gulev, S. K., and Kollet, S. (2010). “Changing structure of European precipitation: longer wet periods leading to more abundant rainfalls”. In: *Geophysical Research Letters* 37.6. DOI: 10.1029/2010gl042468.

Zolina, O., Simmer, C., Kapala, A., Bachner, S., Gulev, S., and Maechel, H. (2008). “Seasonally dependent changes of precipitation extremes over Germany since 1950 from a very dense observational network”. In: *Journal of Geophysical Research: Atmospheres* 113.D6. DOI: 10.1029/2007jd008393.

Zolina, O., Simmer, C., Kapala, A., and Gulev, S. (2005). “On the robustness of the estimates of centennial-scale variability in heavy precipitation from station data over Europe”. In: *Geophysical Research Letters* 32.14. DOI: 10.1029/2005gl023231.

Author's declaration

I prepared this dissertation without illegal assistance. The work is original except where indicated by special reference in the text and no part of the dissertation has been submitted for any other degree.

This dissertation has not been presented to any other University for examination, neither in Germany nor in another country.

Aline Murawski

Potsdam, December 2017